NACA TN 3876

# NATIONAL ADVISORY COMMITTEE FOR AERONAUTICS

## TECHNICAL NOTE 3876

### AN INVESTIGATION AT LOW SPEED OF THE FLOW

### OVER A SIMULATED FLAT PLATE AT SMALL

### ANGLES OF ATTACK USING PITOT-STATIC

### AND HOT-WIRE PROBES

By Donald E. Gault

Ames Aeronautical Laboratory
Moffett Field, Calif.

NACA

Washington

March 1957

K

NATIONAL ADVISORY COMMITTEE FOR AERONAUTICS

———————

TECHNICAL NOTE 3876

———————

AN INVESTIGATION AT LOW SPEED OF THE FLOW

OVER A SIMULATED FLAT PLATE AT SMALL

ANGLES OF ATTACK USING PITOT-STATIC

AND HOT-WIRE PROBES

By Donald E. Gault

SUMMARY


Results are presented from pitot-static and hot-wire anemometer surveys at low speed of the flow over a thin, sharp-edge airfoil which simulated a flat plate. The investigation was undertaken to obtain detailed measurements of the flow associated with the so-called thin-airfoil type of stall. The measurements were obtained for angles of attack of $2^{\circ}$, $4^{\circ}$, and $6^{\circ}$ at a Reynolds number of $4 \times 10^{6}$. Data are presented in graphical as well as tabular form.

It was found that the large regions of reverse flow (bubbles) which are characteristic of the flow for a thin-airfoil stall cannot be considered regions of "dead" air; mean velocities of about 0.3 of the free-stream velocity and velocity fluctuations up to 0.65 of the local velocities were measured in these regions. The reverse flow appears to be part of a more general circulatory or vortex-type flow. The largest velocity fluctuations (absolute magnitude) were found to occur along a narrow band in the detached flow above the bubbles; these fluctuations amounted to 0.30 of the free-stream velocity and are of the same relative magnitude as have been observed for a turbulent jet. This turbulent flow originated so near the leading edge of the plate that no separated laminar flow was detected.

INTRODUCTION


A classification of stalling and the accompanying flow-separation phenomena into three categories is presented in reference 1 for airfoil sections at low speed. Although stalling and flow separation are considered only in two-dimensional flow, the classifications and illustrative data contained in the reference have proven useful in providing explanations for many flow phenomena which have been encountered in three-dimensional flow fields about complete wings (e.g., ref. 2). The present report is concerned solely with the flow which is associated with what reference 1 describes as the thin-airfoil type of stall.

Briefly, for the thin-airfoil stall, the flow separates from the
leading edge and subsequently reattaches to the upper surface of the air-
foil at a position along the chord which moves progressively downstream
with increasing angle of attack.  The angle of attack for which the flow
first separates is dependent primarily on the geometry (roundness) of the
leading edge.  When the position of flow reattachment is near the trailing
edge, the lift coefficient begins to decrease with continued increases
in angle of attack and, for present purposes, the airfoil section is con-
sidered to have stalled.  A reverse flow is established inside the large
region underlying the detached flow; this region of reverse flow will
hereinafter be referred to as the "thin-airfoil" bubble.  This thin-airfoil
bubble should not be confused, however, with the laminar-separation bubble
discussed in reference 1 in connection with the so-called leading-edge
stall.  Although there appears to be some relationship between the thin-
airfoil and laminar-separation bubbles (ref. 1), the characteristics of
the two are vastly different.  Specific investigations of the laminar-
separation bubble are reported in references 3, 4, and 5.

The data which form the basis for defining the thin-airfoil stall in
reference 1 and the preceding brief description were originally reported
by McCullough and Gault for an NACA 64A006 airfoil (ref. 6) and by Rose
and Altman for a modified double-wedge airfoil (ref. 7).  It is pointed
out in references 6 and 7 that the quantitative value of the flow surveys
of the thin-airfoil flow is uncertain due to limitations in the experi-
mental techniques and certain characteristics of the flow peculiar to
thin-airfoil stall.  For this reason only a limited amount of the survey
data is presented in the references, and these are included with the
intent of illustrating the general features of the mean flow rather than
defining specific details of the flow.  It is to be noted that no cor-
rections were applied to the survey data for the effects of the exceedingly
turbulent flow encountered during the investigations nor were any measure-
ments obtained in the region of reverse flow.

The investigation reported herein was instigated for the specific
purpose of obtaining more detailed and refined measurements than are
available in references 6 and 7 of the flow which precedes the thin-
airfoil stall.  It was anticipated that the results would aid in clarifying
the mechanics of the flow associated with the thin-airfoil stall and, at
the same time, could be of value in ascertaining differences between the
thin-airfoil and laminar-separation bubbles.

In order to obtain as clear and distinct an example of the thin-
airfoil type of separated flow as possible, a thin, sharp-edged airfoil
was employed for this investigation which effectively simulated a flat
plate.  Surveys of the flow from the leading edge to the 80-percent-chord
station were obtained by pitot-static and hot-wire anemometer techniques,
the latter providing measurements of both mean and fluctuating components
of the flow.  All surveys were obtained for a Reynolds number of $4 \times 10^6$,
based on the chord of the plate, and for angles of attack of $2^\circ$, $4^\circ$, and
$6^\circ$.  The pressure distributions along the surface of the plate also were

measured.  Due to the bulk of the data, only representative results are shown graphically herein; however, all data are presented in tabular form.

## NOTATION

$c$       chord of plate, 5 ft

$C_p$       static pressure coefficient, $\dfrac{\bar{p} - p_\infty}{\frac{1}{2}\rho U_\infty^2}$

$C_{p_t}$       total pressure coefficient, $\dfrac{p_{t_\infty} - \bar{p}_t}{\frac{1}{2}\rho U_\infty^2}$

$p$       static pressure, lb/sq ft

$p_t$       total pressure, lb/sq ft

$u$       resultant velocity, ft/sec
        (The mean resultant velocity $\bar{u}$ is equal to $\sqrt{\bar{u}_x^2 + \bar{u}_y^2}$.)

$\Delta u, \Delta v, \Delta w$ fluctuating components of the resultant velocity, ft/sec

$R$       Reynolds number, $\dfrac{U_\infty c}{\nu}$

$u_x, u_y$       velocity components in the $x$ and $y$ directions, respectively, ft/sec

$U$       reference velocity, ft/sec

$x$       distance from the leading edge along flat surface of model, ft

$y$       distance normal from the surface, ft

$\alpha$       angle of attack, deg
        (See discussion under section entitled "TESTS.")

$\gamma$       direction of mean resultant velocity $\bar{u}$ relative to the longitudinal axis of the pitot-static probes, deg

$\rho$       density of air, slugs/cu ft

$\nu$       kinematic viscosity, ft$^2$/sec

$\theta$        direction of mean resultant velocity $\bar{u}$ relative to the flat

surface of model ($\theta$ = arctan $\bar{u}_y/\bar{u}_x$ with $-180^{\circ} \leq \theta \leq 180^{\circ}$

and $\bar{u}_y$ positive when directed away from the surface), deg

Barred symbols (e.g., $\bar{u}$) indicate the temporal mean of the quantity.

## Subscripts

$\infty$        free-stream conditions

m        a measured quantity (uncorrected for the effects of velocity
fluctuations)

## APPARATUS

### Wind Tunnel

The investigation reported herein was conducted in one of the Ames 7- by 10-foot wind tunnels, modified to provide a 4- by 10-foot test section (fig. 1). The false floor and ceiling, approximately 3 inches thick, were 25 feet long and extended an equal distance upstream and downstream of the original test section. Hot-wire anemometer measurements have indicated that the turbulence level of the free stream $\sqrt{\overline{\Delta u_{\infty}^2}}/U_{\infty}$ is 0.15 to 0.20 percent.

### Model

Figure 2 presents dimensions of the simulated flat plate and a photograph of the model installed in the wind tunnel. The model spanned the 4-foot dimension of the modified test section and was fabricated from steel, except for a thin mahogany veneer in the region of the rounded crest line of the double-wedge profile of the lower surface. Static-pressure orifices were provided along the midspan station of the model. Circular end plates, 6 feet in diameter, were attached to the ends of the model and served as parts of the false floor and ceiling. The rectangular fences (1 by 5 feet) visible in figure 2, were added during the course of the investigation to improve the two-dimensionality of the flow; the span between the fences was 3.33 feet.

## Flow-Survey Equipment

The survey apparatus used to obtain the pitot-static and hot-wire anemometer measurements was remotely controlled from outside the wind tunnel. Two devices were employed; one, shown in figure 3, was capable of traversing 5 inches in the  y  direction and a second mechanism of similar design was capable of a 9-inch traverse. The frames of these devices screwed into holes tapped in the lower surface of the model. Nine tapped holes were provided along the chord (3 inches above the mid-span station) which permitted flow surveys to be made at any chordwise position between the leading edge and the 80-percent-chord station. When not being used, the tapped holes were filled with plugs which had been machined as integral parts of the surface during construction of the model.

The mechanical counter shown in figure 3 was read by telescope from outside the wind tunnel. Although the least count on the counter corresponded to 0.0002-inch traverse, backlash and other mechanical tolerances limited the accuracy of positioning the probes to ±0.002 inch.

## Survey Probes and Related Equipment

Pitot static.- Photographs of the pitot-static probes employed during this investigation are presented as figure 4. Both the conventional probe and the probe used for measurements of the reverse flow consisted of four 0.030-inch-outside-diameter stainless-steel tubes. The center tube of the three tubes grouped together provided a measure of the total pressure while the two adjoining tubes, beveled $45^\circ$, furnished a means for ascertaining the direction $\theta$ of the mean resultant flow $\bar{u}$. The single static-pressure tube was offset laterally about 0.5 inch from the total-pressure tube and contained four 0.008-inch-diameter orifices, spaced $90^\circ$ apart, at the plane of survey. All four tubes were soldered into a 0.125-inch-outside-diameter tube which fitted tightly into the ends of the probe holders (see fig. 3).

Hot wire.- Tungsten wire with a nominal diameter of 0.00015 inch was employed for the hot-wire probes. The wires, approximately 0.10 inch long, were welded across the ends of two 0.010-inch-diameter drill-rod prongs which were embedded in a 0.125-inch-diameter bakelite-rod base. The prongs had an unsupported length of 0.75 inch and were ground to a conical shape at the ends where the tungsten wire was attached. The bakelite base fitted into the same holders of the traversing mechanism as were employed for the pitot-static probes.

The electronic equipment required for obtaining measurements with the hot wires was designed to operate the wires at a constant mean resistance (i.e., variable heating current) throughout the speed range. The amplifying circuit has a flat response (within 2 percent) from 30 cycles to approximately 40 kilocycles per second; the response is down

3 db at 8 cycles and 55 kilocycles. The amplifier contains a resistance-capacitance circuit to compensate for thermal lag of the hot wires. The square-wave technique described by Kovasznay in reference 8 was employed to ascertain the proper compensation. For the turbulence measurements, a millivoltmeter indicates the output from a thermocouple which is heated by the current output from the compensated amplifier. A sinusoidal output from a commercial oscillator was used for calibrating the output from the thermocouple.

All wires were calibrated in a small (2- by 7.5-inch test section) wind tunnel. Air was drawn through this wind tunnel by means of a constant-speed centrifugal blower. Speed control was obtained by a throttle on the blower discharge line and velocities up to approximately 400 feet per second were attainable.

## EXPERIMENTAL PROCEDURE AND PROBE CALIBRATIONS

### Test Conditions

All measurements of the flow about the simulated flat plate were obtained for a Reynolds number of $4 \times 10^6$, based on the chord of the plate. For average test conditions this corresponds to a free-stream velocity $U_\infty$ of approximately 130 feet per second and a dynamic pressure of 20 pounds per square foot.

The values of angle of attack listed herein are referenced to that angle of attack for which free-stream total pressure was attained at a pressure orifice in the 0.020-inch thick leading edge of the plate. Due to the camber in the model this reference angle is $0.3^\circ$ greater than the geometric angle of attack referred to the upper (flat) surface of the plate.

Although measurements of the surface pressure distributions were obtained for angles of attack from $-8^\circ$ to $8^\circ$ in one degree increments, surveys of the flow about the plate were obtained only for angles of attack of $2^\circ$, $4^\circ$, and $6^\circ$. For angles less than $2^\circ$, the region of separated flow was too small to define easily in any detail. For angles greater than $6^\circ$, the position of flow reattachment was downstream of the most rearward position for which flow surveys could be obtained ($x/c = 0.80$). The type of surveys and chordwise stations for which measurements were obtained are listed in the following table:

| x/c | Type of survey | x/c | Type of survey | x/c | Type of survey |
|-----|----------------|-----|----------------|-----|----------------|
| 0 | Pitot and wire | 0.2 | Pitot and wire | 0.5 | Pitot |
| .01 | Pitot and wire | .25 | Pitot | .55 | Pitot |
| .025 | Pitot | .3 | Pitot and wire | .6 | Pitot and wire |
| .05 | Pitot and wire | .35 | Pitot | .65 | Pitot |
| .075 | Pitot | .4 | Pitot | .7 | Pitot |
| .10 | Pitot and wire | .45 | Pitot and wire | .8 | Pitot and wire |
| .15 | Pitot | | | | |

Hot-wire anemometer measurements were also made at several stations upstream of the leading edge and results are presented for values of x/c  of -0.00025 and -0.00010.

All pressures were read to the nearest 0.01 inch of water from differential reading U-tube manometers. Approximately 60 feet of 0.063-inch-inside-diameter tubing were employed in the lines between the probes and the manometers. Although this caused a 3- to 5-minute time lag for the manometers to attain equilibrium readings, such a procedure was used in order to damp out the large irregular pressure fluctuations which are characteristic of the flow under consideration.

## Calibration of Probes

The pitot-static probes were calibrated prior to and periodically concurrent with the pitot-static surveys. These calibrations were conducted in an unmodified 7- by 10-foot wind tunnel and a typical calibration is presented in figure 5. The pitot-static, as well as the hot-wire, probes were calibrated in the holders (fig. 3) as complete units. Before and after each run (consisting of a single traverse for fixed values of x/c and $\alpha$) the hot wires were calibrated. This procedure was necessary because of changes in the calibrations caused by the accumulation of microscopic dirt particles on the wires. In general, changes in the calibrations were sufficiently small so they could be prorated on a time basis for data-reduction purposes. When the changes in the calibrations were excessive, all data were discarded and the measurements were repeated. Despite the presence of foreign material in the air stream, wire breakage was a minor problem.

## Corrections Applied to Data for the Effects of Turbulence

All values of mean velocity presented herein have had corrections applied for the influence of the turbulent flow on the pitot-static and hot-wire measurements. The bases for the corrections are that: (1) either all or part of the energy of the turbulent flow is included as part

of the pitot-static pressures; and (2) the voltage-velocity relationship
for a hot wire is nonlinear for the usual hot-wire anemometry practice
in which constant current is maintained for any given value of the mean
velocity.  The net effect of the turbulence is to cause the indicated
mean velocities from the pitot-static measurements to be larger and from
the hot-wire measurements to be smaller than the true mean velocities.
For the extremely high values of turbulence encountered during the present
investigation, the differences in the measured mean velocities between
the two techniques amounted to as much as 0.2 of the free-stream velocity.

Details of the methods for correcting the pitot-static and hot-wire
measurements are described in Appendixes A and B, respectively.  Although
the methods are rather crude, it is believed that the corrections are, in
general, good first-order approximations for the effects of the turbulent
flow.  The accuracy of the final results is difficult to assess, but some
indication of the validity of the procedure used for correcting the data
for turbulence is evidenced by the fact that the results from the hot-wire
and pitot-static surveys agree for the most part within 3 or 4 percent of
the free-stream velocity.  As might be expected, the greatest discrepancies
(10 to 20 percent of the free-stream velocity) occur for results obtained
in regions of reversed flow.  It is to be emphasized that no corrections
have been applied to the measurements of velocity fluctuations $\sqrt{\overline{\Delta u^2}}$.

## RESULTS AND DISCUSSION

### Preliminary Tests

Prior to the main studies of this investigation, a series of tests
were made to examine and improve the two-dimensionality of the flow about
the simulated flat plate.  These tests were undertaken after tuft studies
had revealed that (without the rectangular fences shown in fig. 2) span-
wise flow developed in the region of separated flow for about $3^\circ$ angle of
attack and became very pronounced for angles of attack of $5^\circ$ or greater.
The addition of the fences delayed the onset of the spanwise flow indi-
cated by the tufts to an angle of attack of approximately $6^\circ$.  With or
without the fences, the spanwise flow was symmetrical about the midspan
of the model and was visible only near the 5-percent-chord station.

Inasmuch as tuft studies provide, at best, a qualitative description
of the flow, a series of total- and static-pressure surveys were con-
ducted to examine further the two-dimensionality of the flow.  Conven-
tional rakes of total- and static-pressure tubes were employed to survey
the flow at five spanwise and three chordwise stations.  These measure-
ments revealed unexpectedly that, either with or without the fences and
independent of the angle of attack (up to $6^\circ$), the height of the region
of viscous flow (as well as the shape of the velocity profiles) was
independent of spanwise position except along the bottom 15 inches of
the 48-inch span of the plate.  The spanwise change in the height (and
velocity profiles) of the region of viscous flow occurred on both the

upper (flat) and lower surfaces of the model but, significantly, in an opposite sense for the two surfaces (i.e., an increase in thickness for one surface and a decrease for the other surface). This result was interpreted and subsequently verified as having been caused by a spanwise variation in the stream angle along the bottom portion of the plate. It is estimated that the variation along the bottom 15 inches of the span did not exceed $0.3^{\circ}$. Since this stream defect could not be corrected readily, the preliminary tests for improving the two-dimensionality of the flow were terminated at this point in the investigation.

The experimental results presented herein, therefore, were not obtained in strictly two-dimensional flow. However, all measurements were obtained along the upper spanwise stations of the plate for which the thickness of the boundary layer was found not to vary with spanwise position. It seems probable that with the rectangular fences installed, a good approximation to two-dimensional conditions was achieved for angles of attack of $2^{\circ}$ and $4^{\circ}$. For $6^{\circ}$ angle of attack, some spanwise flow is believed to have occurred and the two-dimensionality of the data are suspect. Some further discussion and evidence of the limitation to the data are presented in a subsequent section.

## Pressure Distributions

Distributions of pressure along the upper (flat) surface of the model for angles of attack from $-8^{\circ}$ to $+8^{\circ}$ are presented as figure 6. The representative distributions for negative angles of attack are included to provide an indication of the distributions along the lower surface of a flat plate. These data together with additional results for negative angles of attack are also presented in table I.

The distributions shown in figure 6 are effectively the same as those which have been obtained for other thin- and sharp-edged airfoil sections (refs. 6 and 7). The regions of approximately constant pressure at the positive angles of attack depict graphically the development of the so-called thin-airfoil type of separated flow and its fairly rapid extension downstream from the leading edge as the angle of attack is increased.

## Mean Flow Measurements

Some typical results from the pitot-static surveys of the mean flow over the flat surface of the model for $2^{\circ}$, $4^{\circ}$, and $6^{\circ}$ angle of attack are given in figure 7. The data, which are presented only for the chordwise stations for which hot-wire measurements were obtained, include the hot-wire determinations of the mean velocity. A complete presentation of the flow-survey data will be found in tables II and III.

With regard to figure 7, it is convenient to consider first the agreement obtained between the two types of measurements for the mean velocity ū.  Toward this end, figure 8 is presented to illustrate some typical comparisons at a larger scale than is employed in figure 7.  At the same time, figure 8 demonstrates: (1) the magnitude of the corrections applied for the influence of the turbulent flow and (2) the correlation obtained between the results from the conventional and reverse flow probes.

It will be seen that, in general, the pitot-static and hot-wire measurements are in good agreement.  The agreement is excellent for some conditions (fig.8(a)) while for other conditions the agreement is not so good but is still felt to be satisfactory (figs. 8(b) and 8(c)).  The discrepancy shown in figure 8(b) for values of $y/c$ between 0.03 to 0.05 occurs in the region of separated flow where the direction of the mean resultant flow changed rapidly approximately $180^\circ$ (see fig. 7(f)).  In such regions, disagreement is probably caused by a number of effects including: (1) the inherent loss of accuracy in the pitot-static surveys for small manometer deflections, (2) the sensitivity for small velocity ratios of the corrections to the pitot-static measurements for turbulence (see Appendix A and fig. 14), and (3) in conjunction with (2), the probability of errors in the measured values of turbulence due to their magnitude and the nonlinear voltage-velocity characteristics of the hot-wire anemometer.  It should not be implied, however, that such discrepancies as that shown in figure 8(b) are caused solely by limitations in the pitot-static technique.  The mean velocities indicated by the hot wire are also subject to error (Appendix B).  Although the magnitude of the probable errors in hot-wire results are indeterminate, it will be noted that hot-wire data are more regular than the pitot-static results for conditions where $\theta$ is changing rapidly with $y$.

The survey data shown in figure 7 reveal several interesting features of the flow about the simulated flat plate.  One of the most interesting is that the magnitudes of the velocities of the reverse flow are (except near the leading edge) greater than $0.2\ U_\infty$ and as large as 0.35 to $0.40\ U_\infty$ for certain chordwise locations.  The thin-airfoil bubble is not, therefore, a region of dead or stagnant air.  It will be noted, in addition, that the static pressure through the regions of separated flow is not constant.  The pressure first decreases and then increases with increasing distance above the surface.  (Note that the static pressures measured near the plate surface with the pitot-static probes agree well with the static pressures measured by the flush orifice in the surface of the model.)  The maximum variations in the static pressure occur in the detached flow above the regions of reverse flow and, in some cases, amount to 0.5 of the free-stream dynamic pressure (fig. 7(b)).  These pressure variations in the $y$ direction gradually lessen with distance downstream of the region of reverse flow and for the smaller angles of attack eventually disappear completely.  The pressure variations in the $y$ direction together with the occurrence of the fairly strong reverse flow, as mentioned in references 6 and 7, are suggestive of a vortex flow.  The changes in the direction of the flow which should be expected for a vortex-type flow are clearly evident in figure 7.

The shape and extent of the thin-airfoil bubbles derived from the mean flow surveys are presented in figure 9.  The bubble is defined for present purposes as the region bounded by the plate surface and the contour above the plate surface along which the $\bar{u}_x$ component of the mean velocity is zero (i.e., $\theta = \pm 90^\circ$).  The figure also includes the distribution of the mean flow into and out of the bubble (i.e., the $\bar{u}_y$ component of velocity along the contour where $\bar{u}_x = 0$).

The rapid increase in extent and thickness of the bubble with increasing angle of attack is apparent.  These data together with the surface pressure-distribution measurements (fig. 6) indicate that the separated flow from the leading edge of the plate reattaches to the surface at the termination (approximately) of the rapid pressure rise downstream of the region of essentially constant pressure.  On this basis it is estimated that flow reattachment probably occurred at chordwise stations of 0.02, 0.14, and 0.42 for angles of attack of $1^\circ$, $3^\circ$, and $5^\circ$, respectively. Estimates for higher angles of attack are not warranted because of the vagueness of the terminal points and the probability of spanwise flow.

It is interesting to compare the extent and maximum thickness of the bubbles from the current studies with those reported by Rose and Altman (ref. 7) for a modified double-wedge airfoil having a thickness-chord ratio of 0.0423.  Although the surface pressure distributions from the two investigations are very similar except for minor differences attributable to the differences in thickness distribution, the results of the flow surveys are markedly different.  Figure 10 shows that at least up to $6^\circ$ angle of attack, the extent and thickness of the bubbles encountered in the current investigation are considerably larger than those measured on the double-wedge airfoil in reference 7.  The differences between the results of the two investigations are in the proper direction to be explained by the effects of the exceedingly turbulent flow for which corrections were not applied to the data of reference 7.  The magnitude of the differences, however, are too great to be explained by the turbulence effects.  Based on estimates from pressure distributions, the extent of the bubbles for the two investigations should agree very well (fig. 10). The large discrepancies are, therefore, somewhat puzzling and cannot be explained.  It does not seem likely that the possible occurrence of spanwise flow and the differences in thickness distribution are the major factors leading to the disagreement.

The flow into and out of the bubbles shown in figure 9 gives some evidence of the spanwise flow observed during the preliminary tests. From continuity considerations the volume inflow should be equal to the volume outflow for conditions of two-dimensional flow.  Any differences between the two volumes must be manifested as flow in the spanwise direction.  The accompanying table, evaluated from figure 9 by mechanical integration, indicates that for all angles of attack investigated the inflow exceeded the outflow.

| $\alpha$, deg | $\dfrac{a_{inflow}}{cU_\infty}$ | $\dfrac{a_{outflow}}{cU_\infty}$ | $\dfrac{a_{(inflow-outflow)}}{cU_\infty}$ |
|---|---|---|---|
| 2 | 0.006 | 0.005 | 0.001 |
| 4 | .040 | .016 | .024 |
| 6 | .091 | .036 | .055 |

[a] per unit span

The accuracy of the measurements involved, however, is poor. The numerical results should be interpreted only as an indication of an increasing tendency for spanwise flow with increasing angle of attack.

Velocity Fluctuation Measurements

Results of hot-wire anemometer measurements of the velocity fluctuations are presented in figure 11 and in table III. The extremely high levels of turbulence in the flow are readily apparent. In an absolute sense (fig. 11), the largest fluctuations measured were (root-mean-square values) approximately 30 percent of the free-stream velocity. In a relative sense (table III), the largest fluctuations measured were approximately 65 percent of the local mean velocity. As discussed in Appendix B, measurements of such high levels of turbulence should be considered qualitative due to the nonlinear voltage-velocity characteristics of a hot wire. It is of interest that these fluctuations are of considerably greater magnitude than those measured by Schubauer and Klebanoff (ref. 9) in a turbulent boundary layer approaching separation. It is not surprising, perhaps, that the fluctuations presented herein are of similar magnitude to those reported by Corrisin and Uberoi (ref. 10) for a turbulent jet.[1]

Figure 12, which is presented to summarize graphically some of the salient features of the pitot-static and hot-wire results, illustrates that between the leading edge and the position of reattachment the largest (absolute) velocity fluctuations occur along a band in the detached flow approximately midway between the bubble and the outer edge of the detached flow. The detached flow is, therefore, a region of intense turbulent

---

[1] A paper by M. Arie and H. Rouse ("Experiments on Two-Dimensional Flow Over a Normal Wall", Jour. of Fluid Mech., vol. 1, pt. 2, July 1956, pp. 129-141) became available while the present report was being prepared for publication. Measurements are presented of velocity, pressure, and velocity fluctuations behind flat plates normal to the air stream with splitter plates in the wake to prevent vortex streets. Arie and Rouse show that the flow separates from the edges of the plates and subsequently reattaches to the splitter plates; the characteristics of the entire region of separated flow are remarkably similar to those of the present investigation, particularly the magnitude of the reverse flow in what corresponds to the bubble and also the magnitude and distribution of the velocity fluctuations.

mixing and, not unlike a jet, it expands rapidly downstream from its
origin at the leading edge of the plate. Although it is not evident in
figure 12 (see, rather, fig. 11), the intensity of the turbulent motion
along the band gradually decreases as the flow passes downstream of the
position of reattachment. The band of maximum intensity tends, moreover,
to move inward toward the surface over the downstream portion of the
bubbles. For $2^o$ angle of attack the band becomes adjacent to the surface
(i.e., just above the laminar sublayer) between the chordwise stations
of 0.45 and 0.80; the intensity and distribution of the fluctuations are
similar to those measured by Klebanoff and Diehl (ref. 11) for a turbulent
boundary layer on a flat plate. This is not surprising since the pressure
gradient is almost zero downstream of the 0.10-chord station. The data
for $4^o$ (and to a lesser extent, for $6^o$) angle of attack show the same
trends downstream of the bubble as for $2^o$. However, the extent of flow
through the region of approximately zero pressure gradient is too short
to allow as complete a readjustment.

<div align="center">Observations and Measurements of the Flow in the Immediate<br>Vicinity of the Leading Edge</div>

As mentioned previously, there was intense turbulent mixing in the
detached flow in the immediate vicinity of the leading edge of the plate.
This is demonstrated by the data in figure 13 which show that at the
0-percent-chord station the largest root-mean-square values measured for
the velocity fluctuations were 15 to 25 percent of the free-stream
velocity. Moreover, observations of the output from the hot wire on
cathode-ray oscilloscope verified that the velocity fluctuations were of
the completely random type characteristic of turbulent flow. Measurements
were also obtained at several additional stations upstream of the leading
edge in an effort to pinpoint the onset of transition. This permitted
surveying at negative values of $y$; that is, surveys could be made in the
region of the separated flow which passes around the leading edge from
the position of stagnation on the lower surface. Results of some of
these measurements also are presented in figure 13. No indication of
turbulent flow is shown nor was any detected visually on an oscilloscope.
For negative values of $x/c$, the decrease in the local velocity as $y$
increases negatively is not associated with a loss in total pressure.
It is, rather, attributable to a decrease in the velocity of the potential
flow which would occur as the position of stagnation is approached.

Although it is not impossible that these results are peculiar to
the flow around a sharp leading edge, the results strongly suggest that
the extent of separated laminar flow along a thin-airfoil bubble is
virtually zero. It is of interest to note that this differs considerably
from the laminar-separation bubbles discussed in references 3 to 5.
Reference 3 reports that approximately 80 percent of the extent of a
laminar-separation bubble is covered by separated laminar flow. Since,
however, there is also a large difference in the actual physical dimen-
sions of the two types of bubbles, it is, perhaps, more correct to express

the difference on the basis of a Reynolds number

$$R_L = \frac{U_{sep}L}{\nu}$$

where $U_{sep}$ is the velocity of the outer potential flow at the position of separation and $L$ is the extent of separated laminar flow. A maximum value of $R_L$ for the thin-airfoil bubbles reported herein is estimated to be 5000; whereas a corresponding value for a laminar-separation bubble (ref. 3) would be at least ten times as great or of the order of 50,000. The physical significance, if any, of this difference between the two types of separated flow is not readily apparent.

## SUMMARY OF RESULTS

The principal results from pitot-static and hot-wire anemometer surveys of the low-speed flow over a simulated flat plate at small angles of attack are as follows:

1. In the regions or bubbles of reverse flow which are characteristic of the flow associated with the so-called thin-airfoil stall, resultant mean velocities of about 30 percent of the free-stream velocity and velocity fluctuations up to 65 percent of the local velocities were measured.

2. The reverse flow in the bubbles appears to be part of a more general vortex-type flow.

3. The magnitude of the turbulent velocity fluctuations in the regions of separated flow above the bubbles is comparable to that which has been observed for a turbulent jet. The largest velocity fluctuations measured amounted to 30 percent of the free-stream velocity.

4. No separated laminar flow was detected at the forward edge of the bubbles.

Ames Aeronautical Laboratory
     National Advisory Committee for Aeronautics
          Moffett Field, Calif., Nov. 23, 1956

# APPENDIX A

## CORRECTIONS APPLIED TO THE PITOT-STATIC MEASUREMENTS

## FOR THE EFFECTS OF TURBULENT FLOW

The relationships used as a basis for correcting the pitot-static measurements for the effects of turbulent flow are due to Goldstein (ref. 12) and Fage (ref. 13). Goldstein and Fage indicate that a static-pressure probe, aligned with a turbulent stream having a resultant mean velocity $\bar{u}$, measures a static pressure $\bar{p}_m$ such that

$$\bar{p}_m = \bar{p} + \frac{1}{2}\rho k_1(\overline{\Delta v^2} + \overline{\Delta w^2}) \tag{A1}$$

where $k_1$ is a constant which depends to some extent on the geometry of the probe. Goldstein also demonstrates that under similar flow conditions a total-pressure probe measures a pressure $(\bar{p}_t)_m$ where

$$(\bar{p}_t)_m = \bar{p}_t + \frac{1}{2}\rho(\overline{\Delta u^2} + \overline{\Delta v^2} + \overline{\Delta w^2}) \tag{A2}$$

or, since $\bar{p}_t - \bar{p} = \frac{1}{2}\rho\bar{u}^2$

$$(\bar{p}_t)_m = \bar{p} + \frac{1}{2}\rho\bar{u}^2 + \frac{1}{2}\rho(\overline{\Delta u^2} + \overline{\Delta v^2} + \overline{\Delta w^2}) \tag{A3}$$

If equations (A1) and (A3) are combined and a reference dynamic pressure $\frac{1}{2}\rho U_\infty^2$ is introduced, there results

$$\left(\frac{\bar{u}_m}{U_\infty}\right)^2 = \left(\frac{\bar{u}}{U_\infty}\right)^2 + \left(\frac{\overline{\Delta u}}{U_\infty}\right)^2 + (1 - k_1)\left[\left(\frac{\overline{\Delta v}}{U_\infty}\right)^2 + \left(\frac{\overline{\Delta w}}{U_\infty}\right)^2\right] \tag{A4}$$

Similarly, the relationship between the measured and the true static- and total-pressure coefficients becomes

$$\left(C_p\right)_m = C_p - k_1\left[\left(\frac{\overline{\Delta v}}{U_\infty}\right)^2 + \left(\frac{\overline{\Delta w}}{U_\infty}\right)^2\right] \tag{A5}$$

$$\left(C_{p_t}\right)_m = C_{p_t} + \left[\left(\frac{\overline{\Delta u}}{U_\infty}\right)^2 + \left(\frac{\overline{\Delta v}}{U_\infty}\right)^2 + \left(\frac{\overline{\Delta w}}{U_\infty}\right)^2\right] \tag{A6}$$

Unfortunately these simple expressions could not be applied directly to the present results for several reasons: (1) Only one component of the turbulent velocity fluctuations was measured, $\overline{\Delta u}$; (2) the probes were

seldom aligned with the resultant flow during the course of the pitot-static surveys; and (3) equations (A1) and (A2) provide no information on any differential effects which the velocity fluctuations might have on the two $45^\circ$ beveled tubes employed to ascertain the direction $\gamma$ of the resultant flow. The latter is significant because an erroneous indication of $\gamma$ for values between $10^\circ$ and $45^\circ$ would have caused errors in the corrections which were required for the measured static and total pressures as a function of $\gamma$ (see fig. 5).

In order to circumvent the difficulty stemming from the measurement of only one component of the velocity fluctuations, it was assumed that

$$k_2(\overline{\Delta u^2}) = (\overline{\Delta u^2} + \overline{\Delta v^2} + \overline{\Delta w^2})$$

so that

$$(k_2 - 1)(\overline{\Delta u^2}) = (\overline{\Delta v^2} + \overline{\Delta w^2}) \tag{A7}$$

An analysis of the results of Schubauer and Klebanoff (ref. 9) revealed that a value for $k_2$ for turbulent boundary-layer flow would vary from 1.5 near the wall to 2.1 near the outer edge of the boundary layer. Moreover, this variation was virtually independent of the shape of the mean-velocity profiles. The results of Laufer (ref. 14) and Ruetenik (ref. 15) for turbulent flow in a two-dimensional channel indicate a similar variation for $k_2$ from the wall to the center of the channel. Although the general applicability of these results to the problem at hand is admittedly open to some question, in the absence of any better criterion, an average value of 1.8 was selected for $k_2$ to provide a means for correcting the present pitot-static measurements.

If the value of $k_1$ is taken to be 0.5 on the basis of Fage's empirical results (ref. 13) for a static-pressure probe similar to those employed during this investigation, equations (A4), (A5), and (A6) become

$$\left(\frac{\bar{u}_m}{U_\infty}\right)^2 = \left(\frac{\bar{u}}{U_\infty}\right)^2 + \left(\frac{\overline{\Delta u}}{U_\infty}\right)^2\left[1 + (1 - k_1)(k_2 - 1)\right] = \left(\frac{\bar{u}}{U_\infty}\right)^2 + 1.4\left(\frac{\overline{\Delta u}}{U_\infty}\right)^2$$

$$\frac{\bar{u}_m}{U_\infty} = \frac{\bar{u}}{U_\infty} + \Delta\left(\frac{\bar{u}}{U_\infty}\right) \tag{A8}$$

$$\left(C_p\right)_m = C_p - k_1(k_2 - 1)\left(\frac{\overline{\Delta u}}{U_\infty}\right)^2 = C_p - 0.4\left(\frac{\overline{\Delta u}}{U_\infty}\right)^2$$

$$\left(C_p\right)_m = C_p - \Delta C_p \tag{A9}$$

$$\left(c_{p_t}\right)_m = c_{p_t} + k_2\left(\frac{\overline{\Delta u}}{U_\infty}\right)^2 = c_{p_t} + 1.8\left(\frac{\overline{\Delta u}}{U_\infty}\right)^2$$

$$\left(c_{p_t}\right)_m = c_{p_t} + \Delta c_{p_t} \tag{A10}$$

The numerical value for $k_1$ determined by Fage was derived from measurements of turbulent flow in a pipe. Its general applicability is unknown but the use of a value of 0.5 is not inconsistent with the over-all accuracy which should be expected from the corrections, considering the assumptions introduced by the use of the constant $k_2$. The incremental corrections $\Delta(\overline{u}/U_\infty)$, $\Delta c_p$, and $\Delta c_{p_t}$ defined by equations (A8) to (A10) are shown graphically in figure 14.

The corrections for turbulence described in the preceding paragraphs are appropriate only when the longitudinal axis of the probe is aligned with the resultant flow (i.e., $\gamma = 0$), a condition which, as mentioned previously, was seldom encountered during the course of the present surveys. It is apparent, for example, that when the local flow is oblique to the longitudinal axis of the probe, the $\Delta u$ component of the velocity fluctuations can contribute to the measured static pressure. At the same time, particularly for large values of $\gamma$, one would expect that the response of the total-pressure probe to the velocity fluctuations would differ from that given by equation (A3). In order, therefore, to determine the influence of $\gamma$ on the preceding relationships for $\overline{u}_m/U_\infty$, $(c_p)_m$, and $(c_{p_t})_m$, and at the same time assess any differential effects of the turbulent flow on the pressure difference measured between the two 45° beveled pressure tubes, a calibration of the conventional pitot-static probe (fig. 4) was conducted in the small wind tunnel for measured turbulence levels $\sqrt{\overline{\Delta u^2}}/\overline{u}$ of approximately 0.25 and 0.43. The calibrations covered a range of $\gamma$ from 0 to 45° and the results were assumed applicable for negative values of $\gamma$. The results were also applied to the reverse-flow probe shown in figure 4.

For these measurements the influence of $\gamma$ was considered in the following manner:

$$(\overline{p}_t - \overline{p})_m = (\overline{p}_t - \overline{p}) + f(\gamma)\left(\frac{1}{2}\rho\overline{\Delta u}^2\right) \tag{A11}$$

$$(\overline{p}_1 - \overline{p}_2)_m = (\overline{p}_1 - \overline{p}_2) + g(\gamma)\left(\frac{1}{2}\rho\overline{\Delta u}^2\right) \tag{A12}$$

where

$(\overline{p}_t - \overline{p})$    dynamic pressure at the probe

$(\overline{p}_1 - \overline{p}_2)$    the pressure difference between the two 45° beveled tubes

$\left.\begin{array}{l}f(\gamma)\\g(\gamma)\end{array}\right\}$    unknown functions of $\gamma$ to be determined experimentally

The functions $f(\gamma)$ and $g(\gamma)$ derived from the measurements are shown in figure 15. The results are surprisingly good considering that they were evaluated from small differences between relatively large numerical values. The results for $g(\gamma)$ indicate that there is a considerable differential effect of the velocity fluctuations on the two $45^{\circ}$ beveled tubes. The effect, as might be expected, increases rapidly as $\gamma$ increases. The quantity $f(\gamma)$ decreases slowly from a value somewhere between 1.6 and 1.2, when $\gamma = 0$, to a value of approximately 1.0 when $\gamma = 30^{\circ}$; thereafter $f(\gamma)$ decreases rapidly. Note that a value between 1.2 and 1.6 is consistent with equation (A8) for which $f(\gamma)$ should be identical with $1 + (k_2 - 1)(1 - k_1) = 1.4$. The effects of turbulence on the directional characteristics of the probes also are illustrated in figure 15. It is readily apparent that under certain conditions the effects of velocity fluctuations are large.

On the basis of the preceding discussion and experimental results, the procedure employed herein to correct the pitot-static measurements for the effects of turbulence is summarized as follows:

(1) The value of $\gamma$ was determined from charts similar to that shown in figure 15.

(2) With the value of $\gamma$ from (1) above, the measured values of total and static pressure were corrected using charts similar to those shown in figure 5.

(3) The quantities $(C_p)_m$, $(C_{p_t})_m$, and $\bar{u}_m/U_\infty$ were computed and then corrected for the effects of turbulence using charts similar to figure 14.

As suggested by $f(\gamma)$ in figure 15, the corrections applied in step (3) above should have been, strictly speaking, considered a function of $\gamma$. Although this was possible in the case of $\bar{u}_m$ which depends only on $f(\gamma)$, such a procedure was not possible for $(C_p)_m$ and $(C_{p_t})_m$ since $k_1$ and $k_2$ were not evaluated as separate functions of $\gamma$. It will be noted, however, that with only a few exceptions, most of the pitot-static measurements correspond to values of $-20^{\circ} < \gamma < 20^{\circ}$ (when $\gamma = 0$, $\theta = 0$ or $\pm 180^{\circ}$). Figure 15 demonstrates that over this range of $\gamma$, $f(\gamma)$ appears to be essentially constant; this result carries the implication that $k_1$ and $k_2$ probably vary only a small amount[1] out to $\gamma = 20^{\circ}$. Thus, for the present pitot-static measurements the dependence of the corrections for turbulence on $\gamma$ was, effectively, a second-order effect and was ignored.

---

[1]It seems probable that an increase in $\gamma$ would cause $k_1$ to increase and $k_2$ to decrease but would only cause a small change in $f(\gamma)$ if $f(\gamma) \equiv 1 + (k_2 - 1)(1 - k_1)$ as in equation (A8).

APPENDIX B


CORRECTIONS APPLIED TO THE HOT-WIRE ANEMOMETER MEASUREMENTS

FOR THE EFFECT OF LARGE VELOCITY FLUCTUATIONS


The basis for correcting the hot-wire measurements may be illustrated
by the accompanying sketch.  The sketch presents the typical relationship
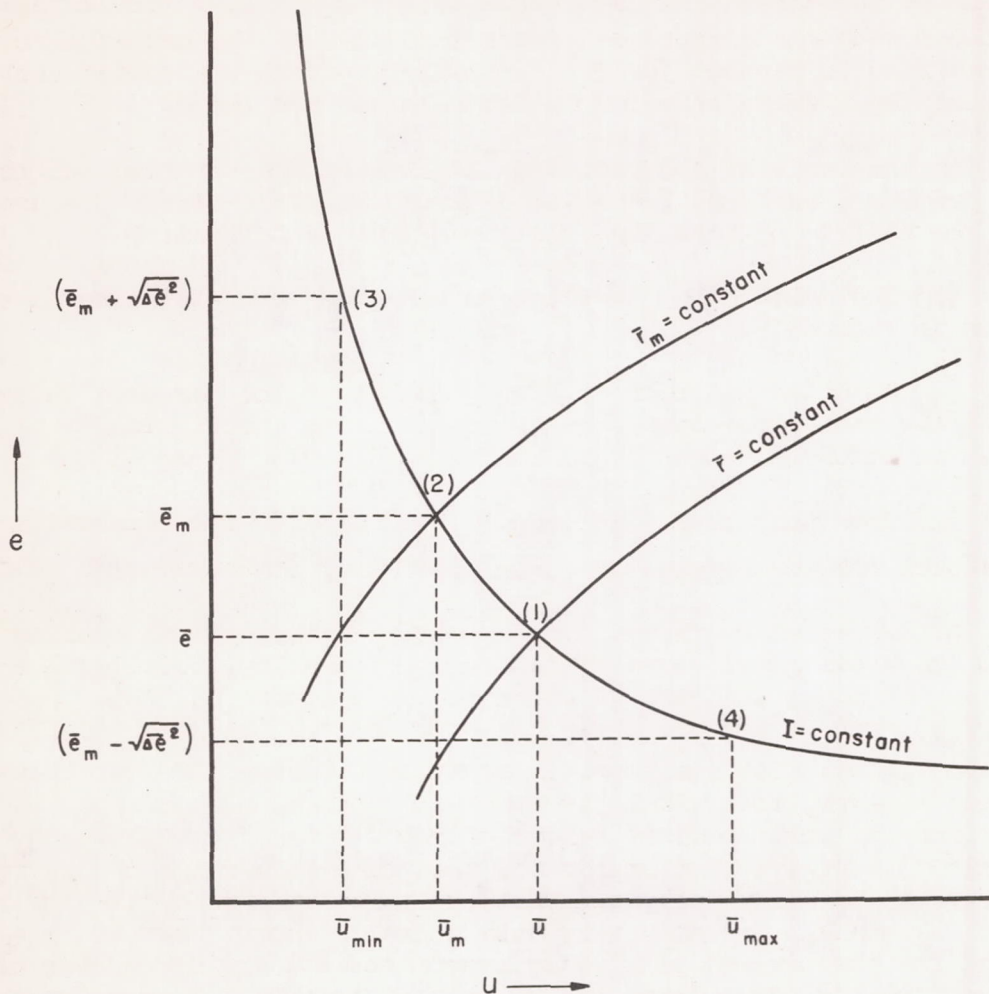


which exists between the heating current  I  supplied to the wire, the
resistance  r  of the wire, the voltage drop  e  across the wire, and the
velocity component  u  normal to the axis of the wire.[1]  Point (1)

_____

[1]The sketch is strictly applicable only to steady or quasi-steady
flow conditions.  It is assumed, however, for present purposes, that it
is applicable also to conditions with unsteady (turbulent) flow.

represents conditions in a hypothetical flow having zero turbulence. The current is of an arbitrary magnitude $I$ to maintain the wire resistance at a desired value $\bar{r}$. The corresponding values for the velocity and voltage are, respectively, $\bar{u}$ and $\bar{e}$. If turbulence is introduced into this hypothetical flow in such a manner that the mean velocity is unchanged from the value $\bar{u}$, the nonlinear voltage-velocity characteristics of the wire for constant current operation lead to a mean voltage $\bar{e}_m$ which is greater than the original voltage $\bar{e}$. As a result the mean resistance is $\bar{r}_m$ (greater than $\bar{r}$) and the indicated mean velocity $\bar{u}_m$ in the turbulent flow is less than the true mean velocity $\bar{u}$. Moreover, since it is assumed in hot-wire anemometry that $\Delta u$ is proportional to $\Delta e$, it is apparent that the nonlinearity can cause an erroneous determination of the velocity fluctuations. The difference between the measured and the true mean quantities, of course, increases with increasing magnitude of the velocity fluctuations.

With reference to the preceding sketch the corrections applied to the hot-wire measurements were accomplished in the following manner: point (2) represents the resistance $\bar{r}_m$ set during the tests by applying an arbitrary current $I$. The voltage drop across the wire is $\bar{e}_m$ and the indicated mean velocity is $\bar{u}_m$. Using the mean-square voltage-fluctuation signal from the wire $\Delta\bar{e}^2$, uncompensated for the thermal lag,[2] the quantities $\left(\bar{e}_m + \sqrt{\overline{\Delta e^2}}\right)$ and $\left(\bar{e}_m - \sqrt{\overline{\Delta e^2}}\right)$ were employed to ascertain the hypothetical velocities $\bar{u}_{min}$ and $\bar{u}_{max}$ (points (3) and (4), respectively). A simple average value of these two velocities $\bar{u}_{av}$ was taken to be the true mean velocity and is presented herein as $\bar{u}$. The quantity $\left(\sqrt{\overline{\Delta u^2}}/\bar{u}\right)_m$ was computed using the compensated voltage signals from the wire and the measured mean properties at point (2). No corrections were applied, however, to the absolute values of $\left(\sqrt{\overline{\Delta u^2}}\right)_m$ for the nonlinear voltage-velocity relationship; $\sqrt{\overline{\Delta u^2}}$, as presented herein, is identical to $\left(\sqrt{\overline{\Delta u^2}}\right)_m$.

This procedure, as mentioned previously, is intended to furnish no more than approximate corrections to mean-flow measurements. The agreement obtained between the pitot-static- and hot-wire-survey results is, perhaps, ample evidence that the method successfully fulfills its purpose. However, in order to provide some further indication of the validity of the method, results of calculations are presented in the table of the idealized response of a hot wire (typical to those employed during this investigation) to large sinusoidal velocity fluctuations. The numerical values in columns (2) to (6) are slightly dependent on the magnitude of $\bar{u}$ used in the computations ($\bar{u} = 100$ ft sec ), but the effect is too small to be considered in an analysis of this type.

---

[2]Only the uncompensated signal is a true measure of the actual voltage fluctuations which occur across the wire.

| Calculated (idealized) response of a hot-wire anemometer to large sinsusoidal velocity fluctuations | | | | | |
|---|---|---|---|---|---|
| (1) | (2) | (3) | (4) | (5) | (6) |
| $\dfrac{\sqrt{\overline{\Delta u^2}}}{\bar{u}}$ | $\dfrac{\bar{u}_m}{\bar{u}}$ | $\dfrac{\bar{u}_{av}}{\bar{u}}$ | $\dfrac{(\sqrt{\overline{\Delta u^2}})_m}{\bar{u}_m}$ | $\dfrac{(\sqrt{\overline{\Delta u^2}})_m}{\bar{u}_{av}}$ | $\dfrac{(\sqrt{\overline{\Delta u^2}})_m}{\bar{u}}$ |
| 0.10 | 0.99 | 1.00 | 0.12 | 0.12 | 0.12 |
| .20 | .97 | 1.00 | .24 | .23 | .23 |
| .30 | .93 | 1.00 | .38 | .35 | .35 |
| .40 | .86 | 1.02 | .54 | .46 | .45 |
| .50 | .78 | 1.06 | .74 | .55 | .58 |
| .60 | .65 | 1.19 | 1.03 | .57 | .67 |

Two significant results are apparent from the tabulation.  The first and most important item to be noted is that the method of correcting the mean-flow measurements herein appears to be satisfactory (cf., columns (2) and (3) - for complete correction column (3) should, of course, be unity); and the second is that, as expected, the values of turbulence presented herein are probably too large (cf., columns (1) and (4) to (6)).  Further discussion is not warranted in view of the many ramifications involved. It is sufficient to conclude that the calculated results for the mean velocity are not inconsistent with the agreement shown by the experimental results.

REFERENCES

1.  McCullough, George B., and Gault, Donald E.:  Examples of Three
        Representative Types of Airfoil-Section Stall at Low Speed.  NACA
        TN 2502, 1951.

2.  Küchemann, D.:  Types of Flow on Swept Wings with Special Reference
        to Free Boundaries and Vortex Sheets.  Jour. Roy. Aero. Soc. of
        London, vol. 57, no. 684, Nov. 1953, pp. 683-699.

3.  Gault, Donald E.:  An Experimental Investigation of Regions of
        Separated Laminar Flow.  NACA TN 3505, 1955.

4.  Burnsall, William J., and Loftin, Laurence K., Jr.:  Experimental
        Investigation of Localized Regions of Laminar-Boundary-Layer
        Separation.  NACA TN 2338, 1951.

5.  Maekawa, T., and Atsumi, S.:  Transition Caused by the Laminar Flow
        Separation.  NACA TM 1352, 1952.

6.  McCullough, George B., and Gault, Donald E.:  Boundary-Layer and
        Stalling Characteristics of the NACA 64A006 Airfoil Section.
        NACA TN 1923, 1949.

7.  Rose, Leonard M., and Altman, John M.:  Low-Speed Investigation of
        the Stalling of a Thin, Faired, Double-Wedge Airfoil with Nose
        Flap.  NACA TN 2172, 1950.

8.  Kovasznay, Laszlo:  Calibration and Measurements in Turbulence
        Research by the Hot-Wire Method.  NACA TM 1130, 1947.

9.  Schubauer, G. B., and Klebanoff, P. S.:  Investigation of Separation
        of the Turbulent Boundary Layer.  NACA Rep. 1030, 1951.

10. Corrsin, Stanley, and Uberoi, Mahinder S.:  Further Experiments on
        the Flow and Heat Transfer in a Heated Turbulent Air Jet.  NACA
        Rep. 998, 1950.

11. Klebanoff, P. S., and Diehl, Z. W.:  Some Features of Artificially
        Thickened Fully Developed Turbulent Boundary Layers with Zero
        Pressure Gradient.  NACA TN 2475, 1951.

12. Goldstein, S.:  A Note on the Measurement of Total Head and Static
        Pressure in a Turbulent Stream.  Proc. Roy. Soc. of London, Series
        A, vol. 155, July 1, 1936, pp. 570-575.

13. Fage, A.:  On the Static Pressure in Fully-Developed Turbulent Flow.
        Proc. Roy. Soc. of London, Series A, vol. 155, July 1, 1936,
        pp. 576-596.

14.  Laufer, John:  Investigation of Turbulent Flow in a Two-Dimensional
        Channel.  NACA Rep. 1053, 1951.

15.  Ruetenik, J. R.:  The Investigation of Equilibrium Flow in a
        Slightly Divergent Channel.  The Johns Hopkins University, Dept.
        of Mech. Engineering.  Rep. I-19, Aug. 1954.

# TABLE I.- STATIC-PRESSURE DISTRIBUTIONS

| $\alpha$ \ $x/c$ | 0° | 1° | 2° | 3° | 4° | 5° | 6° | 7° | 8° | -1° | -2° | -3° | -4° | -5° | -6° | -7° | -8° |
|---|---|---|---|---|---|---|---|---|---|---|---|---|---|---|---|---|---|
| 0 | 0.974 | 0.800 | 0.073 | -0.586 | -1.018 | -.943 | -0.942 | -0.943 | -0.955 | 0.843 | 0.143 | -0.890 | -1.359 | -1.300 | -1.238 | -1.203 | -1.139 |
| .005 | .216 | -.542 | -.899 | -.916 | -.886 | -.906 | -.930 | -.943 | -.955 | .854 | .657 | .802 | .885 | .943 | .973 | 1.000 | .993 |
| .010 | .152 | -.503 | -.918 | -.928 | -.889 | -.906 | -.936 | -.943 | -.955 | .348 | .536 | .682 | .771 | .840 | .885 | .920 | .928 |
| .020 | .114 | -.079 | -.930 | -.941 | -.898 | -.918 | -.942 | -.943 | -.955 | .248 | .404 | .536 | .632 | .705 | .758 | .801 | .806 |
| .030 | .087 | -.067 | -.881 | -.954 | -.905 | -.918 | -.949 | -.949 | -.961 | .204 | .353 | .466 | .556 | .632 | .682 | .728 | .742 |
| .040 | .075 | -.067 | -.712 | -.973 | -.917 | -.930 | -.955 | -.949 | -.967 | .186 | .314 | .416 | .505 | .578 | .632 | .675 | .678 |
| .050 | .052 | -.060 | -.470 | -.979 | -.929 | -.943 | -.955 | -.955 | -.967 | .166 | .283 | .390 | .473 | .538 | .593 | .636 | .640 |
| .075 | .049 | -.041 | -.152 | -.891 | -.942 | -.956 | -.968 | -.968 | -.973 | .141 | .238 | .334 | .404 | .468 | .517 | .554 | .563 |
| .100 | .049 | -.034 | -.109 | -.649 | -.942 | -.968 | -.980 | -.980 | -.980 | .123 | .213 | .302 | .365 | .425 | .466 | .503 | .511 |
| .125 | .029 | -.034 | -.102 | -.396 | -.905 | -.992 | -1.004 | -.992 | -1.004 | .110 | .188 | .264 | .328 | .386 | .429 | .457 | .459 |
| .150 | .029 | -.034 | -.102 | -.218 | -.817 | -.980 | -1.018 | -1.004 | -1.004 | .103 | .175 | .238 | .302 | .355 | .396 | .425 | .421 |
| .175 | .049 | -.015 | -.083 | -.155 | -.654 | -.956 | -1.018 | -1.004 | -1.004 | .103 | .162 | .232 | .289 | .340 | .378 | .397 | .395 |
| .200 | .023 | -.028 | -.083 | -.142 | -.516 | -.918 | -1.030 | -1.024 | -1.030 | .097 | .150 | .213 | .264 | .317 | .353 | .333 | .332 |
| .250 | .037 | -.021 | -.071 | -.104 | -.291 | -.770 | -.992 | -1.024 | -1.030 | .085 | .137 | .188 | .238 | .283 | .314 | .296 | .293 |
| .300 | .037 | -.015 | -.071 | -.091 | -.153 | -.584 | -.930 | -1.024 | -1.042 | .072 | .118 | .162 | .213 | .250 | .277 | .274 | .267 |
| .350 | .037 | -.002 | -.059 | -.079 | -.116 | -.411 | -.818 | -.992 | -1.042 | .072 | .112 | .156 | .201 | .237 | .264 | .250 | .241 |
| .400 | .037 | -.002 | -.047 | -.079 | -.090 | -.287 | -.681 | -.930 | -1.004 | .066 | .105 | .150 | .175 | .216 | .238 | .223 | .216 |
| .450 | .037 | -.002 | -.047 | -.066 | -.090 | -.201 | -.544 | -.855 | -.967 | .060 | .090 | .137 | .162 | .195 | .213 | .205 | .177 |
| .500 | .037 | -.002 | -.041 | -.066 | -.078 | -.151 | -.420 | -.756 | -.917 | .060 | .086 | .125 | .150 | .180 | .201 | .181 | .164 |
| .550 | .017 | -.015 | -.041 | -.066 | -.083 | -.139 | -.333 | -.656 | -.842 | .054 | .080 | .105 | .137 | .160 | .175 | .172 | .139 |
| .600 | .017 | -.009 | -.041 | -.066 | -.083 | -.127 | -.283 | -.557 | -.767 | .054 | .080 | .099 | .125 | .149 | .162 | .154 | .120 |
| .650 | .037 | .004 | -.021 | -.054 | -.071 | -.108 | -.208 | -.444 | -.679 | .054 | .074 | .099 | .112 | .124 | .137 | .131 | .120 |
| .700 | .037 | .004 | -.021 | -.041 | -.059 | -.101 | -.170 | -.370 | -.566 | .048 | .061 | .086 | .105 | .113 | .131 | .126 | .100 |
| .750 | .037 | .004 | -.015 | -.041 | -.053 | -.095 | -.146 | -.295 | -.491 | .054 | .061 | .086 | .099 | .113 | .112 | .108 | .075 |
| .800 | .037 | .010 | .003 | -.028 | -.033 | -.077 | -.121 | -.233 | -.416 | .060 | .061 | .061 | .074 | .080 | .074 | .062 | .010 |
| .850 | .023 | .010 | -.009 | -.028 | -.033 | -.077 | -.115 | -.208 | -.353 | .048 | .049 | .049 | .061 | .065 | .061 | .035 | -.028 |
| .900 | .023 | .010 | .003 | -.015 | -.033 | -.065 | -.096 | -.170 | -.291 | .042 | .042 | .036 | .049 | .042 | .023 | -.011 | -.079 |
| .950 | .023 | .010 | .003 | -.002 | -.009 | -.053 | -.071 | -.134 | -.228 | .035 | .036 | .036 | .049 | .042 | .023 | -.011 | -.079 |

## TABLE II.- RESULTS FROM PITOT-STATIC SURVEYS

**$x/c = 0;\ \alpha = 2°$**

| $y/c$ | $\theta$, deg | $\bar{u}/U_\infty$ | $c_p$ | $c_{p_t}$ |
|---|---|---|---|---|
| 0.0002 | 40.2 | 1.145 | 0.348 | 0.035 |
| .0003 | 39.3 | 1.163 | .349 | -.003 |
| .0005 | 37.3 | 1.204 | .368 | -.082 |
| .0007 | 34.2 | 1.233 | .526 | -.078 |
| .0010 | 33.5 | 1.229 | .529 | .007 |
| .0013 | 35.5 | 1.222 | .455 | -.084 |
| .0020 | 33.2 | 1.206 | .452 | -.018 |

**$x/c = 0;\ \alpha = 4°$**

| $y/c$ | $\theta$, deg | $\bar{u}/U_\infty$ | $c_p$ | $c_{p_t}$ |
|---|---|---|---|---|
| .0002 | 30.0 | .922 | .880 | 1.030 |
| .0006 | 38.7 | .894 | .633 | .618 |
| .0009 | 37.9 | 1.161 | .613 | .264 |
| .0013 | 37.8 | 1.181 | .619 | .224 |
| .0019 | 37.8 | 1.195 | .600 | .170 |
| .0023 | 39.6 | 1.207 | .565 | .107 |
| .0026 | 41.6 | 1.219 | .508 | .018 |
| .0029 | 42.7 | 1.198 | .431 | -.007 |

**$x/c = 0;\ \alpha = 6°$**

| $y/c$ | $\theta$, deg | $\bar{u}/U_\infty$ | $c_p$ | $c_{p_t}$ |
|---|---|---|---|---|
| .0002 | 23.7 | .329 | 1.043 | 1.935 |
| .0006 | 10.0 | .518 | 1.064 | 1.797 |
| .0008 | 20.9 | .775 | 1.055 | 1.455 |
| .0009 | 29.3 | .965 | .998 | 1.068 |
| .0011 | 38.5 | 1.112 | .762 | .526 |
| .0013 | 39.5 | 1.139 | .754 | .460 |
| .0021 | 37.2 | 1.138 | .847 | .552 |
| .0038 | 39.6 | 1.148 | .760 | .441 |
| .0038 | 39.5 | 1.148 | .769 | .449 |
| .0046 | 46.4 | 1.187 | .598 | .188 |

**$x/c = 0.010;\ \alpha = 2°$**

| $y/c$ | $\theta$, deg | $\bar{u}/U_\infty$ | $c_p$ | $c_{p_t}$ |
|---|---|---|---|---|
| .0050 | 10.8 | .948 | .875 | .978 |
| .0053 | 12.6 | 1.112 | .843 | .603 |
| .0057 | 13.0 | 1.221 | .799 | .298 |
| .0060 | 13.5 | 1.288 | .780 | .117 |
| .0063 | 14.2 | 1.308 | .763 | .048 |
| .0067 | 14.3 | 1.307 | .750 | .035 |
| .0073 | 14.5 | 1.298 | .715 | .026 |
| .0090 | 14.3 | 1.283 | .673 | .020 |
| .0107 | 14.0 | 1.248 | .607 | .046 |

**[1]$x/c = 0.010;\ \alpha = 2°$**

| $y/c$ | $\theta$, deg | $\bar{u}/U_\infty$ | $c_p$ | $c_{p_t}$ |
|---|---|---|---|---|
| .0033 | 0 | --- | .876 | 1.992 |
| .0037 | 0 | .180 | .882 | 1.849 |
| .0040 | 0 | .264 | .914 | 1.844 |
| .0043 | 3.5 | .458 | .917 | 1.708 |
| .0047 | 6.5 | .665 | .923 | 1.482 |
| .0048 | 8.3 | .751 | .922 | 1.358 |
| .0050 | 9.2 | .881 | .911 | 1.139 |
| .0052 | 10.5 | .935 | .894 | 1.018 |
| .0053 | 11.4 | 1.043 | .881 | .791 |
| .0055 | 10.0 | 1.110 | .865 | .629 |
| .0055 | 12.0 | 1.120 | .850 | .593 |
| .0057 | 13.0 | 1.165 | .838 | .478 |
| .0058 | 13.5 | 1.229 | .823 | .315 |
| .0060 | 14.3 | 1.272 | .791 | .172 |
| .0063 | 14.6 | 1.311 | .776 | .055 |
| .0067 | 14.7 | 1.311 | .749 | .026 |
| .0073 | 15.4 | 1.300 | .715 | .019 |
| .0080 | 15.4 | 1.290 | .691 | .021 |
| .0087 | 15.3 | 1.288 | .678 | .015 |

**$x/c = 0.010;\ \alpha = 4°$**

| $y/c$ | $\theta$, deg | $\bar{u}/U_\infty$ | $c_p$ | $c_{p_t}$ |
|---|---|---|---|---|
| .0067 | 3.9 | .177 | .946 | 1.914 |
| .0070 | 6.7 | .289 | .949 | 1.864 |
| .0073 | 9.8 | .405 | .967 | 1.806 |
| .0077 | 13.0 | .523 | .988 | 1.715 |
| .0080 | 17.0 | .683 | .995 | 1.528 |
| .0083 | 18.5 | .896 | 1.010 | 1.207 |

**[1]$x/c = 0.010;\ \alpha = 4°$**

| $y/c$ | $\theta$, deg | $\bar{u}/U_\infty$ | $c_p$ | $c_{p_t}$ |
|---|---|---|---|---|
| 0.0067 | 6.8 | 0.283 | 0.921 | 1.840 |
| .0073 | 12.8 | .452 | .957 | 1.752 |
| .0080 | 17.9 | .604 | .938 | 1.572 |
| .0083 | 19.1 | .846 | .915 | 1.200 |
| .0087 | 21.0 | .995 | .874 | .883 |
| .0090 | 21.7 | 1.100 | .850 | .634 |
| .0093 | 21.8 | 1.216 | .846 | .367 |
| .0093 | 21.5 | 1.243 | .895 | .351 |
| .0097 | 22.5 | 1.298 | .863 | .175 |
| .0100 | 23.8 | 1.308 | .787 | -.068 |
| .0107 | 25.8 | 1.297 | .686 | .001 |
| .0113 | 26.5 | 1.276 | .628 | -.005 |
| .0127 | 26.2 | 1.265 | .595 | -.009 |
| .0160 | 26.5 | 1.246 | .514 | -.041 |
| .0193 | 23.8 | 1.240 | .554 | .013 |
| .0227 | 22.8 | 1.244 | .561 | .010 |
| .0260 | 21.8 | 1.246 | .563 | .008 |

**$x/c = 0.010;\ \alpha = 6°$**

| $y/c$ | $\theta$, deg | $\bar{u}/U_\infty$ | $c_p$ | $c_{p_t}$ |
|---|---|---|---|---|
| .0083 | 0 | .176 | .915 | 1.883 |
| .0100 | 11.8 | .433 | 1.016 | 1.827 |
| .0107 | 17.6 | .640 | 1.057 | 1.647 |
| .0110 | 19.5 | .724 | 1.057 | 1.533 |
| .0113 | 21.3 | .985 | 1.316 | 1.343 |
| .0117 | 22.3 | .960 | 1. | 1.119 |
| .0120 | 23.8 | 1.013 | .966 | .914 |
| .0123 | 25.4 | 1.087 | .886 | .700 |
| .0127 | 27.2 | 1.134 | .788 | .500 |
| .0130 | 28.5 | 1.203 | .721 | .271 |
| .0137 | 31.3 | 1.247 | .621 | .067 |
| .0153 | 33.8 | 1.262 | .558 | -.035 |
| .0187 | 33.0 | 1.238 | .512 | -.025 |
| .0220 | 31.5 | 1.218 | .500 | .011 |
| .0253 | 30.3 | 1.213 | .487 | .011 |
| .0287 | 29.5 | 1.205 | .463 | .007 |
| .0303 | 28.5 | 1.198 | .438 | 0 |
| .0353 | 27.5 | 1.195 | .431 | 0 |
| .0420 | 26.0 | 1.195 | .440 | .010 |
| .0487 | 24.5 | 1.203 | .455 | .003 |
| .0562 | 22.8 | 1.218 | .501 | .017 |

**$x/c = 0.025;\ \alpha = 2°$**

| $y/c$ | $\theta$, deg | $\bar{u}/U_\infty$ | $c_p$ | $c_{p_t}$ |
|---|---|---|---|---|
| .0055 | 5.0 | .199 | .969 | 1.927 |
| .0072 | .2 | .609 | .970 | 1.624 |
| .0080 | .1 | 1.035 | .944 | .875 |
| .0088 | 6.4 | 1.101 | .926 | .716 |
| .0097 | 7.0 | 1.247 | .877 | .333 |
| .0105 | 6.9 | 1.314 | .847 | .139 |
| .0122 | 6.9 | 1.329 | .794 | .045 |
| .0138 | 7.0 | 1.313 | .741 | .031 |
| .0155 | 6.3 | 1.295 | .690 | .025 |
| .0172 | 3.1 | 1.275 | .639 | .027 |

**[2]$x/c = 0.025;\ \alpha = 2°$**

| $y/c$ | $\theta$, deg | $\bar{u}/U_\infty$ | $c_p$ | $c_{p_t}$ |
|---|---|---|---|---|
| .0002 | 174.7 | .316 | .898 | 1.797 |
| .0012 | 176.3 | .341 | .912 | 1.794 |
| .0028 | 171.5 | .264 | .930 | 1.860 |
| .0045 | 158.1 | .105 | .938 | 1.928 |

**$x/c = 0.025;\ \alpha = 4°$**

| $y/c$ | $\theta$, deg | $\bar{u}/U_\infty$ | $c_p$ | $c_{p_t}$ |
|---|---|---|---|---|
| .0080 | 4.2 | .140 | .911 | 1.891 |
| .0122 | 9.7 | .273 | .934 | 1.858 |
| .0130 | 12.8 | .401 | .940 | 1.779 |
| .0138 | 13.5 | .612 | .962 | 1.585 |
| .0147 | 15.2 | .790 | .977 | 1.352 |
| .0155 | 15.5 | 1.014 | .971 | .944 |
| .0163 | 16.7 | 1.188 | .955 | .537 |
| .0172 | 17.5 | 1.302 | .950 | .246 |
| .0188 | 18.0 | 1.354 | .912 | .076 |
| .0205 | 18.0 | 1.354 | .886 | .048 |
| .0222 | 17.5 | 1.345 | .863 | .049 |
| .0238 | 17.2 | 1.335 | .824 | .036 |

**[2]$x/c = 0.025;\ \alpha = 4°$**

| $y/c$ | $\theta$, deg | $\bar{u}/U_\infty$ | $c_p$ | $c_{p_t}$ |
|---|---|---|---|---|
| 0.0002 | 159.8 | 0.077 | 0.895 | 1.888 |
| .0012 | 167.5 | .082 | .898 | 1.890 |
| .0028 | 171.9 | .194 | .893 | 1.870 |
| .0045 | 173.0 | .161 | .900 | 1.873 |
| .0062 | 177.2 | .184 | .902 | 1.867 |
| .0078 | 176.8 | .183 | .902 | 1.867 |
| .0095 | 170.0 | .156 | .900 | 1.874 |

**$x/c = 0.025;\ \alpha = 6°$**

| $y/c$ | $\theta$, deg | $\bar{u}/U_\infty$ | $c_p$ | $c_{p_t}$ |
|---|---|---|---|---|
| .0166 | 15.8 | .007 | .990 | 1.989 |
| .0176 | 17.8 | .253 | .976 | 1.912 |
| .0186 | 15.7 | .421 | .983 | 1.805 |
| .0196 | 16.9 | .600 | 1.022 | 1.662 |
| .0206 | 18.0 | .822 | 1.058 | 1.381 |
| .0216 | 19.8 | 1.031 | 1.070 | 1.002 |
| .0226 | 21.6 | 1.219 | 1.045 | .532 |
| .0236 | 23.8 | 1.334 | .984 | .182 |
| .0246 | 24.8 | 1.362 | .954 | .080 |
| .0256 | 25.1 | 1.369 | .923 | .033 |
| .0266 | 25.3 | 1.361 | .891 | .028 |
| .0276 | 25.1 | 1.362 | .889 | .024 |

**[2]$x/c = 0.025;\ \alpha = 6°$**

| $y/c$ | $\theta$, deg | $\bar{u}/U_\infty$ | $c_p$ | $c_{p_t}$ |
|---|---|---|---|---|
| .0045 | 168.6 | .061 | .930 | 1.925 |
| .0078 | 176.8 | .106 | .939 | 1.926 |
| .0112 | 179.3 | .140 | .950 | 1.929 |

**$x/c = 0.050;\ \alpha = 2°$**

| $y/c$ | $\theta$, deg | $\bar{u}/U_\infty$ | $c_p$ | $c_{p_t}$ |
|---|---|---|---|---|
| .0056 | -15.5 | .381 | .738 | 1.602 |
| .0073 | -11.4 | .492 | .769 | 1.530 |
| .0089 | -8.7 | .794 | .756 | 1.188 |
| .0106 | -6.7 | 1.011 | .773 | .755 |
| .0123 | -2.6 | 1.128 | .595 | .324 |
| .0139 | -3.0 | 1.181 | .537 | .137 |
| .0156 | -2.0 | 1.203 | .508 | .070 |
| .0173 | -1.5 | 1.203 | .470 | .033 |
| .0189 | -1.3 | 1.202 | .441 | .018 |

**[1]$x/c = 0.050;\ \alpha = 2°$**

| $y/c$ | $\theta$, deg | $\bar{u}/U_\infty$ | $c_p$ | $c_{p_t}$ |
|---|---|---|---|---|
| .0034 | -28.9 | .174 | .701 | 1.671 |
| .0040 | -25.5 | .144 | .724 | 1.691 |
| .0047 | -20.7 | .270 | .712 | 1.639 |
| .005 | -20.3 | .309 | .743 | 1.647 |
| .0060 | -16.4 | .420 | .746 | 1.562 |
| .0067 | -16.1 | .476 | .741 | 1.519 |
| .0074 | -12.4 | .556 | .737 | 1.427 |
| .0080 | -11.5 | .603 | .744 | 1.381 |
| .0087 | -9.0 | .729 | .752 | 1.219 |
| .0094 | -8.3 | .798 | .733 | 1.094 |
| .0100 | -7.1 | .932 | .699 | .841 |
| .0107 | -6.3 | 1.013 | .693 | .679 |
| .0114 | -5.7 | 1.084 | .652 | .489 |

**[2]$x/c = 0.050;\ \alpha = 2°$**

| $y/c$ | $\theta$, deg | $\bar{u}/U_\infty$ | $c_p$ | $c_{p_t}$ |
|---|---|---|---|---|
| .0003 | -174.3 | .335 | .666 | 1.571 |
| .0007 | -179.1 | .344 | .679 | 1.560 |
| .0010 | -179.1 | .322 | .699 | 1.598 |
| .0013 | -179.0 | .292 | .693 | 1.607 |
| .0017 | -178.5 | .267 | .696 | 1.624 |
| .0020 | -179.1 | .256 | .701 | 1.634 |
| .0023 | -179.1 | .232 | 1.714 | 1.659 |

**$x/c = 0.050;\ \alpha = 4°$**

| $y/c$ | $\theta$, deg | $\bar{u}/U_\infty$ | $c_p$ | $c_{p_t}$ |
|---|---|---|---|---|
| .0156 | -2.7 | .106 | .976 | 1.964 |
| .0173 | 4.0 | .383 | 1.024 | 1.841 |
| .0206 | 9.3 | .563 | 1.004 | 1.709 |
| .0223 | 9.9 | .769 | 1.018 | 1.427 |
| .0239 | 11.4 | .990 | .992 | 1.013 |

[1]Repeat run.
[2]Reverse-flow probe.

## TABLE II.- RESULTS FROM PITOT-STATIC SURVEYS - Continued

| $\frac{y}{c}$ | $\theta$, deg | $\frac{\bar{u}}{U_\infty}$ | $c_p$ | $c_{p_t}$ |
|---|---|---|---|---|
| 0.0256 | 12.5 | 1.175 | 0.969 | 0.584 |
| .0273 | 13.8 | 1.279 | .905 | .263 |
| .0289 | 13.2 | 1.332 | .863 | .097 |
| .0323 | 13.2 | 1.338 | .809 | .040 |
| .0389 | 12.8 | 1.323 | .756 | .025 |
| .0456 | 12.5 | 1.304 | .707 | .019 |

²x/c = 0.050; α = 4°

| $\frac{y}{c}$ | $\theta$, deg | $\frac{\bar{u}}{U_\infty}$ | $c_p$ | $c_{p_t}$ |
|---|---|---|---|---|
| .0002 | 166.3 | .128 | .907 | 1.889 |
| .0011 | 173.3 | .153 | .921 | 1.899 |
| .0027 | 174.2 | .196 | .924 | 1.882 |
| .0046 | 174.2 | .214 | .922 | 1.876 |
| .0077 | 171.7 | .213 | .920 | 1.875 |
| .0110 | 169.9 | .203 | .938 | 1.894 |

x/c = 0.050; α = 6°

| $\frac{y}{c}$ | $\theta$, deg | $\frac{\bar{u}}{U_\infty}$ | $c_p$ | $c_{p_t}$ |
|---|---|---|---|---|
| .0256 | 13.5 | .233 | 1.009 | 1.955 |
| .0273 | 12.9 | .375 | 1.018 | 1.906 |
| .0289 | 12.8 | .469 | 1.025 | 1.803 |
| .0306 | 14.0 | .712 | 1.052 | 1.547 |
| .0323 | 14.2 | .900 | 1.061 | 1.244 |
| .0339 | 15.3 | 1.112 | 1.056 | .821 |
| .0356 | 16.3 | 1.268 | 1.069 | .457 |
| .0373 | 17.7 | 1.353 | 1.053 | .214 |
| .0389 | 18.3 | 1.373 | 1.025 | .123 |
| .0423 | 18.5 | 1.395 | .992 | .068 |
| .0456 | 17.8 | 1.390 | .976 | .065 |
| .0489 | 17.8 | 1.380 | .952 | .065 |

²x/c = 0.050; α = 6°

| $\frac{y}{c}$ | $\theta$, deg | $\frac{\bar{u}}{U_\infty}$ | $c_p$ | $c_{p_t}$ |
|---|---|---|---|---|
| .0002 | 166.3 | .054 | .953 | 1.949 |
| .0046 | 165.6 | .055 | .959 | 1.955 |
| .0077 | 172.1 | .139 | .951 | 1.931 |
| .0144 | 173.5 | .141 | .964 | 1.942 |
| .0211 | 173.3 | .134 | 1.950 | .972 |

x/c = 0.075; α = 2°

| $\frac{y}{c}$ | $\theta$, deg | $\frac{\bar{u}}{U_\infty}$ | $c_p$ | $c_{p_t}$ |
|---|---|---|---|---|
| .0055 | -11.6 | .554 | .341 | 1.036 |
| .0072 | -10.1 | .652 | .373 | .948 |
| .0088 | -8.8 | .755 | .384 | .815 |
| .0100 | -5.8 | .905 | .357 | .536 |
| .0120 | -4.4 | .953 | .307 | .339 |
| .0140 | -4.2 | 1.111 | .432 | .197 |
| .0150 | -3.3 | 1.073 | .269 | .097 |
| .0190 | -5.8 | 1.102 | .253 | .041 |
| .0220 | -6.6 | 1.105 | .252 | .032 |

¹x/c = 0.075; α = 2°

| $\frac{y}{c}$ | $\theta$, deg | $\frac{\bar{u}}{U_\infty}$ | $c_p$ | $c_{p_t}$ |
|---|---|---|---|---|
| .0002 | 0 | .240 | .203 | 1.145 |
| .0027 | -11.7 | .413 | .275 | 1.105 |
| .0034 | -12.5 | .444 | .285 | 1.088 |
| .0041 | -12.6 | .482 | .284 | 1.053 |
| .0047 | -12.7 | .517 | .302 | 1.035 |

²x/c = 0.075; α = 4°

| $\frac{y}{c}$ | $\theta$, deg | $\frac{\bar{u}}{U_\infty}$ | $c_p$ | $c_{p_t}$ |
|---|---|---|---|---|
| .0003 | 178.0 | .203 | .977 | 1.933 |
| .0030 | 178.5 | .277 | .989 | 1.910 |
| .0063 | 177.3 | .277 | .990 | 1.912 |
| .0096 | 176.1 | .274 | .993 | 1.917 |
| .0130 | 173.7 | .239 | 1.006 | 1.947 |
| .0163 | 169.4 | .169 | 1.021 | 1.990 |
| .0196 | 151.2 | .074 | 1.026 | 2.020 |

x/c = 0.075; α = 4°

| $\frac{y}{c}$ | $\theta$, deg | $\frac{\bar{u}}{U_\infty}$ | $c_p$ | $c_{p_t}$ |
|---|---|---|---|---|
| .0105 | .3 | --- | .980 | 1.983 |
| .0172 | -5.8 | .218 | .981 | 1.932 |
| .0188 | -2.6 | .181 | 1.021 | 1.989 |
| .0205 | .6 | .292 | 1.027 | 1.940 |
| .0222 | 2.6 | .424 | 1.042 | 1.860 |

| $\frac{y}{c}$ | $\theta$, deg | $\frac{\bar{u}}{U_\infty}$ | $c_p$ | $c_{p_t}$ |
|---|---|---|---|---|
| 0.0238 | 4.4 | .527 | 1.059 | 1.780 |
| .0255 | 6.1 | .655 | 1.073 | 1.645 |
| .0272 | 7.1 | .811 | 1.071 | 1.412 |
| .0288 | 8.6 | 1.015 | 1.011 | 1.134 |
| .0305 | 9.7 | 1.081 | 1.024 | .764 |
| .0322 | 10.0 | .428 | 1.223 | 1.044 |
| .0355 | 9.7 | 1.304 | .881 | .175 |
| .0388 | 9.5 | 1.327 | .835 | .062 |
| .0422 | 9.0 | 1.326 | .807 | .046 |
| .0455 | 9.0 | 1.317 | .769 | .033 |
| .0488 | 7.5 | 1.313 | .762 | .033 |

²x/c = 0.075; α = 6°

| $\frac{y}{c}$ | $\theta$, deg | $\frac{\bar{u}}{U_\infty}$ | $c_p$ | $c_{p_t}$ |
|---|---|---|---|---|
| .0006 | 172.5 | .151 | .958 | 1.975 |
| .0023 | 173.2 | .201 | .954 | 1.935 |
| .0040 | 173.3 | .100 | .982 | 1.914 |
| .0056 | 174.6 | .072 | .986 | 1.973 |
| .0073 | 175.1 | .001 | .981 | 1.979 |
| .0089 | 175.9 | .132 | .984 | 1.985 |
| .0106 | 173.0 | .171 | .984 | 1.955 |
| .0123 | 176.8 | .170 | .985 | 1.956 |
| .0140 | 175.0 | .148 | .993 | 1.971 |
| .0156 | 175.5 | .137 | .984 | 1.965 |
| .0173 | 176.0 | .108 | .992 | 1.981 |
| .0190 | 176.5 | .185 | .981 | 1.947 |
| .0206 | 177.2 | .160 | .990 | 1.964 |
| .0240 | 177.0 | .087 | .983 | 1.975 |
| .0273 | 180.0 | .081 | .998 | 1.991 |

²x/c = 0.075; α = 4°

| $\frac{y}{c}$ | $\theta$, deg | $\frac{\bar{u}}{U_\infty}$ | $c_p$ | $c_{p_t}$ |
|---|---|---|---|---|
| .0003 | 178.0 | .203 | .977 | 1.933 |
| .0030 | 178.5 | .277 | .989 | 1.910 |
| .0063 | 177.3 | .277 | .990 | 1.912 |
| .0096 | 176.1 | .274 | .993 | 1.917 |
| .0130 | 173.7 | .239 | 1.006 | 1.947 |
| .0163 | 169.4 | .169 | 1.021 | 1.990 |
| .0196 | 151.2 | .074 | 1.026 | 2.020 |

x/c = 0.075; α = 6°

| $\frac{y}{c}$ | $\theta$, deg | $\frac{\bar{u}}{U_\infty}$ | $c_p$ | $c_{p_t}$ |
|---|---|---|---|---|
| .0272 | 14.0 | .103 | .991 | 1.978 |
| .0322 | 11.7 | .287 | 1.023 | 1.938 |
| .0338 | 10.6 | .362 | 1.040 | 1.909 |
| .0372 | 11.5 | .593 | 1.068 | 1.715 |
| .0388 | 13.2 | .737 | 1.098 | 1.570 |
| .0405 | 12.8 | .864 | 1.088 | 1.343 |
| .0405 | 14.7 | .867 | 1.090 | 1.361 |
| .0422 | 16.1 | .985 | 1.062 | 1.073 |
| .0438 | 16.0 | 1.121 | 1.056 | .795 |
| .0455 | 16.0 | 1.225 | 1.041 | .538 |
| .0472 | 15.8 | 1.301 | .996 | .299 |
| .0505 | 15.5 | 1.355 | .954 | .112 |
| .0535 | 15.7 | 1.363 | .925 | .063 |
| .0572 | 14.3 | 1.350 | .885 | .061 |
| .0605 | 12.1 | 1.350 | .872 | .046 |

x/c = 0.100; α = 2°

| $\frac{y}{c}$ | $\theta$, deg | $\frac{\bar{u}}{U_\infty}$ | $c_p$ | $c_{p_t}$ |
|---|---|---|---|---|
| .0002 | 1.5 | .440 | .119 | .926 |
| .0007 | -1.5 | .515 | .126 | .859 |
| .0014 | -2.7 | .562 | .142 | .828 |
| .0027 | -3.3 | .609 | .171 | .798 |
| .0044 | -4.3 | .662 | .180 | .738 |
| .0060 | -4.4 | .727 | .180 | .648 |
| .0077 | -3.7 | .790 | .195 | .572 |
| .0094 | -3.5 | .849 | .196 | .476 |
| .0110 | -2.9 | .914 | .180 | .346 |
| .0127 | -2.6 | .963 | .176 | .250 |
| .0144 | -2.2 | .996 | .158 | .161 |
| .0160 | -2.0 | 1.028 | .150 | .095 |
| .0177 | -2.0 | 1.046 | .141 | .053 |
| .0194 | -2.0 | 1.055 | .139 | .029 |
| .0227 | -2.0 | 1.061 | .132 | .006 |
| .0260 | -2.0 | 1.061 | .132 | .007 |

x/c = 0.100; α = 4°

| $\frac{y}{c}$ | $\theta$, deg | $\frac{\bar{u}}{U_\infty}$ | $c_p$ | $c_{p_t}$ |
|---|---|---|---|---|
| 0.0194 | -8.4 | .150 | 1.051 | 2.028 |
| .0227 | -2.9 | .334 | 1.058 | 1.947 |
| .0260 | 0 | .507 | 1.079 | 1.818 |
| .0277 | -2.2 | .605 | 1.091 | 1.726 |
| .0294 | 2.5 | .695 | 1.082 | 1.600 |
| .0310 | 2.4 | .799 | 1.088 | 1.450 |
| .0327 | 2.7 | .885 | 1.082 | 1.298 |
| .0344 | 4.3 | .992 | 1.143 | 1.061 |
| .0360 | 5.8 | 1.096 | 1.017 | .811 |
| .0377 | 6.1 | 1.187 | .979 | .563 |
| .0394 | 7.1 | 1.251 | .931 | .361 |
| .0410 | 7.8 | 1.287 | .900 | .242 |
| .0427 | 8.3 | 1.312 | .867 | .139 |
| .0444 | 7.7 | 1.324 | .841 | .078 |
| .0460 | 8.2 | 1.335 | .820 | .036 |
| .0494 | 8.1 | 1.330 | .794 | .021 |
| .0527 | 7.9 | 1.322 | .755 | .006 |

²x/c = 0.100; α = 4°

| $\frac{y}{c}$ | $\theta$, deg | $\frac{\bar{u}}{U_\infty}$ | $c_p$ | $c_{p_t}$ |
|---|---|---|---|---|
| .0002 | -177.0 | .272 | .979 | 1.904 |
| .0027 | -179.2 | .349 | 1.002 | 1.880 |
| .0061 | -178.0 | .332 | 1.012 | 1.902 |
| .0094 | -176.7 | .314 | 1.025 | 1.927 |
| .0127 | -175.0 | .265 | 1.027 | 1.956 |
| .0161 | -173.0 | .209 | 1.034 | 1.990 |
| .0194 | -163.2 | .088 | 1.063 | 2.056 |

x/c = 0.100; α = 6°

| $\frac{y}{c}$ | $\theta$, deg | $\frac{\bar{u}}{U_\infty}$ | $c_p$ | $c_{p_t}$ |
|---|---|---|---|---|
| .0327 | 11.6 | .194 | 1.037 | 1.998 |
| .0360 | 10.4 | .227 | 1.058 | 2.007 |
| .0394 | 9.2 | .394 | 1.079 | 1.923 |
| .0929 | 11.3 | .554 | 1.098 | 1.790 |
| .0460 | 11.6 | .740 | 1.113 | 1.561 |
| .0494 | 13.5 | .944 | 1.091 | 1.196 |
| .0527 | 15.1 | 1.153 | 1.018 | .685 |
| .0560 | 16.5 | 1.271 | .938 | .317 |
| .0594 | 17.3 | 1.325 | .865 | .104 |
| .0627 | 17.1 | 1.344 | .848 | .039 |
| .0660 | 16.7 | 1.344 | .822 | .011 |
| .0695 | 16.6 | 1.341 | .802 | -.002 |

²x/c = 0.100; α = 6°

| $\frac{y}{c}$ | $\theta$, deg | $\frac{\bar{u}}{U_\infty}$ | $c_p$ | $c_{p_t}$ |
|---|---|---|---|---|
| .0002 | 172.0 | .124 | .984 | 1.968 |
| .0027 | 172.0 | .206 | .985 | 1.943 |
| .0061 | 174.0 | .225 | .990 | 1.938 |
| .0094 | 176.0 | .225 | .997 | 1.947 |
| .0161 | 180.0 | .232 | 1.005 | 1.951 |
| .0227 | 180.0 | .225 | 1.011 | 1.961 |
| .0294 | 180.0 | .168 | 1.029 | 1.999 |

x/c = 0.150; α = 2°

| $\frac{y}{c}$ | $\theta$, deg | $\frac{\bar{u}}{U_\infty}$ | $c_p$ | $c_{p_t}$ |
|---|---|---|---|---|
| .0002 | -1.7 | .439 | .027 | .836 |
| .0010 | -.5 | .564 | .026 | .711 |
| .0023 | -1.5 | .633 | .027 | .627 |
| .0063 | -1.7 | .699 | .028 | .541 |
| .0130 | -1.5 | .837 | .029 | .331 |
| .0197 | -.5 | .92 | .031 | .181 |
| .0263 | 0 | .95 | .018 | .023 |
| .0330 | 0 | .999 | .015 | .019 |
| .0460 | 0 | .999 | .015 | .017 |
| .0630 | 0 | .999 | .015 | .019 |

x/c = 0.150; α = 4°

| $\frac{y}{c}$ | $\theta$, deg | $\frac{\bar{u}}{U_\infty}$ | $c_p$ | $c_{p_t}$ |
|---|---|---|---|---|
| .0250 | 9.4 | .383 | .996 | 1.846 |
| .0266 | 7.9 | .452 | 1.000 | 1.797 |
| .0299 | 5.0 | .584 | 1.009 | 1.670 |
| .0333 | 4.3 | .704 | 1.001 | 1.437 |
| .0366 | 3.0 | .860 | .977 | 1.236 |
| .0399 | 1.0 | 1.009 | .939 | .918 |
| .0433 | 0 | 1.133 | .867 | .577 |
| .0466 | -.5 | 1.222 | .822 | .320 |

¹Repeat run.
²Reverse-flow probe.

# TABLE II.- RESULTS FROM PITOT-STATIC SURVEYS - Continued

**Left column**

| $y/c$ | $\theta$, deg | $\bar{u}/U_\infty$ | $c_p$ | $c_{p_t}$ |
|---|---|---|---|---|
| 0.0499 | -1.5 | 1.268 | 0.777 | 0.168 |
| .0533 | -1.7 | 1.278 | .723 | .085 |
| .0599 | -2.5 | 1.282 | .681 | .035 |
| .0666 | -3.0 | 1.270 | .634 | .019 |
| .0799 | -3.3 | 1.232 | .537 | .019 |

[2]$x/c = 0.150$; $\alpha = 4°$

| $y/c$ | $\theta$, deg | $\bar{u}/U_\infty$ | $c_p$ | $c_{p_t}$ |
|---|---|---|---|---|
| .0002 | -176.0 | .335 | .846 | 1.732 |
| .0004 | -177.8 | .345 | .850 | 1.730 |
| .0024 | -180.0 | .387 | .867 | 1.716 |
| .0058 | -180.0 | .349 | .845 | 1.772 |
| .0091 | -180.0 | .312 | .923 | 1.826 |
| .0124 | -178.5 | .262 | .926 | 1.856 |
| .0158 | -177.8 | .198 | .957 | 1.917 |
| .0191 | -174.6 | .006 | .977 | 1.996 |
| .0224 | -173.0 | .003 | .970 | 1.974 |
| .0258 | -164.3 | .002 | .970 | 2.021 |

$x/c = 0.150$; $\alpha = 6°$

| $y/c$ | $\theta$, deg | $\bar{u}/U_\infty$ | $c_p$ | $c_{p_t}$ |
|---|---|---|---|---|
| .0466 | 5.6 | .382 | 1.138 | 1.992 |
| .0499 | 6.5 | .512 | 1.153 | 1.893 |
| .0533 | 7.4 | .611 | 1.180 | 1.809 |
| .0566 | 8.7 | .756 | 1.193 | 1.622 |
| .0599 | 9.0 | .913 | 1.195 | 1.362 |
| .0633 | 10.1 | 1.077 | 1.175 | 1.010 |
| .0666 | 10.0 | 1.212 | 1.154 | .681 |
| .0699 | 11.6 | 1.297 | 1.135 | .449 |
| .0733 | 11.4 | 1.357 | 1.108 | .262 |
| .0733 | 11.4 | 1.369 | 1.093 | .215 |
| .0766 | 12.2 | 1.399 | 1.094 | .133 |
| .0799 | 11.8 | 1.422 | 1.118 | .075 |
| .0866 | 11.4 | 1.404 | 1.003 | .029 |
| .0899 | 11.4 | 1.404 | .993 | .018 |
| .0967 | 11.6 | 1.392 | .953 | .009 |

[2]$x/c = 0.150$; $\alpha = 6°$

| $y/c$ | $\theta$, deg | $\bar{u}/U_\infty$ | $c_p$ | $c_{p_t}$ |
|---|---|---|---|---|
| .0002 | 178.2 | .143 | .991 | 1.970 |
| .0024 | 178.0 | .234 | .982 | 1.928 |
| .0091 | 180.0 | .303 | 1.026 | 1.935 |
| .0158 | 179.0 | .276 | 1.038 | 1.961 |
| .0224 | 178.5 | .213 | 1.029 | 1.984 |
| .0291 | 177.3 | .224 | 1.029 | 1.979 |
| .0358 | 175.0 | .001 | 1.053 | 2.054 |

$x/c = 0.200$; $\alpha = 2°$

| $y/c$ | $\theta$, deg | $\bar{u}/U_\infty$ | $c_p$ | $c_{p_t}$ |
|---|---|---|---|---|
| .0003 | -2.0 | .558 | .100 | .794 |
| .0030 | 0 | .761 | .106 | .525 |
| .0063 | 0 | .809 | .118 | .461 |
| .0063 | 0 | .822 | .124 | .446 |
| .0097 | 1.0 | .856 | .118 | .383 |
| .0163 | 0 | .933 | .117 | .240 |
| .0230 | -1.0 | .998 | .098 | .103 |
| .0297 | -1.0 | 1.028 | .088 | .133 |
| .0363 | -1.0 | 1.032 | .083 | .018 |
| .0430 | -1.0 | 1.037 | .083 | .010 |

$x/c = 0.200$; $\alpha = 4°$

| $y/c$ | $\theta$, deg | $\bar{u}/U_\infty$ | $c_p$ | $c_{p_t}$ |
|---|---|---|---|---|
| .0183 | -19.0 | .281 | .735 | 1.656 |
| .0201 | -19.0 | .307 | .736 | 1.643 |
| .0235 | -15.0 | .383 | .754 | 1.606 |
| .0268 | -10.5 | .510 | .758 | 1.498 |
| .0301 | -8.8 | .582 | .752 | 1.413 |
| .0335 | -8.2 | .665 | .754 | 1.314 |
| .0401 | -5.3 | .879 | .731 | .960 |
| .0468 | -3.3 | 1.080 | .636 | .468 |
| .0535 | -3.0 | 1.175 | .573 | .184 |
| .0601 | -2.3 | 1.207 | .526 | .064 |
| .0668 | -1.5 | 1.209 | .492 | .030 |
| .0735 | -1.0 | 1.208 | .481 | .020 |
| .0868 | 0 | 1.193 | .436 | .011 |

**Middle column**

[2]$x/c = 0.200$; $\alpha = 4°$

| $y/c$ | $\theta$, deg | $\bar{u}/U_\infty$ | $c_p$ | $c_{p_t}$ |
|---|---|---|---|---|
| 0 | -172.0 | .248 | .594 | 1.533 |
| .0026 | -180.0 | .280 | .625 | 1.544 |
| .0059 | -180.0 | .221 | .661 | 1.614 |
| .0093 | -178.5 | .184 | .681 | 1.648 |
| .0126 | -177.6 | .114 | .703 | 1.690 |

$x/c = 0.200$; $\alpha = 6°$

| $y/c$ | $\theta$, deg | $\bar{u}/U_\infty$ | $c_p$ | $c_{p_t}$ |
|---|---|---|---|---|
| .0401 | -6.6 | .071 | 1.135 | 2.128 |
| .0468 | -1.3 | .262 | 1.124 | 2.055 |
| .0535 | 2.7 | .463 | 1.148 | 1.949 |
| .0601 | 3.4 | .627 | 1.158 | 1.787 |
| .0668 | 5.0 | .875 | 1.155 | 1.494 |
| .0735 | 6.5 | 1.052 | 1.110 | 1.009 |
| .0801 | 8.0 | 1.218 | 1.022 | .530 |
| .0868 | 8.5 | 1.300 | .944 | .293 |
| .0935 | 9.1 | 1.340 | .883 | .082 |
| .1001 | 9.1 | 1.337 | .825 | .035 |

[2]$x/c = 0.200$; $\alpha = 6°$

| $y/c$ | $\theta$, deg | $\bar{u}/U_\infty$ | $c_p$ | $c_{p_t}$ |
|---|---|---|---|---|
| 0 | -177.0 | .268 | 1.032 | 1.958 |
| .0026 | -180.0 | .321 | 1.045 | 1.940 |
| .0059 | -179.0 | .351 | 1.060 | 1.927 |
| .0093 | -178.5 | .347 | 1.063 | 1.942 |
| .0159 | -178.0 | .327 | 1.073 | 1.969 |
| .0226 | -176.5 | .303 | 1.073 | 1.983 |
| .0293 | -175.0 | .260 | 1.093 | 2.025 |
| .0359 | -172.4 | .210 | 1.111 | 2.067 |

$x/c = 0.250$; $\alpha = 2°$

| $y/c$ | $\theta$, deg | $\bar{u}/U_\infty$ | $c_p$ | $c_{p_t}$ |
|---|---|---|---|---|
| .0002 | 1.5 | .547 | .090 | .775 |
| .0006 | .6 | .572 | .096 | .754 |
| .0012 | -.8 | .669 | .093 | .628 |
| .0026 | -.8 | .735 | .101 | .537 |
| .0059 | -.9 | .801 | .110 | .453 |
| .0126 | -.9 | .870 | .115 | .344 |
| .0226 | -.8 | .963 | .103 | .160 |
| .0326 | -.5 | 1.018 | .087 | .043 |
| .0426 | -.5 | 1.034 | .082 | .010 |
| .0526 | -.2 | 1.036 | .080 | .005 |

$x/c = 0.250$; $\alpha = 4°$

| $y/c$ | $\theta$, deg | $\bar{u}/U_\infty$ | $c_p$ | $c_{p_t}$ |
|---|---|---|---|---|
| .0002 | .6 | .012 | .404 | 1.412 |
| .0006 | .6 | .050 | .402 | 1.400 |
| .0026 | -9.4 | .093 | .439 | 1.431 |
| .0126 | -22.8 | .204 | .510 | 1.469 |
| .0226 | -16.4 | .401 | .542 | 1.382 |
| .0326 | -10.0 | .658 | .552 | 1.119 |
| .0426 | -6.8 | .870 | .526 | .766 |
| .0526 | -4.3 | 1.054 | .450 | .340 |
| .0626 | -3.4 | 1.129 | .398 | .102 |
| .0726 | -2.9 | 1.147 | .357 | .029 |
| .0826 | -2.1 | 1.152 | .344 | .010 |

[2]$x/c = 0.250$; $\alpha = 4°$

| $y/c$ | $\theta$, deg | $\bar{u}/U_\infty$ | $c_p$ | $c_{p_t}$ |
|---|---|---|---|---|
| .0003 | -168.3 | .071 | .361 | 1.356 |
| .0033 | -177.0 | .054 | .400 | 1.397 |
| .0066 | -167.6 | .001 | .430 | 1.437 |

$x/c = 0.250$; $\alpha = 6°$

| $y/c$ | $\theta$, deg | $\bar{u}/U_\infty$ | $c_p$ | $c_{p_t}$ |
|---|---|---|---|---|
| .0402 | -20.8 | .111 | 1.129 | 2.117 |
| .0502 | -11.0 | .275 | 1.135 | 2.060 |
| .0600 | -4.9 | .480 | 1.164 | 1.936 |
| .0700 | .6 | .698 | 1.159 | 1.670 |
| .0800 | 2.8 | .981 | 1.116 | 1.150 |
| .0900 | 4.0 | 1.209 | 1.016 | .549 |
| .1000 | 5.3 | 1.311 | .916 | .188 |

**Right column**

| $y/c$ | $\theta$, deg | $\bar{u}/U_\infty$ | $c_p$ | $c_{p_t}$ |
|---|---|---|---|---|
| .1100 | 5.4 | 1.329 | 0.859 | 0.102 |
| .1200 | 5.3 | 1.336 | .809 | .020 |
| .1300 | 5.4 | 1.325 | .771 | .010 |
| .1367 | 5.4 | 1.316 | .747 | .010 |

[2]$x/c = 0.250$; $\alpha = 6°$

| $y/c$ | $\theta$, deg | $\bar{u}/U_\infty$ | $c_p$ | $c_{p_t}$ |
|---|---|---|---|---|
| .0003 | -176.5 | .270 | 1.018 | 1.944 |
| .0033 | -180.0 | .546 | 1.033 | 1.737 |
| .0099 | -178.0 | .359 | 1.058 | 1.929 |
| .0166 | -178.0 | .350 | 1.076 | 1.953 |
| .0232 | -177.3 | .315 | 1.085 | 1.986 |
| .0299 | -175.5 | .252 | 1.092 | 2.023 |
| .0366 | -172.4 | .215 | 1.106 | 2.059 |
| .0433 | -166.7 | .129 | 1.119 | 2.101 |

$x/c = 0.300$; $\alpha = 2°$

| $y/c$ | $\theta$, deg | $\bar{u}/U_\infty$ | $c_p$ | $c_{p_t}$ |
|---|---|---|---|---|
| .0002 | 2.5 | .539 | .086 | .778 |
| .0007 | 0 | .620 | .087 | .686 |
| .0027 | -.8 | .756 | .092 | .508 |
| .0061 | -.6 | .813 | .099 | .423 |
| .0161 | -.6 | .894 | .097 | .282 |
| .0294 | -.4 | .995 | .085 | .097 |
| .0427 | -.1 | 1.029 | .072 | .013 |
| .0527 | -.1 | 1.032 | .069 | .006 |

$x/c = 0.300$; $\alpha = 4°$

| $y/c$ | $\theta$, deg | $\bar{u}/U_\infty$ | $c_p$ | $c_{p_t}$ |
|---|---|---|---|---|
| .0002 | 3.0 | .149 | .252 | 1.229 |
| .0007 | -2.3 | .200 | .265 | 1.224 |
| .0027 | -4.5 | .245 | .292 | 1.232 |
| .0061 | -9.9 | .256 | .313 | 1.247 |
| .0161 | -13.2 | .365 | .374 | 1.241 |
| .0294 | -9.6 | .597 | .411 | 1.053 |
| .0427 | -6.0 | .849 | .380 | .657 |
| .0561 | -4.4 | 1.017 | .330 | .295 |
| .0694 | -3.5 | 1.091 | .263 | .059 |
| .0827 | -2.5 | 1.112 | .252 | .018 |
| .0961 | -2.2 | 1.111 | .241 | .008 |

$x/c = 0.300$; $\alpha = 6°$

| $y/c$ | $\theta$, deg | $\bar{u}/U_\infty$ | $c_p$ | $c_{p_t}$ |
|---|---|---|---|---|
| .0427 | -21.3 | .119 | 1.084 | 2.068 |
| .0561 | -10.0 | .371 | 1.111 | 1.973 |
| .0694 | -3.8 | .624 | 1.109 | 1.720 |
| .0827 | -.3 | .928 | 1.061 | 1.199 |
| .0961 | 1.5 | 1.197 | .931 | .497 |
| .1094 | 2.7 | 1.296 | .833 | .142 |
| .1227 | 2.9 | 1.313 | .755 | .030 |
| .1361 | 3.6 | 1.303 | .707 | .006 |

[2]$x/c = 0.300$; $\alpha = 6°$

| $y/c$ | $\theta$, deg | $\bar{u}/U_\infty$ | $c_p$ | $c_{p_t}$ |
|---|---|---|---|---|
| .0003 | -173.4 | .317 | .946 | 1.845 |
| .0033 | -180.0 | .387 | .989 | 1.839 |
| .0066 | -178.5 | .374 | 1.012 | 1.872 |
| .0099 | -178.0 | .318 | 1.027 | 1.926 |
| .0166 | -177.8 | .309 | 1.032 | 1.937 |
| .0232 | -176.7 | .280 | 1.027 | 1.948 |
| .0299 | -173.9 | .187 | 1.064 | 2.028 |
| .0366 | -166.3 | .060 | 1.081 | 2.077 |

$x/c = 0.350$; $\alpha = 2°$

| $y/c$ | $\theta$, deg | $\bar{u}/U_\infty$ | $c_p$ | $c_{p_t}$ |
|---|---|---|---|---|
| .0002 | 1.4 | .558 | .072 | .762 |
| .0005 | .2 | .615 | .068 | .691 |
| .0012 | -.5 | .698 | .072 | .587 |
| .0022 | -.7 | .754 | .073 | .505 |
| .0038 | -.6 | .778 | .060 | .441 |
| .0078 | -.5 | .842 | .076 | .368 |
| .0145 | -.5 | .894 | .075 | .276 |
| .0278 | -.4 | .973 | .073 | .123 |
| .0412 | -.2 | 1.018 | .061 | .024 |
| .0546 | -.1 | 1.026 | .058 | .005 |

[2]Reverse-flow probe.

## TABLE II.- RESULTS FROM PITOT-STATIC SURVEYS - Continued

**$x/c = 0.350$; $\alpha = 4°$**

| $y/c$ | $\theta$, deg | $\bar{u}/U_\infty$ | $c_p$ | $c_{p_t}$ |
|---|---|---|---|---|
| 0.0002 | 0.6 | 0.259 | 0.165 | 1.097 |
| .0005 | -1.1 | .288 | .171 | 1.088 |
| .0022 | -3.9 | .359 | .200 | 1.072 |
| .0078 | -5.8 | .404 | .245 | 1.083 |
| .0212 | -7.7 | .558 | .292 | .981 |
| .0212 | -7.6 | .538 | .293 | 1.003 |
| .0345 | -6.3 | .727 | .297 | .768 |
| .0478 | -4.7 | .899 | .277 | .458 |
| .0612 | -2.7 | 1.015 | .231 | .202 |
| .0745 | -2.4 | 1.062 | .201 | .060 |
| .0878 | -1.7 | 1.082 | .187 | .018 |
| .1012 | -1.4 | 1.085 | .181 | .006 |

**$x/c = 0.350$; $\alpha = 6°$**

| $y/c$ | $\theta$, deg | $\bar{u}/U_\infty$ | $c_p$ | $c_{p_t}$ |
|---|---|---|---|---|
| .0345 | -33.6 | .002 | .992 | 2.003 |
| .0479 | -20.3 | .230 | 1.014 | 1.958 |
| .0612 | -10.3 | .451 | 1.037 | 1.835 |
| .0745 | -5.3 | .709 | 1.021 | 1.518 |
| .0878 | -2.4 | .980 | .965 | 1.006 |
| .1012 | -1.1 | 1.185 | .854 | .443 |
| .1145 | 0 | 1.268 | .755 | .144 |
| .1278 | .3 | 1.282 | .687 | .028 |
| .1395 | 1.0 | 1.284 | .664 | .014 |

**[2]$x/c = 0.350$; $\alpha = 6°$**

| $y/c$ | $\theta$, deg | $\bar{u}/U_\infty$ | $c_p$ | $c_{p_t}$ |
|---|---|---|---|---|
| .0003 | -173.4 | .226 | .824 | 1.776 |
| .0024 | -179.9 | .378 | .892 | 1.749 |
| .0090 | -179.8 | .337 | .925 | 1.811 |
| .0157 | -179.4 | .316 | .939 | 1.840 |
| .0223 | -177.8 | .260 | .964 | 1.896 |
| .0290 | -176.5 | .215 | .974 | 1.927 |
| .0357 | -174.7 | .154 | .993 | 1.969 |
| .0424 | -168.0 | .094 | 1.008 | 2.006 |

**$x/c = 0.400$; $\alpha = 2°$**

| $y/c$ | $\theta$, deg | $\bar{u}/U_\infty$ | $c_p$ | $c_{p_t}$ |
|---|---|---|---|---|
| .0002 | 1.1 | .585 | .057 | .716 |
| .0010 | -.4 | .671 | .052 | .603 |
| .0016 | -.4 | .724 | .056 | .533 |
| .0033 | -.4 | .790 | .057 | .434 |
| .0050 | -.4 | .822 | .059 | .385 |
| .0083 | -.4 | .887 | .060 | .275 |
| .0183 | -.4 | .924 | .058 | .206 |
| .0283 | -.4 | .981 | .054 | .091 |
| .0383 | -.3 | 1.011 | .046 | .024 |
| .0483 | -.1 | 1.017 | .043 | .010 |
| .0550 | -.1 | 1.019 | .043 | .005 |

**$x/c = 0.400$; $\alpha = 4°$**

| $y/c$ | $\theta$, deg | $\bar{u}/U_\infty$ | $c_p$ | $c_{p_t}$ |
|---|---|---|---|---|
| .0003 | -.3 | .304 | .138 | 1.048 |
| .0010 | -1.3 | .385 | .151 | 1.003 |
| .0016 | -1.6 | .421 | .159 | .983 |
| .0050 | -3.0 | .470 | .179 | .957 |
| .0083 | -4.3 | .504 | .202 | .948 |
| .0183 | -5.5 | .556 | .228 | .917 |
| .0283 | -5.6 | .672 | .245 | .792 |
| .0417 | -2.0 | .816 | .236 | .572 |
| .0500 | -2.8 | .945 | .213 | .324 |
| .0683 | -1.6 | 1.019 | .174 | .134 |
| .0817 | -1.3 | 1.046 | .143 | .039 |
| .0950 | -1.2 | 1.061 | .138 | .014 |

**$x/c = 0.400$; $\alpha = 6°$**

| $y/c$ | $\theta$, deg | $\bar{u}/U_\infty$ | $c_p$ | $c_{p_t}$ |
|---|---|---|---|---|
| .0417 | -27.4 | .198 | .905 | 1.864 |
| .0550 | -17.7 | .369 | .913 | 1.777 |
| .0683 | -10.3 | .577 | .930 | 1.594 |
| .0683 | -9.9 | .593 | .908 | 1.553 |
| .0817 | -6.4 | .872 | .888 | 1.201 |
| .0950 | -4.5 | 1.076 | .786 | .654 |
| .1083 | -2.3 | 1.198 | .715 | .276 |
| .1217 | -1.5 | 1.236 | .636 | .791 |
| .1350 | -1.0 | 1.253 | .597 | .054 |
| .1431 | -.7 | 1.251 | .577 | .013 |

**[2]$x/c = 0.400$; $\alpha = 6°$**

| $y/c$ | $\theta$, deg | $\bar{u}/U_\infty$ | $c_p$ | $c_{p_t}$ |
|---|---|---|---|---|
| 0.0003 | -173.4 | 0.279 | 0.754 | 1.666 |
| .0023 | -180.0 | .353 | .772 | 1.646 |
| .0087 | -180.0 | .320 | .812 | 1.709 |
| .0156 | -180.0 | .259 | .838 | 1.770 |
| .0223 | -178.5 | .220 | .856 | 1.808 |
| .0289 | -177.1 | .166 | .880 | 1.852 |
| .0356 | -173.2 | .084 | .900 | 1.893 |

**$x/c = 0.450$; $\alpha = 2°$**

| $y/c$ | $\theta$, deg | $\bar{u}/U_\infty$ | $c_p$ | $c_{p_t}$ |
|---|---|---|---|---|
| .0002 | 1.3 | .568 | .055 | .739 |
| .0004 | 0 | .577 | .048 | .716 |
| .0011 | -.9 | .684 | .043 | .577 |
| .0018 | -1.0 | .735 | .046 | .509 |
| .0034 | -.4 | .795 | .047 | .416 |
| .0051 | -.4 | .823 | .049 | .372 |
| .0084 | -.4 | .862 | .048 | .306 |
| .0151 | -.3 | .907 | .046 | .225 |
| .0284 | -.3 | .976 | .036 | .086 |
| .0417 | -.3 | 1.005 | .029 | .018 |
| .0551 | -.2 | 1.012 | .029 | .005 |

**$x/c = 0.450$; $\alpha = 4°$**

| $y/c$ | $\theta$, deg | $\bar{u}/U_\infty$ | $c_p$ | $c_{p_t}$ |
|---|---|---|---|---|
| .0004 | -.2 | .393 | .121 | .967 |
| .0011 | -1.2 | .467 | .134 | .913 |
| .0051 | -2.2 | .560 | .157 | .843 |
| .0151 | -3.7 | .626 | .184 | .790 |
| .0284 | -3.9 | .725 | .201 | .675 |
| .0417 | -3.2 | .834 | .193 | .498 |
| .0551 | -2.0 | .932 | .167 | .301 |
| .0551 | -2.1 | .932 | .169 | .301 |
| .0684 | -1.2 | .995 | .141 | .147 |
| .0818 | -1.1 | 1.032 | .120 | .057 |
| .0951 | -1.0 | 1.046 | .110 | .019 |
| .1085 | -.4 | 1.051 | .110 | .006 |

**$x/c = 0.450$; $\alpha = 6°$**

| $y/c$ | $\theta$, deg | $\bar{u}/U_\infty$ | $c_p$ | $c_{p_t}$ |
|---|---|---|---|---|
| .0417 | -24.3 | .248 | .767 | 1.706 |
| .0551 | -16.2 | .440 | .776 | 1.594 |
| .0684 | -11.0 | .617 | .775 | 1.393 |
| .0818 | -8.0 | .827 | .748 | 1.061 |
| .0951 | -5.5 | 1.017 | .701 | .666 |
| .1085 | -4.3 | 1.140 | .606 | .303 |
| .1218 | -3.4 | 1.191 | .547 | .109 |
| .1351 | -2.8 | 1.215 | .515 | .041 |
| .1438 | -2.3 | 1.215 | .496 | .021 |

**[2]$x/c = 0.450$; $\alpha = 6°$**

| $y/c$ | $\theta$, deg | $\bar{u}/U_\infty$ | $c_p$ | $c_{p_t}$ |
|---|---|---|---|---|
| .0013 | -170.5 | .209 | .589 | 1.545 |
| .0017 | -180.0 | .281 | .617 | 1.537 |
| .0050 | -180.0 | .272 | .645 | 1.570 |
| .0084 | -180.0 | .230 | .662 | 1.609 |
| .0117 | -179.8 | .204 | .682 | 1.640 |
| .0150 | -177.5 | .179 | .687 | 1.654 |
| .0183 | -176.7 | .151 | .698 | 1.672 |
| .0217 | -174.6 | .119 | .695 | 1.679 |
| .0250 | -173.4 | .076 | .724 | 1.722 |

**$x/c = 0.500$; $\alpha = 2°$**

| $y/c$ | $\theta$, deg | $\bar{u}/U_\infty$ | $c_p$ | $c_{p_t}$ |
|---|---|---|---|---|
| .0002 | -1.0 | .597 | .067 | .712 |
| .0006 | -2.0 | .618 | .057 | .676 |
| .0023 | -2.5 | .758 | .060 | .488 |
| .0040 | -2.4 | .806 | .062 | .415 |
| .0073 | -2.2 | .852 | .065 | .340 |
| .0140 | -2.1 | .900 | .070 | .262 |
| .0273 | -2.2 | .967 | .069 | .136 |
| .0406 | -2.0 | 1.009 | .061 | .043 |
| .0539 | -2.0 | 1.023 | .062 | .005 |

**$x/c = 0.500$; $\alpha = 4°$**

| $y/c$ | $\theta$, deg | $\bar{u}/U_\infty$ | $c_p$ | $c_{p_t}$ |
|---|---|---|---|---|
| 0.0002 | -2.0 | 0.423 | 0.123 | 0.946 |
| .0006 | -2.1 | .465 | .128 | .912 |
| .0023 | -2.5 | .559 | .136 | .825 |
| .0040 | -2.5 | .592 | .140 | .792 |
| .0073 | -3.3 | .619 | .156 | .773 |
| .0140 | -3.4 | .674 | .180 | .736 |
| .0273 | -4.3 | .749 | .196 | .634 |
| .0406 | -3.4 | .842 | .195 | .487 |
| .0539 | -3.6 | .930 | .182 | .322 |
| .0673 | -3.1 | .991 | .166 | .182 |
| .0806 | -2.5 | 1.027 | .142 | .084 |
| .0940 | -2.0 | 1.049 | .128 | .045 |
| .1056 | -2.0 | 1.059 | .127 | .006 |

**$x/c = 0.500$; $\alpha = 6°$**

| $y/c$ | $\theta$, deg | $\bar{u}/U_\infty$ | $c_p$ | $c_{p_t}$ |
|---|---|---|---|---|
| .0140 | -29.3 | .152 | .584 | 1.559 |
| .0273 | -29.3 | .144 | .623 | 1.601 |
| .0406 | -23.4 | .276 | .653 | 1.574 |
| .0539 | -17.0 | .446 | .662 | 1.461 |
| .0673 | -14.0 | .629 | .657 | 1.259 |
| .0806 | -9.8 | .813 | .650 | .987 |
| .0940 | -7.7 | 1.101 | .595 | .381 |
| .1056 | -7.3 | 1.093 | .541 | .341 |
| .1213 | -5.7 | 1.153 | .484 | .150 |
| .1339 | -5.3 | 1.186 | .448 | .051 |
| .1473 | -4.5 | 1.193 | .431 | .018 |

**[2]$x/c = 0.500$; $\alpha = 6°$**

| $y/c$ | $\theta$, deg | $\bar{u}/U_\infty$ | $c_p$ | $c_{p_t}$ |
|---|---|---|---|---|
| .0003 | -166.2 | .155 | .471 | 1.446 |
| .0036 | -180.0 | .192 | .518 | 1.480 |
| .0103 | -177.0 | .070 | .544 | 1.539 |
| .0169 | -170.2 | .051 | .570 | 1.567 |

**$x/c = 0.550$; $\alpha = 2°$**

| $y/c$ | $\theta$, deg | $\bar{u}/U_\infty$ | $c_p$ | $c_{p_t}$ |
|---|---|---|---|---|
| .0002 | 0 | .568 | .045 | .724 |
| .0008 | -2.2 | .632 | .040 | .641 |
| .0024 | -2.5 | .754 | .042 | .474 |
| .0041 | -2.4 | .800 | .040 | .402 |
| .0074 | -2.3 | .847 | .038 | .324 |
| .0141 | -2.3 | .893 | .041 | .243 |
| .0274 | -2.3 | .956 | .034 | .118 |
| .0408 | -2.2 | .996 | .027 | .035 |
| .0541 | -2.2 | 1.008 | .020 | .035 |
| .0674 | -2.1 | 1.008 | .019 | .035 |

**$x/c = 0.550$; $\alpha = 4°$**

| $y/c$ | $\theta$, deg | $\bar{u}/U_\infty$ | $c_p$ | $c_{p_t}$ |
|---|---|---|---|---|
| .0002 | -1.1 | .441 | .107 | .913 |
| .0008 | -2.3 | .495 | .108 | .853 |
| .0024 | -3.1 | .587 | .121 | .758 |
| .0041 | -3.1 | .616 | .121 | .742 |
| .0074 | -3.2 | .657 | .135 | .707 |
| .0141 | -3.3 | .684 | .151 | .681 |
| .0274 | -3.3 | .759 | .162 | .587 |
| .0408 | -4.1 | .823 | .162 | .473 |
| .0541 | -3.6 | .905 | .147 | .330 |
| .0674 | -3.1 | .960 | .129 | .205 |
| .0808 | -2.6 | 1.008 | .109 | .102 |
| .0941 | -2.4 | 1.030 | .098 | .039 |
| .1074 | -2.3 | 1.038 | .092 | .014 |
| .1124 | -2.2 | 1.042 | .092 | .008 |

**$x/c = 0.550$; $\alpha = 6°$**

| $y/c$ | $\theta$, deg | $\bar{u}/U_\infty$ | $c_p$ | $c_{p_t}$ |
|---|---|---|---|---|
| .0002 | 0 | .073 | .387 | 1.380 |
| .0141 | -17.5 | .140 | .474 | 1.453 |
| .0274 | -21.4 | .239 | .511 | 1.454 |
| .0485 | -18.8 | .335 | .545 | 1.433 |
| .0541 | -14.1 | .546 | .542 | 1.271 |
| .0674 | -11.2 | .674 | .549 | 1.097 |
| .0808 | -8.0 | .829 | .545 | .859 |
| .0941 | -8.5 | .956 | .481 | .572 |
| .1074 | -8.0 | 1.051 | .448 | .344 |
| .1074 | -8.3 | 1.056 | .444 | .328 |

[2]Reverse-flow probe.

## TABLE II.- RESULTS FROM PITOT-STATIC SURVEYS - Concluded

| $\frac{y}{c}$ | $\theta$, deg | $\frac{\bar{u}}{U_\infty}$ | $c_p$ | $c_{p_t}$ |
|---|---|---|---|---|
| 0.1124 | -7.7 | 1.081 | 0.423 | 0.253 |
| .1207 | -6.7 | 1.120 | .402 | .147 |
| .1340 | -6.7 | 1.146 | .378 | .061 |
| .1483 | -5.8 | 1.158 | .362 | .023 |

²x/c = 0.550; α = 6°

| $\frac{y}{c}$ | $\theta$, deg | $\frac{\bar{u}}{U_\infty}$ | $c_p$ | $c_{p_t}$ |
|---|---|---|---|---|
| .0003 | -153.8 | 0 | .375 | 1.378 |
| .0029 | -180.0 | .094 | .410 | 1.402 |
| .0096 | -167.4 | 0 | .453 | 1.467 |

x/c = 0.600; α = 2°

| $\frac{y}{c}$ | $\theta$, deg | $\frac{\bar{u}}{U_\infty}$ | $c_p$ | $c_{p_t}$ |
|---|---|---|---|---|
| .0002 | 0 | .537 | .044 | .757 |
| .0012 | -2.2 | .666 | .044 | .601 |
| .0029 | -2.2 | .752 | .042 | .478 |
| .0096 | -2.0 | .856 | .045 | .315 |
| .0229 | -1.9 | .921 | .043 | .197 |
| .0362 | -1.9 | .971 | .042 | .097 |
| .0496 | -1.8 | 1.005 | .036 | .027 |
| .0629 | -1.8 | 1.012 | .035 | .010 |
| .0762 | -1.8 | 1.012 | .030 | .005 |

x/c = 0.600; α = 4°

| $\frac{y}{c}$ | $\theta$, deg | $\frac{\bar{u}}{U_\infty}$ | $c_p$ | $c_{p_t}$ |
|---|---|---|---|---|
| .0006 | -1.5 | .477 | .109 | .902 |
| .0029 | -2.7 | .595 | .120 | .765 |
| .0096 | -2.8 | .677 | .136 | .678 |
| .0229 | -3.3 | .747 | .154 | .596 |
| .0362 | -3.4 | .809 | .157 | .505 |
| .0496 | -2.9 | .874 | .154 | .393 |
| .0629 | -2.8 | .937 | .134 | .259 |
| .0762 | -2.5 | .977 | .119 | .159 |
| .0896 | -2.1 | 1.007 | .109 | .085 |
| .1029 | -1.9 | 1.031 | .097 | .036 |
| .1162 | -1.8 | 1.038 | .095 | .016 |
| .1296 | -1.8 | 1.040 | .092 | .010 |
| .1429 | -1.7 | 1.040 | .087 | .005 |

x/c = 0.600; α = 6°

| $\frac{y}{c}$ | $\theta$, deg | $\frac{\bar{u}}{U_\infty}$ | $c_p$ | $c_{p_t}$ |
|---|---|---|---|---|
| .0002 | 21.5 | .135 | .327 | 1.309 |
| .0029 | -4.8 | .185 | .360 | 1.326 |
| .0162 | -15.3 | .252 | .425 | 1.373 |
| .0362 | -17.8 | .369 | .474 | 1.355 |
| .0562 | -12.5 | .552 | .492 | 1.215 |
| .0762 | -9.4 | .744 | .492 | .940 |
| .0962 | -6.8 | .931 | .443 | .569 |
| .1162 | -5.0 | 1.077 | .390 | .234 |
| .1362 | -4.4 | 1.120 | .350 | .081 |
| .1500 | -3.6 | 1.141 | .336 | .036 |

²x/c = 0.600; α = 6°

| $\frac{y}{c}$ | $\theta$, deg | $\frac{\bar{u}}{U_\infty}$ | $c_p$ | $c_{p_t}$ |
|---|---|---|---|---|
| .0003 | -168.3 | .086 | .341 | 1.332 |
| .0046 | -179.7 | .001 | .367 | 1.372 |

x/c = 0.650; α = 2°

| $\frac{y}{c}$ | $\theta$, deg | $\frac{\bar{u}}{U_\infty}$ | $c_p$ | $c_{p_t}$ |
|---|---|---|---|---|
| 0.0002 | -0.5 | 0.531 | 0.037 | 0.756 |
| .0003 | -2.6 | .747 | .033 | .475 |
| .0161 | -2.4 | .888 | .034 | .245 |
| .0294 | -2.4 | .950 | .033 | .132 |
| .0428 | -2.3 | .984 | .029 | .060 |
| .0561 | -2.3 | 1.004 | .024 | .015 |
| .0694 | -2.3 | 1.008 | .021 | .005 |

x/c = 0.650; α = 4°

| $\frac{y}{c}$ | $\theta$, deg | $\frac{\bar{u}}{U_\infty}$ | $c_p$ | $c_{p_t}$ |
|---|---|---|---|---|
| .0004 | -2.6 | .470 | .093 | .868 |
| .0028 | -2.6 | .625 | .108 | .717 |
| .0161 | -3.4 | .730 | .135 | .602 |
| .0294 | -3.9 | .768 | .141 | .549 |
| .0494 | -3.9 | .864 | .137 | .392 |
| .0694 | -3.3 | .945 | .119 | .224 |
| .0894 | -2.6 | .991 | .099 | .099 |
| .1094 | -2.3 | 1.027 | .088 | .034 |
| .1294 | -2.2 | 1.034 | .083 | .015 |
| .1494 | -1.9 | 1.037 | .081 | .007 |

x/c = 0.650; α = 6°

| $\frac{y}{c}$ | $\theta$, deg | $\frac{\bar{u}}{U_\infty}$ | $c_p$ | $c_{p_t}$ |
|---|---|---|---|---|
| .0002 | -.3 | .138 | .272 | 1.253 |
| .0028 | -.3 | .256 | .302 | 1.241 |
| .0161 | -12.0 | .276 | .357 | 1.280 |
| .0361 | -13.0 | .419 | .400 | 1.223 |
| .0561 | -11.3 | .568 | .420 | 1.097 |
| .0761 | -.9 | .768 | .419 | .830 |
| .0961 | -6.4 | .919 | .385 | .538 |
| .1161 | -5.5 | 1.043 | .336 | .249 |
| .1361 | -4.7 | 1.108 | .303 | .088 |
| .1494 | -4.4 | 1.120 | .292 | .044 |

x/c ≈ 0.700; α = 2°

| $\frac{y}{c}$ | $\theta$, deg | $\frac{\bar{u}}{U_\infty}$ | $c_p$ | $c_{p_t}$ |
|---|---|---|---|---|
| .0002 | .6 | .532 | .030 | .748 |
| .0012 | -1.6 | .653 | .028 | .602 |
| .0078 | -1.4 | .832 | .029 | .339 |
| .0212 | -1.3 | .909 | .027 | .203 |
| .0345 | -1.2 | .958 | .023 | .106 |
| .0478 | -1.1 | .991 | .019 | .038 |
| .0612 | -1.1 | 1.002 | .016 | .013 |
| .0745 | -.9 | 1.004 | .016 | .077 |

x/c ≈ 0.700; α = 4°

| $\frac{y}{c}$ | $\theta$, deg | $\frac{\bar{u}}{U_\infty}$ | $c_p$ | $c_{p_t}$ |
|---|---|---|---|---|
| .0002 | .6 | .458 | .089 | .880 |
| .0012 | -1.4 | .568 | .093 | .772 |
| .0078 | -1.5 | .700 | .109 | .618 |
| .0345 | -2.4 | .812 | .126 | .467 |
| .0545 | -1.7 | .887 | .121 | .335 |
| .0745 | -1.4 | .951 | .095 | .186 |

| $\frac{y}{c}$ | $\theta$, deg | $\frac{\bar{u}}{U_\infty}$ | $c_p$ | $c_{p_t}$ |
|---|---|---|---|---|
| 0.0945 | -1.0 | 1.002 | 0.086 | 0.089 |
| .1145 | -.7 | 1.024 | .075 | .029 |
| .1345 | -.5 | 1.030 | .073 | .013 |
| .1545 | -.2 | 1.033 | .073 | .008 |

x/c = 0.700; α = 6°

| $\frac{y}{c}$ | $\theta$, deg | $\frac{\bar{u}}{U_\infty}$ | $c_p$ | $c_{p_t}$ |
|---|---|---|---|---|
| .0002 | .6 | .198 | .225 | 1.193 |
| .0012 | -2.0 | .259 | .247 | 1.180 |
| .0212 | -9.6 | .807 | .323 | .668 |
| .0412 | -11.1 | .869 | .358 | .603 |
| .0611 | -7.6 | .928 | .363 | .500 |
| .0612 | -7.7 | .675 | .365 | .906 |
| .0812 | -7.3 | .820 | .346 | .676 |
| .1012 | -5.4 | .942 | .326 | .431 |
| .1212 | -4.0 | 1.038 | .285 | .209 |
| .1412 | -4.0 | 1.094 | .266 | .080 |
| .1578 | -3.5 | 1.109 | .254 | .029 |

x/c = 0.800; α = 2°

| $\frac{y}{c}$ | $\theta$, deg | $\frac{\bar{u}}{U_\infty}$ | $c_p$ | $c_{p_t}$ |
|---|---|---|---|---|
| .0002 | .6 | .526 | .019 | .743 |
| .0009 | -1.2 | .618 | .017 | .636 |
| .0076 | -1.2 | .822 | .016 | .342 |
| .0209 | -1.0 | .905 | .013 | .195 |
| .0342 | -.9 | .950 | .146 | .112 |
| .0476 | -.8 | .981 | .008 | .045 |
| .0609 | -.6 | .994 | .001 | .013 |
| .0742 | .5 | .998 | .001 | .005 |

x/c = 0.800; α = 4°

| $\frac{y}{c}$ | $\theta$, deg | $\frac{\bar{u}}{U_\infty}$ | $c_p$ | $c_{p_t}$ |
|---|---|---|---|---|
| .0002 | .6 | .453 | .072 | .867 |
| .0009 | -1.0 | .553 | .073 | .771 |
| .0142 | -1.2 | .746 | .090 | .534 |
| .0342 | -1.5 | .811 | .100 | .442 |
| .0542 | -1.3 | .869 | .091 | .338 |
| .0742 | -1.1 | .928 | .082 | .221 |
| .0942 | -.5 | .982 | .071 | .119 |
| .1142 | -.7 | 1.009 | .061 | .048 |
| .1342 | 0 | 1.020 | .058 | .019 |
| .1542 | 1.0 | 1.024 | .055 | .008 |

x/c = 0.800; α = 6°

| $\frac{y}{c}$ | $\theta$, deg | $\frac{\bar{u}}{U_\infty}$ | $c_p$ | $c_{p_t}$ |
|---|---|---|---|---|
| .0002 | -1.1 | .250 | .177 | 1.114 |
| .0076 | -3.6 | .411 | .227 | 1.058 |
| .0209 | -6.3 | .462 | .262 | 1.048 |
| .0342 | -7.7 | .531 | .280 | .999 |
| .0542 | -7.6 | .635 | .293 | .885 |
| .0742 | -6.6 | .766 | .285 | .699 |
| .0942 | -5.2 | .873 | .278 | .513 |
| .1142 | -4.6 | .966 | .251 | .304 |
| .1342 | -4.6 | .967 | .245 | .296 |
| .1342 | -3.7 | 1.047 | .236 | .135 |
| .1542 | -2.7 | 1.075 | .211 | .061 |

²Reverse-flow probe.

## TABLE III.- RESULTS FROM HOT-WIRE ANEMOMETER SURVEYS

Column headers for all blocks: $\dfrac{y}{c}$ , $\dfrac{\bar{u}}{U_\infty}$ , $\dfrac{\sqrt{\overline{\Delta u^2}}}{\bar{u}}$

**x/c = 0; α = 2°**

| $\frac{y}{c}$ | $\frac{\bar{u}}{U_\infty}$ | $\frac{\sqrt{\overline{\Delta u^2}}}{\bar{u}}$ |
|---|---|---|
| 0.00020 | 0.078 | 0.101 |
| .00027 | .330 | .100 |
| .00033 | 1.252 | .203 |
| .00040 | 1.336 | .009 |
| .00047 | 1.304 | .008 |
| .00060 | 1.278 | .008 |
| .00090 | 1.253 | .008 |
| .00157 | 1.204 | .007 |

**x/c = 0; α = 4°**

| $\frac{y}{c}$ | $\frac{\bar{u}}{U_\infty}$ | $\frac{\sqrt{\overline{\Delta u^2}}}{\bar{u}}$ |
|---|---|---|
| .00013 | .016 | .120 |
| .00023 | .025 | .148 |
| .00035 | .039 | .206 |
| .00047 | .685 | .229 |
| .00060 | 1.318 | .017 |
| .00075 | 1.331 | .017 |
| .00103 | 1.313 | .017 |
| .00150 | 1.299 | .017 |
| .00270 | 1.269 | .015 |

**x/c = 0; α = 6°**

| $\frac{y}{c}$ | $\frac{\bar{u}}{U_\infty}$ | $\frac{\sqrt{\overline{\Delta u^2}}}{\bar{u}}$ |
|---|---|---|
| .00013 | .021 | .155 |
| .00023 | .022 | .212 |
| .00035 | .022 | .273 |
| .00048 | .022 | .356 |
| .00061 | .022 | .432 |
| .00075 | .022 | .439 |
| .00088 | .020 | .490 |
| .00095 | .021 | .480 |
| .00103 | .030 | .432 |
| .00110 | .063 | .429 |
| .00117 | .098 | .444 |
| .00123 | .330 | .344 |
| .00132 | .655 | .250 |
| .00140 | .907 | .201 |
| .00153 | 1.246 | .084 |
| .00167 | 1.305 | .038 |
| .00177 | 1.325 | .034 |
| .00190 | 1.319 | .026 |
| .00238 | 1.300 | .017 |
| .00310 | 1.287 | .013 |
| .00402 | 1.263 | .011 |

**x/c = 0.01; α = 2°**

| $\frac{y}{c}$ | $\frac{\bar{u}}{U_\infty}$ | $\frac{\sqrt{\overline{\Delta u^2}}}{\bar{u}}$ |
|---|---|---|
| .00012 | .057 | .574 |
| .00045 | .152 | .492 |
| .00078 | .181 | .462 |
| .00112 | .180 | .455 |
| .00145 | .178 | .445 |
| .00178 | .178 | .445 |
| .00212 | .172 | .433 |
| .00245 | .164 | .427 |
| .00278 | .151 | .374 |
| .00312 | .163 | .372 |
| .00345 | .235 | .329 |
| .00378 | .267 | .331 |
| .00412 | .479 | .293 |
| .00445 | .681 | .237 |
| .00478 | .931 | .198 |
| .00512 | 1.066 | .125 |
| .00545 | 1.225 | .086 |
| .00595 | 1.313 | .041 |
| .00645 | 1.334 | .022 |
| 0.00695 | 1.329 | 0.015 |
| .00745 | 1.323 | .012 |
| .00825 | 1.318 | .008 |
| .00978 | 1.293 | .006 |
| .01245 | 1.265 | .005 |

**x/c = 0.01; α = 4°**

| $\frac{y}{c}$ | $\frac{\bar{u}}{U_\infty}$ | $\frac{\sqrt{\overline{\Delta u^2}}}{\bar{u}}$ |
|---|---|---|
| .00012 | .031 | .564 |
| .00132 | .062 | .452 |
| .00232 | .079 | .415 |
| .00332 | .086 | .411 |
| .00432 | .101 | .411 |
| .00532 | .105 | .417 |
| .00632 | .148 | .395 |
| .00681 | .255 | .356 |
| .00732 | .442 | .282 |
| .00782 | .700 | .210 |
| .00832 | .875 | .142 |
| .00882 | 1.088 | .084 |
| .00932 | 1.262 | .053 |
| .01032 | 1.310 | .020 |
| .01132 | 1.281 | .013 |
| .01265 | 1.263 | .011 |
| .01598 | 1.253 | .009 |

**x/c = 0.01; α = 6°**

| $\frac{y}{c}$ | $\frac{\bar{u}}{U_\infty}$ | $\frac{\sqrt{\overline{\Delta u^2}}}{\bar{u}}$ |
|---|---|---|
| .00008 | .039 | .127 |
| .00108 | .063 | .333 |
| .00442 | .103 | .314 |
| .00775 | .135 | .323 |
| .00608 | .109 | .319 |
| .00275 | .076 | .332 |
| .00875 | .131 | .318 |
| .00975 | .198 | .330 |
| .01025 | .307 | .316 |
| .01075 | .431 | .259 |
| .01125 | .605 | .209 |
| .01175 | .811 | .166 |
| .01225 | 1.108 | .128 |
| .01275 | 1.191 | .100 |
| .01325 | 1.297 | .065 |
| .01375 | 1.347 | .041 |
| .01425 | 1.358 | .029 |
| .01475 | 1.349 | .026 |
| .01575 | 1.336 | .018 |
| .01708 | 1.315 | .010 |
| .01908 | 1.297 | .007 |
| .02175 | 1.277 | .006 |

**¹x/c = 0.05; α = 2°**

| $\frac{y}{c}$ | $\frac{\bar{u}}{U_\infty}$ | $\frac{\sqrt{\overline{\Delta u^2}}}{\bar{u}}$ |
|---|---|---|
| .00042 | .229 | .383 |
| .00058 | .213 | .381 |
| .00125 | .231 | .371 |
| .00192 | .265 | .379 |
| .00258 | .398 | .337 |

**x/c = 0.05; α = 2°**

| $\frac{y}{c}$ | $\frac{\bar{u}}{U_\infty}$ | $\frac{\sqrt{\overline{\Delta u^2}}}{\bar{u}}$ |
|---|---|---|
| .00017 | .186 | .394 |
| .00103 | .240 | .307 |
| .00353 | .289 | .329 |
| .00603 | .484 | .353 |
| .00887 | .888 | .293 |
| .01137 | 1.098 | .131 |
| 0.01387 | 1.203 | 0.049 |
| .01637 | 1.209 | .025 |
| .01887 | 1.203 | .017 |
| .02137 | 1.215 | .013 |
| .02387 | 1.192 | .010 |

**¹x/c = 0.05; α = 4°**

| $\frac{y}{c}$ | $\frac{\bar{u}}{U_\infty}$ | $\frac{\sqrt{\overline{\Delta u^2}}}{\bar{u}}$ |
|---|---|---|
| .00042 | .102 | .597 |
| .00125 | .123 | .588 |
| .00192 | .141 | .575 |
| .00258 | .146 | .543 |
| .00425 | .171 | .518 |
| .00592 | .180 | .527 |
| .00758 | .173 | .473 |
| .00925 | .216 | .481 |
| .01090 | .301 | .461 |
| .01260 | .389 | .440 |

**x/c = 0.05; α = 4°**

| $\frac{y}{c}$ | $\frac{\bar{u}}{U_\infty}$ | $\frac{\sqrt{\overline{\Delta u^2}}}{\bar{u}}$ |
|---|---|---|
| .00987 | .174 | .348 |
| .01237 | .170 | .308 |
| .01453 | .169 | .286 |
| .01703 | .234 | .281 |
| .01953 | .447 | .301 |
| .02203 | .799 | .283 |
| .02453 | 1.144 | .185 |
| .02703 | 1.282 | .099 |
| .02953 | 1.324 | .039 |
| .03203 | 1.324 | .023 |
| .03608 | 1.304 | .013 |
| .04103 | 1.278 | .009 |
| .04770 | 1.266 | .006 |

**¹x/c = 0.05; α = 6°**

| $\frac{y}{c}$ | $\frac{\bar{u}}{U_\infty}$ | $\frac{\sqrt{\overline{\Delta u^2}}}{\bar{u}}$ |
|---|---|---|
| .00042 | .041 | .650 |
| .00258 | .075 | .510 |
| .00592 | .098 | .521 |
| .00925 | .121 | .481 |
| .01258 | .153 | .480 |
| .01592 | .174 | .489 |
| .01925 | .217 | .473 |
| .02258 | .339 | .443 |

**x/c = 0.05; α = 6°**

| $\frac{y}{c}$ | $\frac{\bar{u}}{U_\infty}$ | $\frac{\sqrt{\overline{\Delta u^2}}}{\bar{u}}$ |
|---|---|---|
| .01960 | .158 | .447 |
| .02220 | .145 | .426 |
| .02470 | .206 | .356 |
| .02720 | .364 | .449 |
| .02970 | .651 | .503 |
| .03160 | .864 | .423 |
| .03410 | 1.184 | .303 |
| .03660 | 1.329 | .174 |
| .03910 | 1.365 | .073 |
| .04160 | 1.378 | .049 |
| .04410 | 1.378 | .033 |
| .04660 | 1.365 | .025 |
| .04910 | 1.358 | .021 |
| .05450 | 1.358 | .016 |

**x/c = 0.10; α = 2°**

| $\frac{y}{c}$ | $\frac{\bar{u}}{U_\infty}$ | $\frac{\sqrt{\overline{\Delta u^2}}}{\bar{u}}$ |
|---|---|---|
| .00008 | .138 | .324 |
| .00075 | .494 | .267 |
| .00242 | .581 | .273 |
| 0.00575 | 0.679 | 0.242 |
| .00908 | .826 | .239 |
| .01242 | .944 | .170 |
| .01575 | .999 | .098 |
| .01908 | 1.040 | .042 |
| .02242 | 1.040 | .025 |
| .02575 | 1.040 | .016 |
| .03242 | 1.046 | .009 |
| .03968 | 1.046 | .005 |

**¹x/c = 0.10; α = 4°**

| $\frac{y}{c}$ | $\frac{\bar{u}}{U_\infty}$ | $\frac{\sqrt{\overline{\Delta u^2}}}{\bar{u}}$ |
|---|---|---|
| 0 | .204 | .548 |
| .00202 | .336 | .416 |
| .00701 | .313 | .424 |
| .01202 | .273 | .456 |
| .01468 | .260 | .439 |
| .01735 | .256 | .441 |
| .02002 | .291 | .440 |
| .02268 | .384 | .421 |
| .02535 | .536 | .388 |

**x/c = 0.10; α = 4°**

| $\frac{y}{c}$ | $\frac{\bar{u}}{U_\infty}$ | $\frac{\sqrt{\overline{\Delta u^2}}}{\bar{u}}$ |
|---|---|---|
| .01110 | .299 | .429 |
| .01610 | .250 | .429 |
| .02110 | .289 | .408 |
| .02610 | .448 | .390 |
| .03110 | .751 | .376 |
| .03610 | 1.160 | .240 |
| .04110 | 1.337 | .109 |
| .04610 | 1.337 | .043 |
| .05110 | 1.333 | .027 |
| .05610 | 1.315 | .016 |
| .06110 | 1.297 | .013 |
| .06610 | 1.290 | .011 |

**¹x/c = 0.10; α = 6°**

| $\frac{y}{c}$ | $\frac{\bar{u}}{U_\infty}$ | $\frac{\sqrt{\overline{\Delta u^2}}}{\bar{u}}$ |
|---|---|---|
| .00035 | .078 | .639 |
| .00202 | .139 | .550 |
| .00702 | .174 | .516 |
| .01202 | .189 | .486 |
| .01702 | .201 | .482 |
| .02202 | .201 | .472 |
| .02702 | .181 | .465 |
| .03202 | .228 | .454 |
| .03702 | .353 | .423 |

**x/c = 0.10; α = 6°**

| $\frac{y}{c}$ | $\frac{\bar{u}}{U_\infty}$ | $\frac{\sqrt{\overline{\Delta u^2}}}{\bar{u}}$ |
|---|---|---|
| .02110 | .190 | .451 |
| .02610 | .190 | .434 |
| .03110 | .186 | .436 |
| .03610 | .222 | .457 |
| .04110 | .419 | .399 |
| .04610 | .774 | .358 |
| .05110 | 1.076 | .237 |
| .05610 | 1.266 | .121 |
| .06110 | 1.325 | .086 |
| .06610 | 1.338 | .028 |
| .07110 | 1.338 | .017 |

**x/c = 0.20; α = 2°**

| $\frac{y}{c}$ | $\frac{\bar{u}}{U_\infty}$ | $\frac{\sqrt{\overline{\Delta u^2}}}{\bar{u}}$ |
|---|---|---|
| .00013 | .145 | .259 |
| .00093 | .655 | .151 |
| .00260 | .767 | .135 |

¹Reverse-flow probe.

## TABLE III.- RESULTS FROM HOT-WIRE ANEMOMETER
### SURVEYS - Concluded

Column headers for all sub-tables: $\frac{y}{c}$, $\frac{\bar{u}}{U_\infty}$, $\frac{\sqrt{\overline{\Delta u^2}}}{\bar{u}}$

| $\frac{y}{c}$ | $\frac{\bar{u}}{U_\infty}$ | $\frac{\sqrt{\overline{\Delta u^2}}}{\bar{u}}$ |
|---|---|---|
| 0.00493 | 0.814 | 0.133 |
| .00827 | .825 | .134 |
| .01490 | .905 | .115 |
| .02160 | .996 | .737 |
| .02830 | 1.025 | .321 |
| .03490 | 1.040 | .152 |
| .04830 | 1.025 | .054 |
| .06160 | 1.015 | .030 |

[1]x/c = 0.20; α = 4°

| $\frac{y}{c}$ | $\frac{\bar{u}}{U_\infty}$ | $\frac{\sqrt{\overline{\Delta u^2}}}{\bar{u}}$ |
|---|---|---|
| .00030 | .190 | .544 |
| .00163 | .269 | .455 |
| .00297 | .261 | .435 |
| .00630 | .260 | .427 |
| .00963 | .256 | .440 |
| .01463 | .270 | .443 |
| .01963 | .299 | .457 |
| .02463 | .360 | .457 |
| .02963 | .491 | .450 |

x/c = 0.20; α = 4°

| $\frac{y}{c}$ | $\frac{\bar{u}}{U_\infty}$ | $\frac{\sqrt{\overline{\Delta u^2}}}{\bar{u}}$ |
|---|---|---|
| .00493 | .286 | .380 |
| .00116 | .286 | .387 |
| .01830 | .306 | .437 |
| .02490 | .402 | .452 |
| .03490 | .772 | .409 |
| .04490 | 1.042 | .252 |
| .05490 | 1.186 | .109 |
| .06490 | 1.203 | .046 |
| .07490 | 1.198 | .025 |
| .08490 | 1.192 | .017 |
| .09830 | 1.167 | .011 |

[1]x/c = 0.20; α = 6°

| $\frac{y}{c}$ | $\frac{\bar{u}}{U_\infty}$ | $\frac{\sqrt{\overline{\Delta u^2}}}{\bar{u}}$ |
|---|---|---|
| .00030 | .147 | .593 |
| .00163 | .260 | .471 |
| .00297 | .269 | .443 |
| .00797 | .283 | .424 |
| .01297 | .307 | .427 |
| .01963 | .261 | .467 |
| .02630 | .259 | .474 |
| .03297 | .229 | .477 |
| .03963 | .229 | .467 |
| .04630 | .251 | .455 |
| .05297 | .332 | .454 |
| .05963 | .507 | .379 |

x/c = 0.20; α = 6°

| $\frac{y}{c}$ | $\frac{\bar{u}}{U_\infty}$ | $\frac{\sqrt{\overline{\Delta u^2}}}{\bar{u}}$ |
|---|---|---|
| .03145 | .263 | .441 |
| .03812 | .260 | .434 |
| .04478 | .285 | .438 |
| .05145 | .370 | .436 |
| .05812 | .524 | .402 |
| .06478 | .732 | .352 |
| .07145 | .920 | .330 |
| .07812 | 1.146 | .217 |
| .08478 | 1.320 | .165 |
| .09145 | 1.352 | .072 |
| .09812 | 1.363 | .044 |
| .10478 | 1.345 | .025 |
| .11145 | 1.320 | .018 |
| .11812 | 1.305 | .015 |

x/c = 0.30; α = 2°

| $\frac{y}{c}$ | $\frac{\bar{u}}{U_\infty}$ | $\frac{\sqrt{\overline{\Delta u^2}}}{\bar{u}}$ |
|---|---|---|
| 0.00017 | 0.199 | 0.262 |
| .00033 | .507 | .147 |
| .00200 | .754 | .118 |
| .00367 | .803 | .108 |
| .00700 | .852 | .103 |
| .01367 | .904 | .099 |
| .02367 | .978 | .080 |
| .03367 | 1.034 | .034 |
| .04367 | 1.040 | .013 |
| .05367 | 1.046 | .007 |

x/c = 0.30; α = 4°

| $\frac{y}{c}$ | $\frac{\bar{u}}{U_\infty}$ | $\frac{\sqrt{\overline{\Delta u^2}}}{\bar{u}}$ |
|---|---|---|
| .00017 | .040 | .488 |
| .00037 | .106 | .652 |
| .00203 | .171 | .546 |
| .00370 | .206 | .519 |
| .00703 | .254 | .507 |
| .01370 | .348 | .494 |
| .02303 | .471 | .447 |
| .03700 | .714 | .348 |
| .05036 | .956 | .235 |
| .06370 | 1.078 | .115 |
| .07703 | 1.084 | .048 |
| .09030 | 1.084 | .025 |
| .10360 | 1.090 | .016 |

[1]x/c = 0.30; α = 6°

| $\frac{y}{c}$ | $\frac{\bar{u}}{U_\infty}$ | $\frac{\sqrt{\overline{\Delta u^2}}}{\bar{u}}$ |
|---|---|---|
| .00020 | .151 | .514 |
| .00135 | .358 | .448 |
| .00635 | .366 | .396 |
| .01300 | .349 | .400 |
| .01967 | .345 | .436 |
| .02636 | .310 | .453 |
| .03333 | .292 | .451 |
| .03970 | .286 | .439 |
| .04620 | .301 | .462 |
| .05300 | .335 | .457 |
| .05970 | .422 | .438 |

x/c = 0.30; α = 6°

| $\frac{y}{c}$ | $\frac{\bar{u}}{U_\infty}$ | $\frac{\sqrt{\overline{\Delta u^2}}}{\bar{u}}$ |
|---|---|---|
| .02200 | .330 | .444 |
| .03200 | .296 | .451 |
| .04200 | .285 | .468 |
| .05200 | .354 | .455 |
| .06200 | .477 | .441 |
| .07200 | .682 | .400 |
| .08200 | .935 | .321 |
| .09200 | 1.167 | .207 |
| .10200 | 1.289 | .141 |
| .11200 | 1.300 | .079 |
| .12200 | 1.300 | .034 |
| .13200 | 1.300 | .024 |

x/c = 0.45; α = 2°

| $\frac{y}{c}$ | $\frac{\bar{u}}{U_\infty}$ | $\frac{\sqrt{\overline{\Delta u^2}}}{\bar{u}}$ |
|---|---|---|
| .00013 | .150 | .191 |
| .00053 | .605 | .107 |
| .00187 | .737 | .092 |
| .00353 | .788 | .086 |
| .00507 | .834 | .080 |

| $\frac{y}{c}$ | $\frac{\bar{u}}{U_\infty}$ | $\frac{\sqrt{\overline{\Delta u^2}}}{\bar{u}}$ |
|---|---|---|
| 0.00840 | 0.884 | 0.075 |
| .01186 | .906 | .067 |
| .02190 | .954 | .061 |
| .03190 | .990 | .044 |
| .04140 | .992 | .021 |
| .05190 | .992 | .009 |

x/c = 0.45; α = 4°

| $\frac{y}{c}$ | $\frac{\bar{u}}{U_\infty}$ | $\frac{\sqrt{\overline{\Delta u^2}}}{\bar{u}}$ |
|---|---|---|
| .00017 | .121 | .451 |
| .00057 | .384 | .362 |
| .00190 | .473 | .320 |
| .00856 | .584 | .283 |
| .02190 | .692 | .257 |
| .03520 | .790 | .236 |
| .04860 | .866 | .195 |
| .06190 | .967 | .136 |
| .07520 | 1.003 | .087 |
| .08860 | 1.022 | .043 |
| .10180 | 1.030 | .026 |

[1]x/c = 0.45; α = 6°

| $\frac{y}{c}$ | $\frac{\bar{u}}{U_\infty}$ | $\frac{\sqrt{\overline{\Delta u^2}}}{\bar{u}}$ |
|---|---|---|
| .00233 | .248 | .468 |
| .00400 | .248 | .448 |
| .00733 | .254 | .420 |
| .01400 | .278 | .432 |
| .02733 | .279 | .450 |
| .04066 | .330 | .448 |
| .06066 | .511 | .440 |

x/c = 0.45; α = 6°

| $\frac{y}{c}$ | $\frac{\bar{u}}{U_\infty}$ | $\frac{\sqrt{\overline{\Delta u^2}}}{\bar{u}}$ |
|---|---|---|
| .01824 | .255 | .452 |
| .02490 | .260 | .471 |
| .03160 | .286 | .479 |
| .03820 | .330 | .491 |
| .05160 | .390 | .481 |
| .06490 | .553 | .437 |
| .07820 | .763 | .399 |
| .09140 | .918 | .285 |
| .10480 | 1.097 | .183 |
| .11820 | 1.181 | .105 |
| .13160 | 1.186 | .053 |
| .13960 | 1.208 | .043 |

x/c = 0.60; α = 2°

| $\frac{y}{c}$ | $\frac{\bar{u}}{U_\infty}$ | $\frac{\sqrt{\overline{\Delta u^2}}}{\bar{u}}$ |
|---|---|---|
| .00010 | .193 | .199 |
| .00050 | .590 | .123 |
| .00220 | .726 | .095 |
| .00550 | .827 | .077 |
| .00880 | .860 | .072 |
| .01550 | .897 | .065 |
| .02550 | .936 | .054 |
| .03880 | .980 | .036 |
| .05220 | 1.000 | .016 |
| .06550 | 1.100 | .007 |

x/c = 0.60; α = 4°

| $\frac{y}{c}$ | $\frac{\bar{u}}{U_\infty}$ | $\frac{\sqrt{\overline{\Delta u^2}}}{\bar{u}}$ |
|---|---|---|
| .00001 | .107 | .295 |
| .00050 | .458 | .253 |
| .00180 | .564 | .227 |
| .00520 | .620 | .222 |
| .00680 | .675 | .213 |
| .02020 | .737 | .204 |

| $\frac{y}{c}$ | $\frac{\bar{u}}{U_\infty}$ | $\frac{\sqrt{\overline{\Delta u^2}}}{\bar{u}}$ |
|---|---|---|
| .03350 | .811 | .198 |
| .04690 | .878 | .182 |
| .06020 | .960 | .149 |
| .07350 | 1.003 | .120 |
| .08680 | 1.012 | .064 |
| .10020 | 1.020 | .040 |
| .11350 | 1.020 | .021 |

x/c = 0.60; α = 6°

| $\frac{y}{c}$ | $\frac{\bar{u}}{U_\infty}$ | $\frac{\sqrt{\overline{\Delta u^2}}}{\bar{u}}$ |
|---|---|---|
| .00010 | .079 | .403 |
| .00050 | .119 | .580 |
| .00190 | .158 | .514 |
| .00520 | .188 | .488 |
| .01850 | .264 | .468 |
| .03180 | .362 | .466 |
| .04520 | .425 | .457 |
| .05850 | .538 | .433 |
| .07850 | .727 | .353 |
| .09850 | .956 | .242 |
| .11850 | 1.077 | .145 |
| .13850 | 1.087 | .069 |
| .15040 | 1.102 | .050 |
| .16900 | 1.119 | .031 |

x/c = 0.80; α = 2°

| $\frac{y}{c}$ | $\frac{\bar{u}}{U_\infty}$ | $\frac{\sqrt{\overline{\Delta u^2}}}{\bar{u}}$ |
|---|---|---|
| .00017 | .222 | .043 |
| .00067 | .572 | .063 |
| .00233 | .705 | .069 |
| .00400 | .760 | .067 |
| .01733 | .886 | .052 |
| .03070 | .943 | .050 |
| .04400 | .984 | .036 |
| .05735 | .995 | .014 |
| .07733 | 1.000 | .005 |
| .09070 | 1.000 | .003 |

x/c = 0.80; α = 4°

| $\frac{y}{c}$ | $\frac{\bar{u}}{U_\infty}$ | $\frac{\sqrt{\overline{\Delta u^2}}}{\bar{u}}$ |
|---|---|---|
| .00037 | .427 | .208 |
| .00237 | .618 | .176 |
| .00403 | .654 | .167 |
| .01070 | .718 | .162 |
| .02402 | .773 | .157 |
| .04402 | .840 | .146 |
| .06402 | .900 | .137 |
| .08402 | .956 | .106 |
| .10402 | .980 | .074 |
| .12402 | .994 | .037 |
| .14402 | .999 | .020 |
| .16000 | 1.000 | .013 |

x/c = 0.80; α = 6°

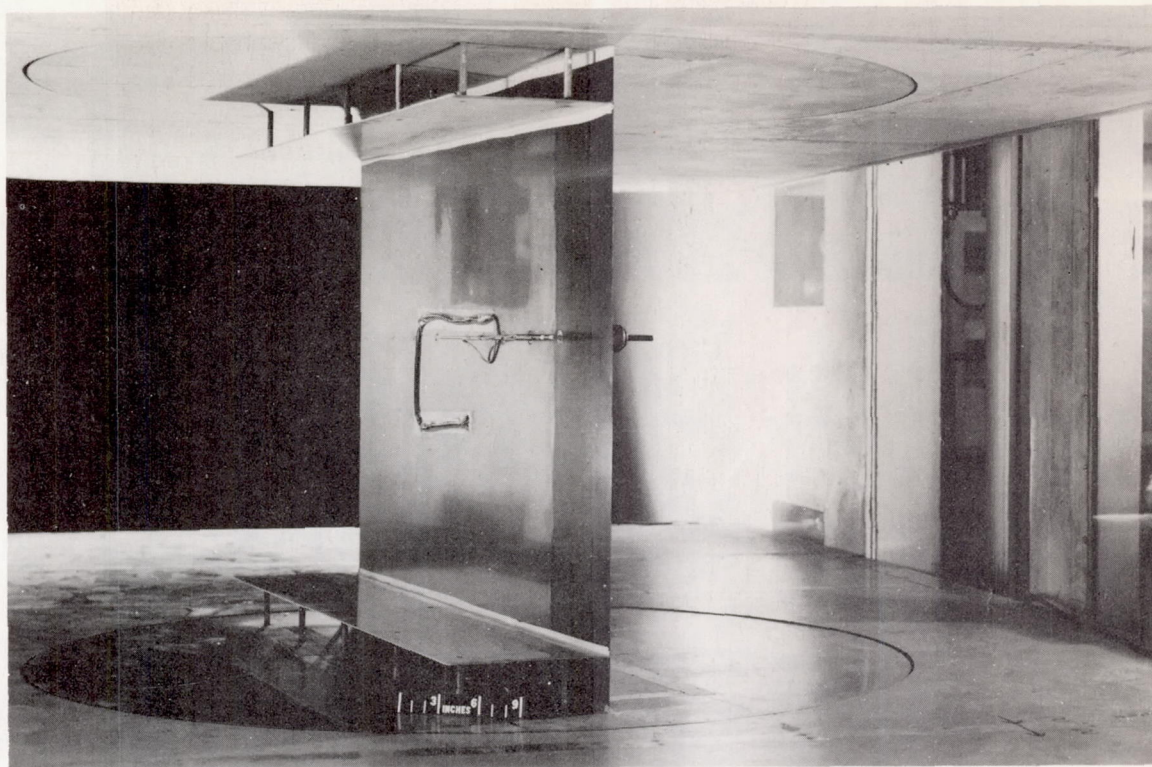| $\frac{y}{c}$ | $\frac{\bar{u}}{U_\infty}$ | $\frac{\sqrt{\overline{\Delta u^2}}}{\bar{u}}$ |
|---|---|---|
| .00037 | .164 | .564 |
| .00237 | .271 | .478 |
| .00403 | .321 | .429 |
| .01070 | .383 | .413 |
| .02402 | .425 | .387 |
| .04402 | .540 | .358 |
| .06402 | .639 | .319 |
| .08402 | .769 | .265 |
| .10402 | .900 | .208 |
| .12402 | .958 | .129 |
| .14402 | .984 | .082 |
| .16000 | 1.000 | .052 |

[1]Reverse-flow probe.

A-19240

Figure 1.- General arrangement of the Ames 7- by 10-foot wind tunnel
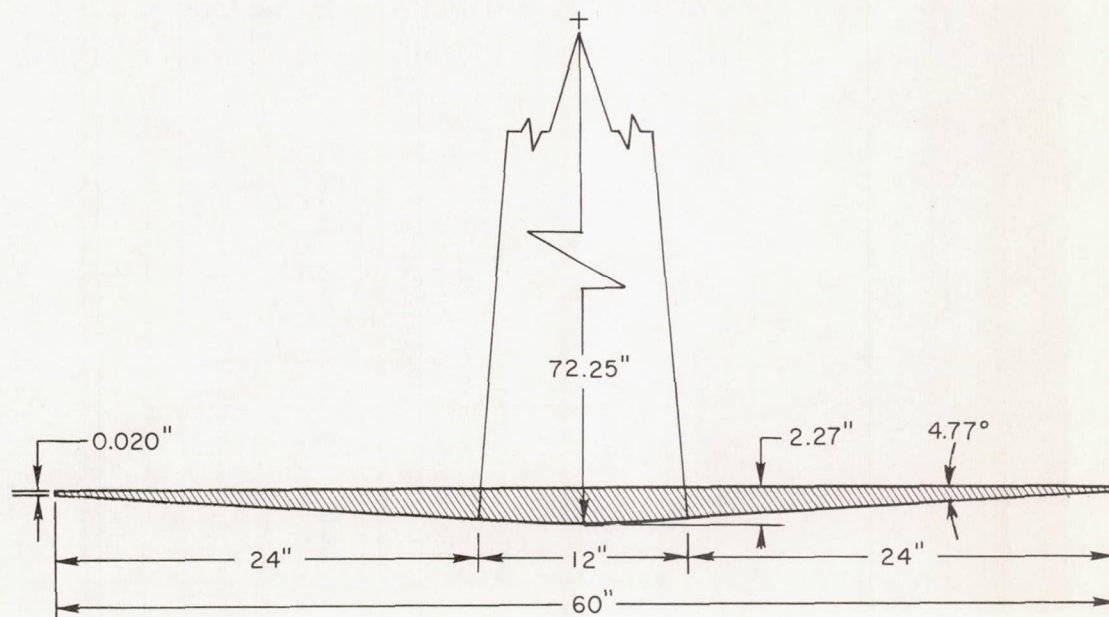with the false floor and ceiling installed.
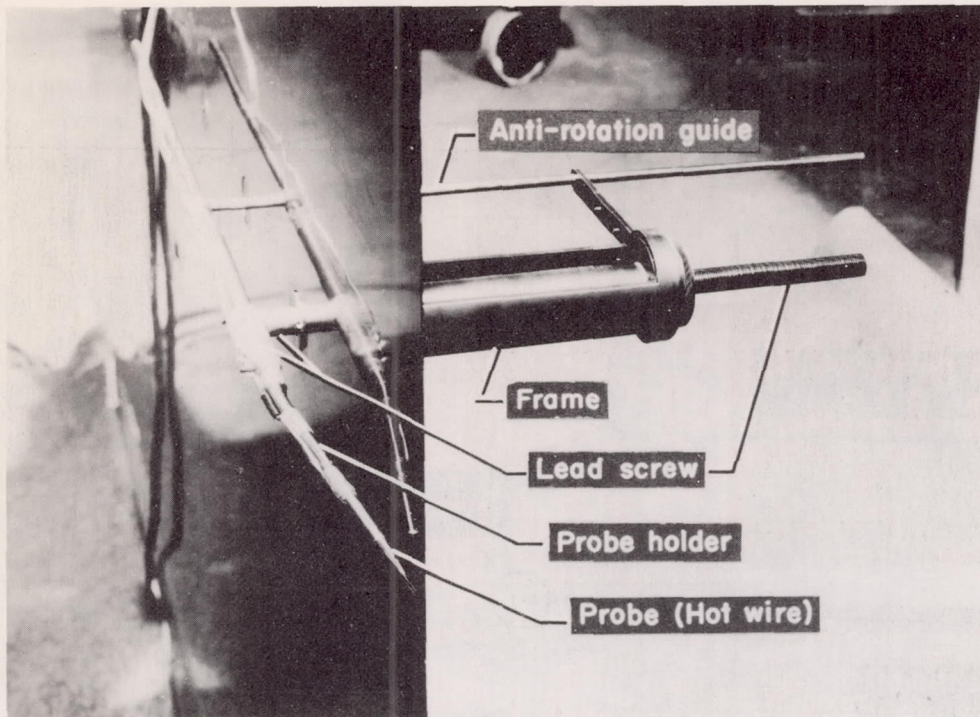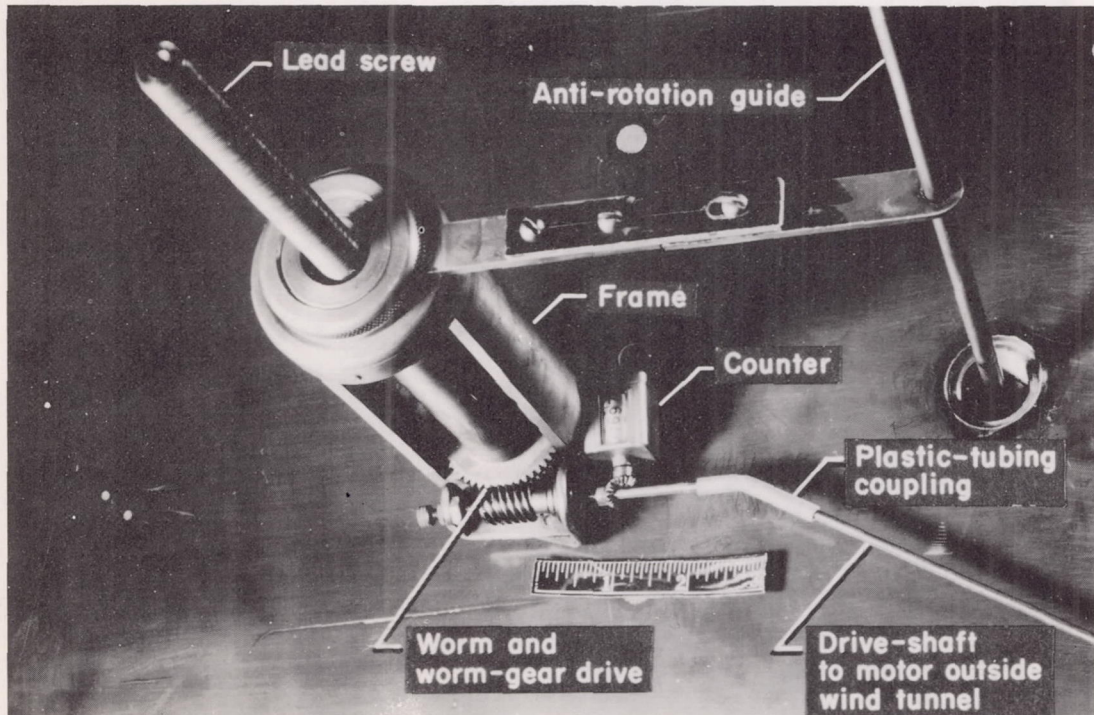
A-21009

Figure 2.- The geometry of the simulated flat plate and a view of the
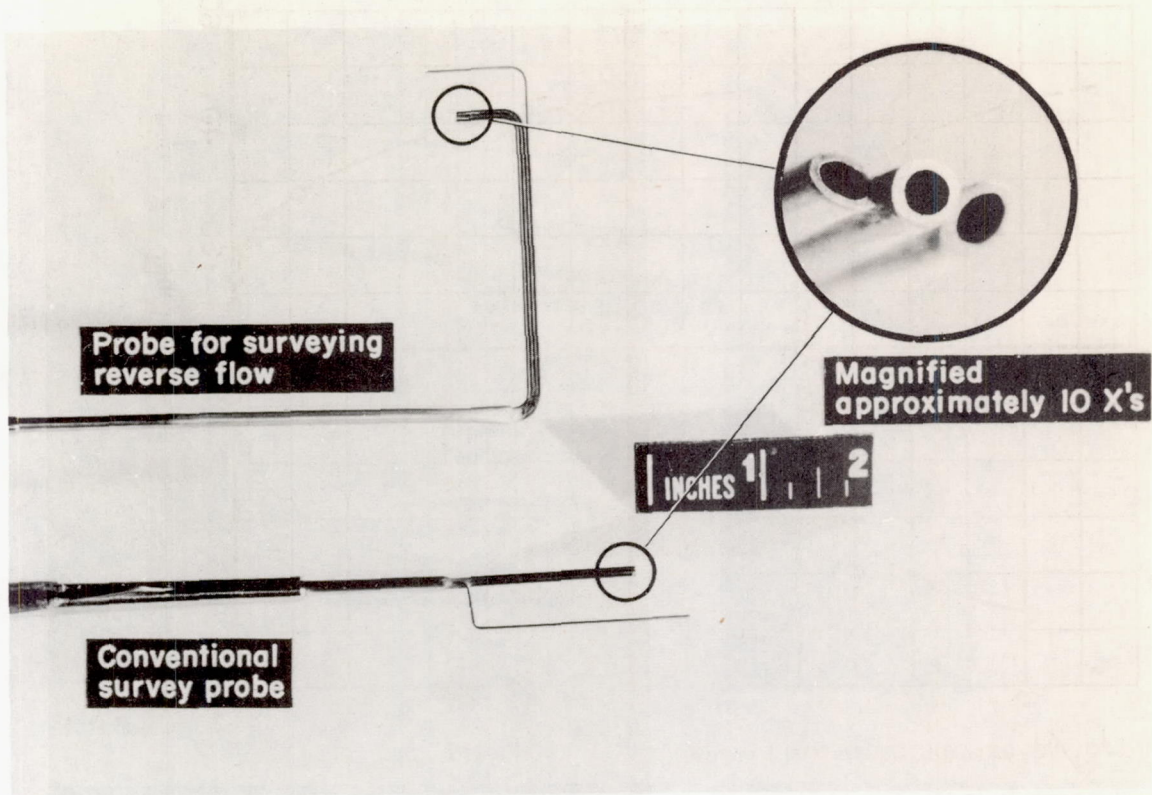model installed in the wind tunnel.
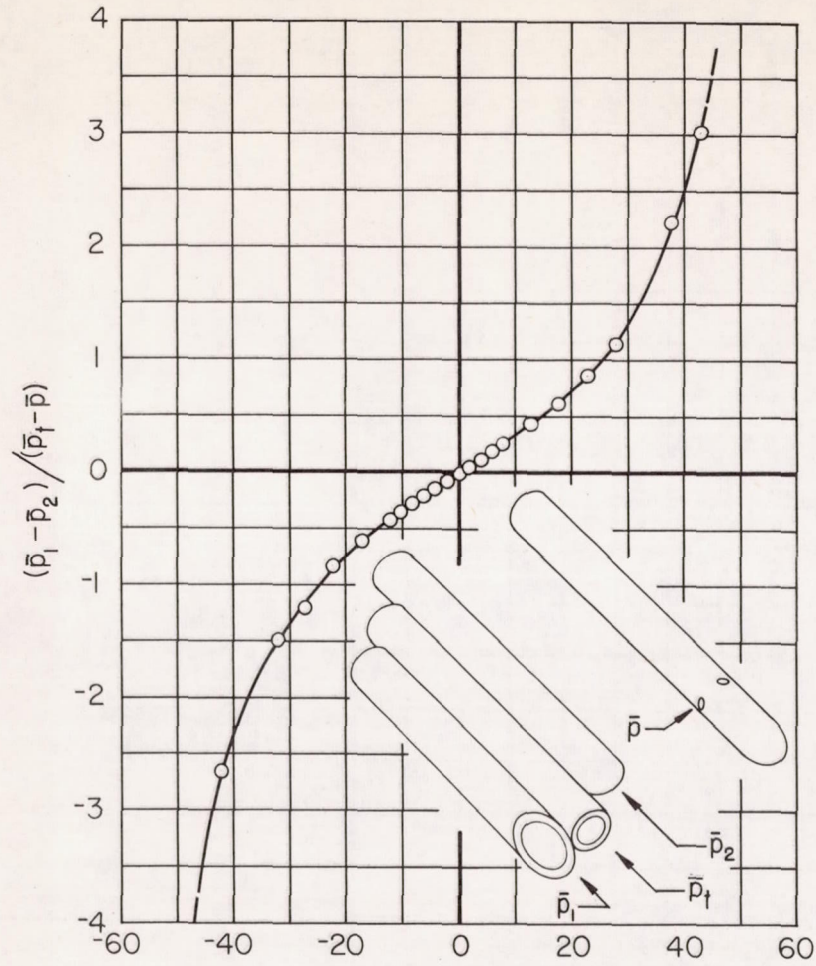
A-21007.1



A-21008.1

Figure 3.- The traversing mechanism employed for the pitot-static and
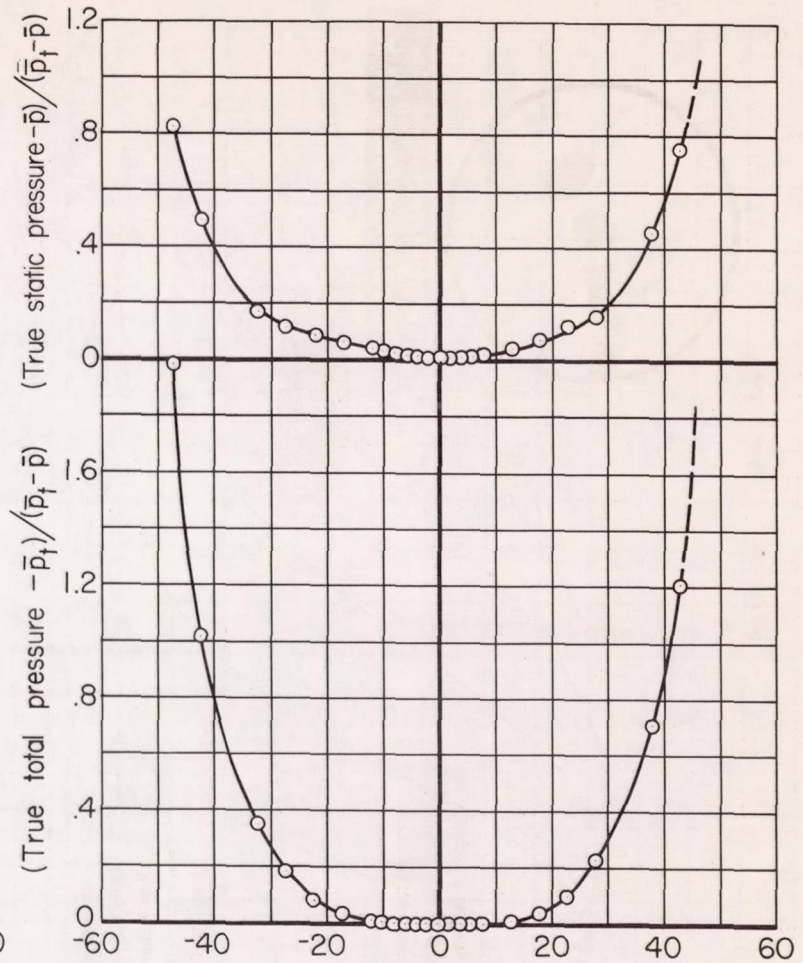hot-wire anemometer surveys.

A-21001.1

Figure 4.- The probes employed for the pitot-static surveys.
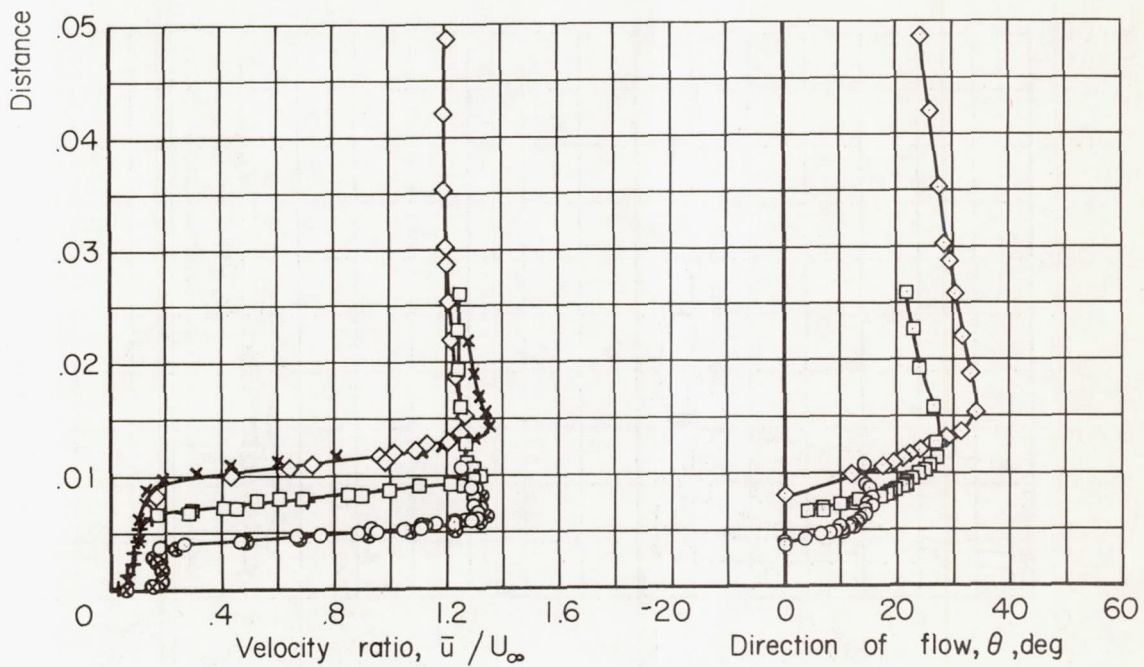
Figure 5.- A typical calibration for the pitot-static probes.
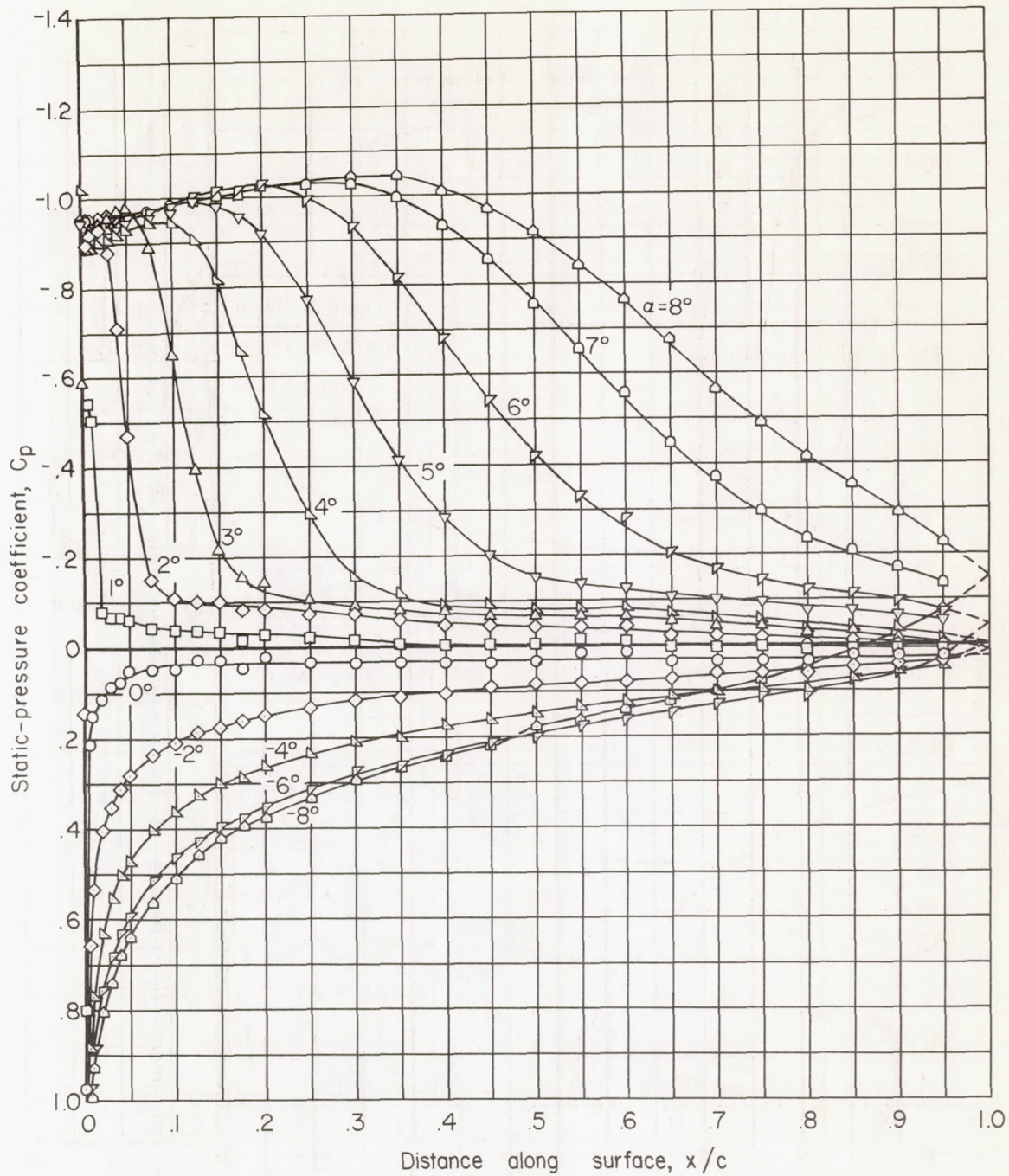
Figure 6.- Pressure distributions along the surface of the simulated flat plate.
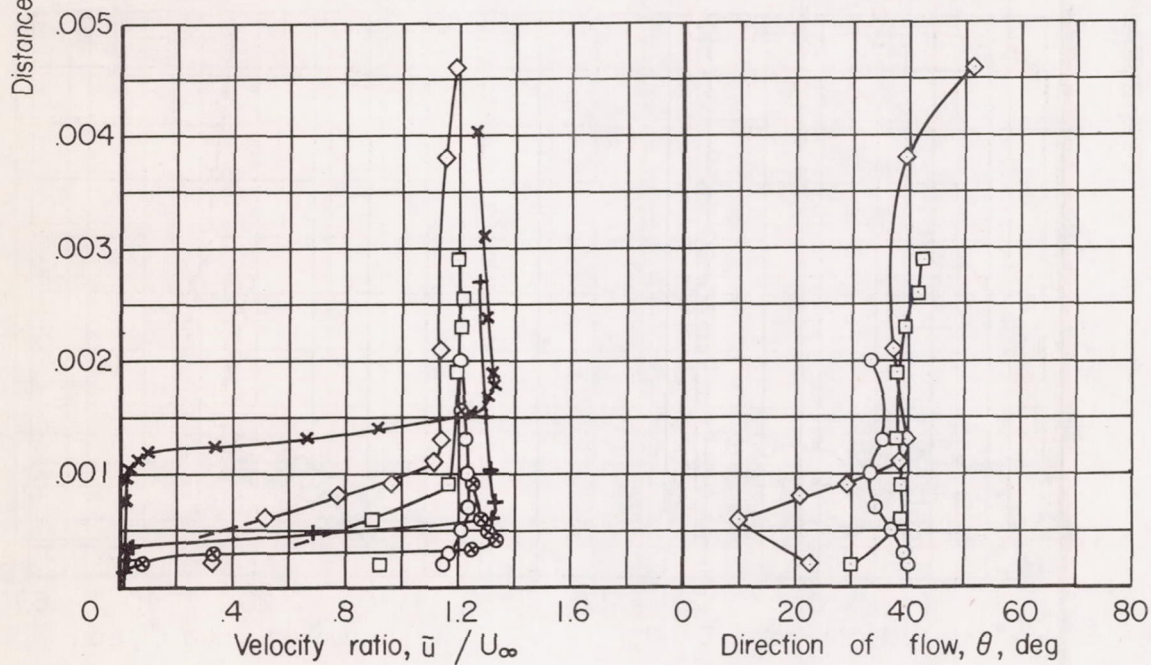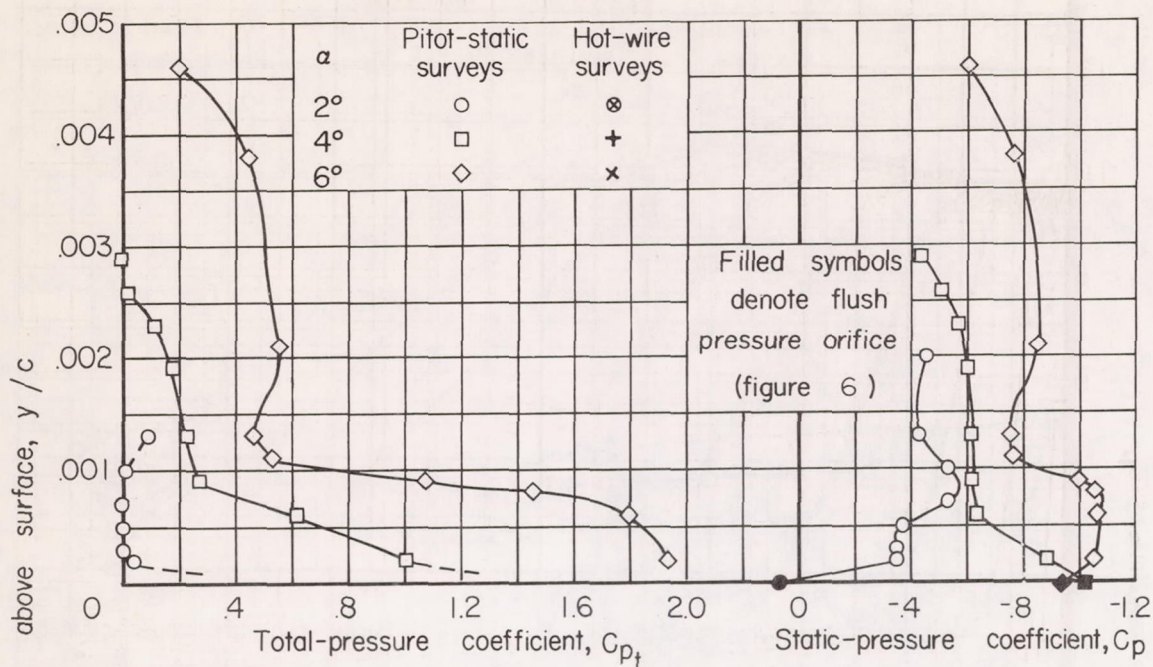
(a) x/c = 0

Figure 7.- Results from the pitot-static and hot-wire measurements of the mean flow.
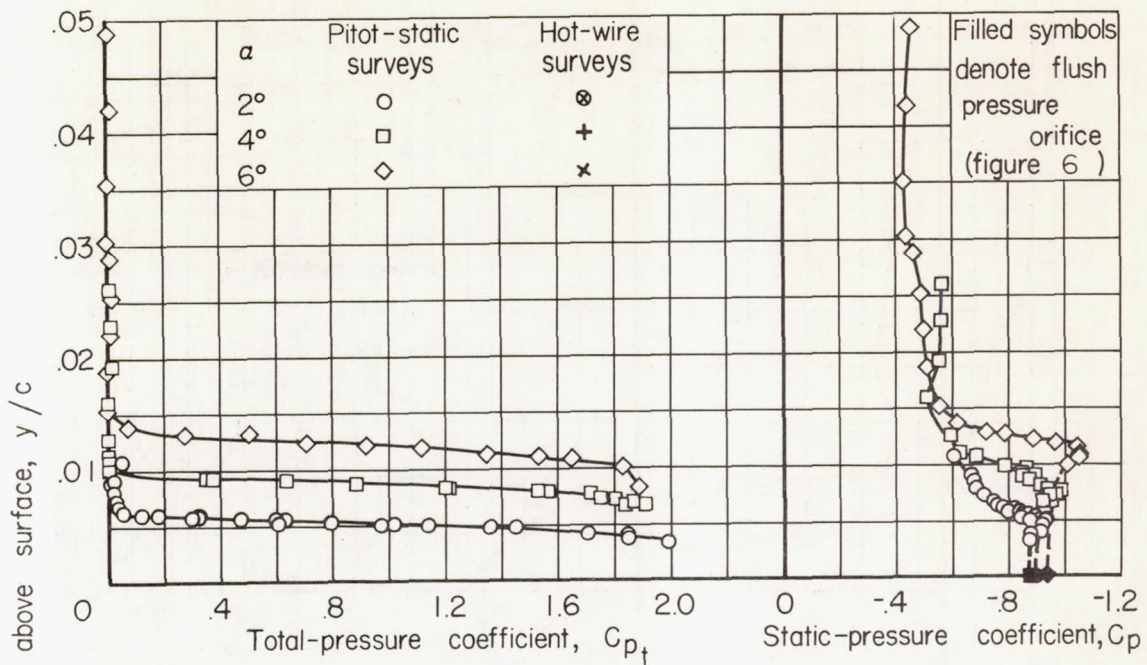
(b) x/c = 0.01

Figure 7.- Continued.
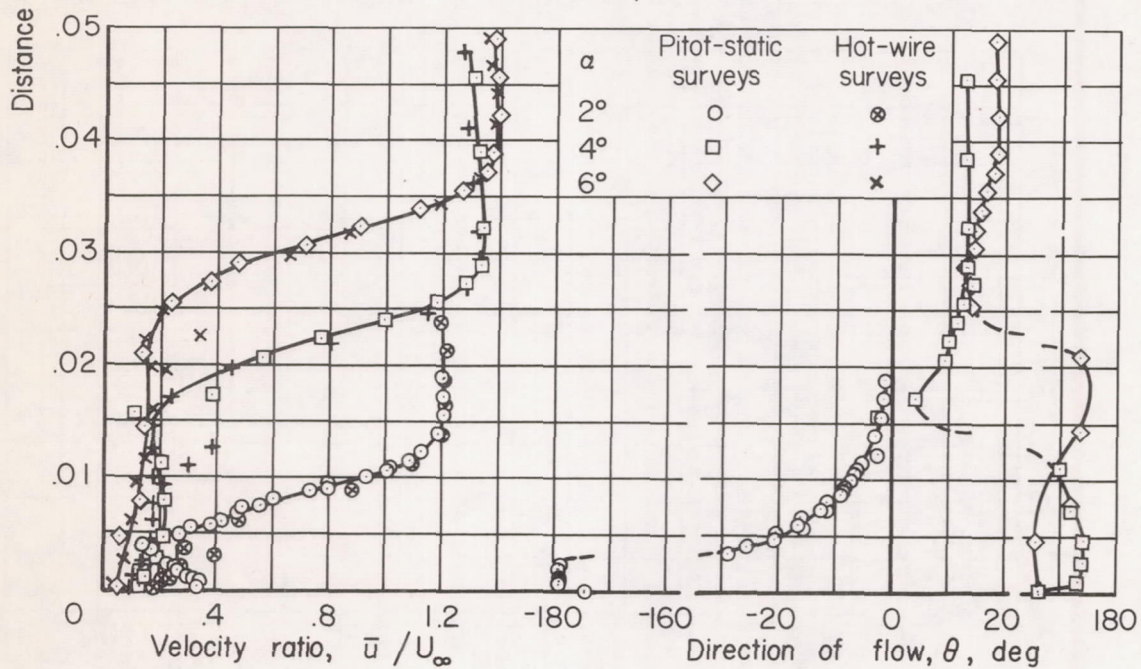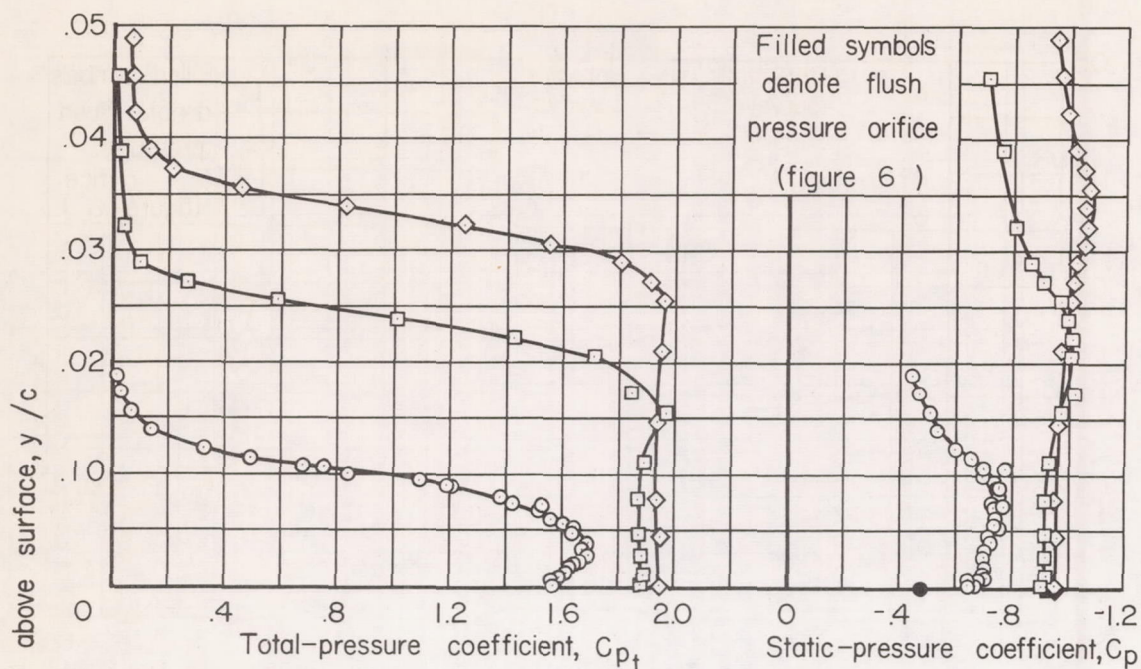
(c) x/c = 0.05

Figure 7.- Continued.
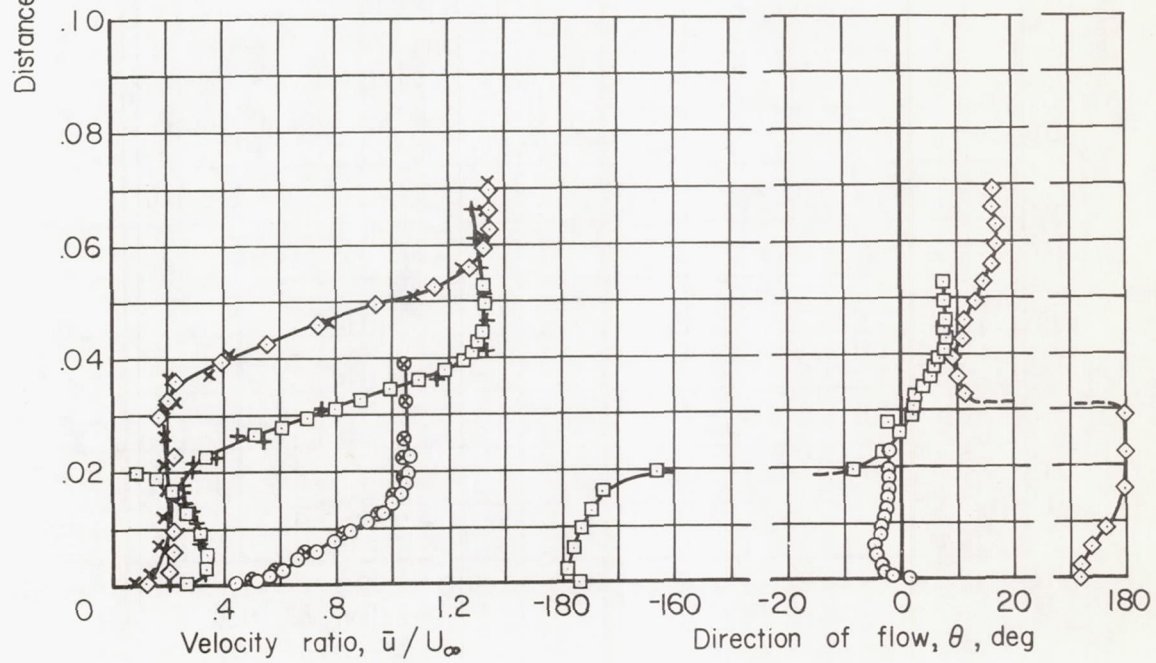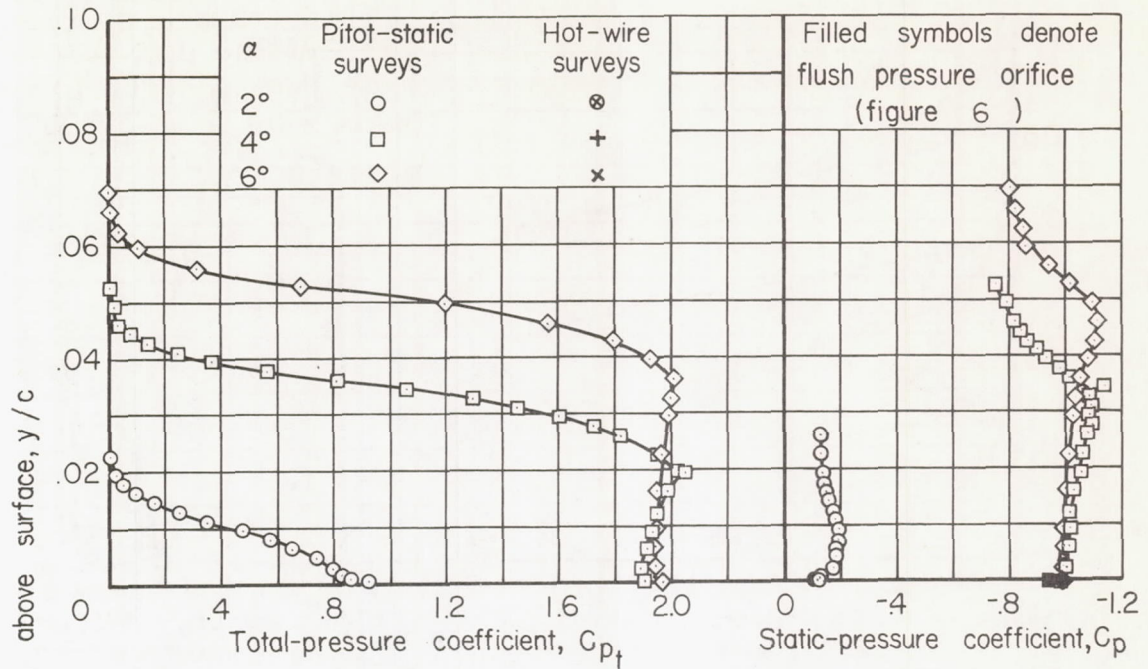
(d) x/c = 0.10

Figure 7.- Continued.
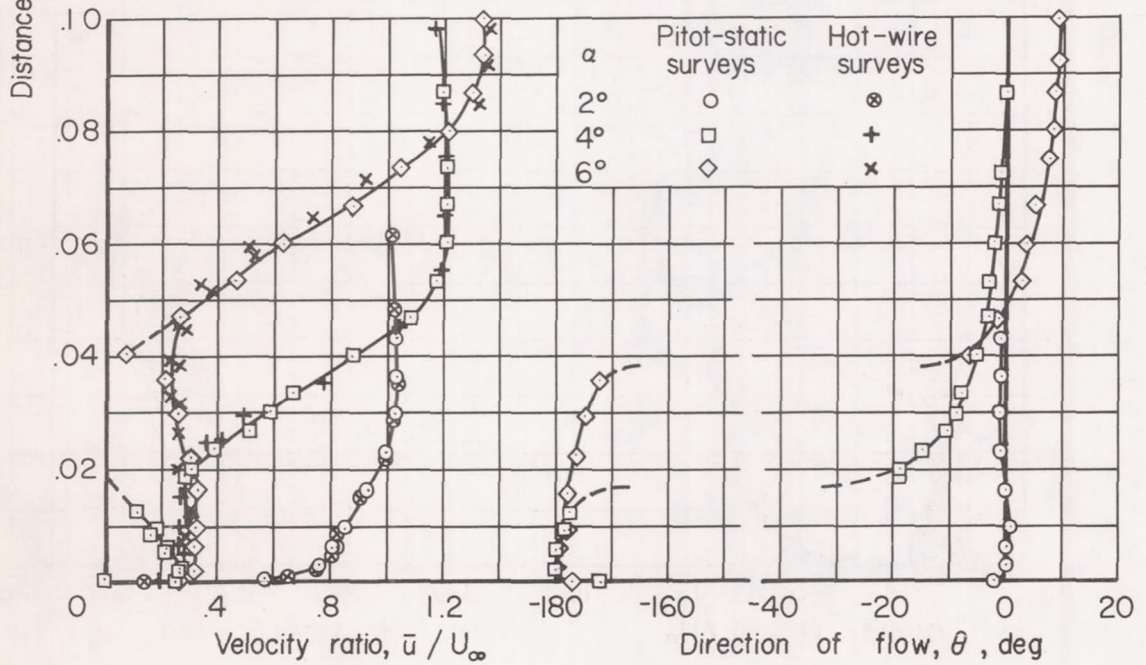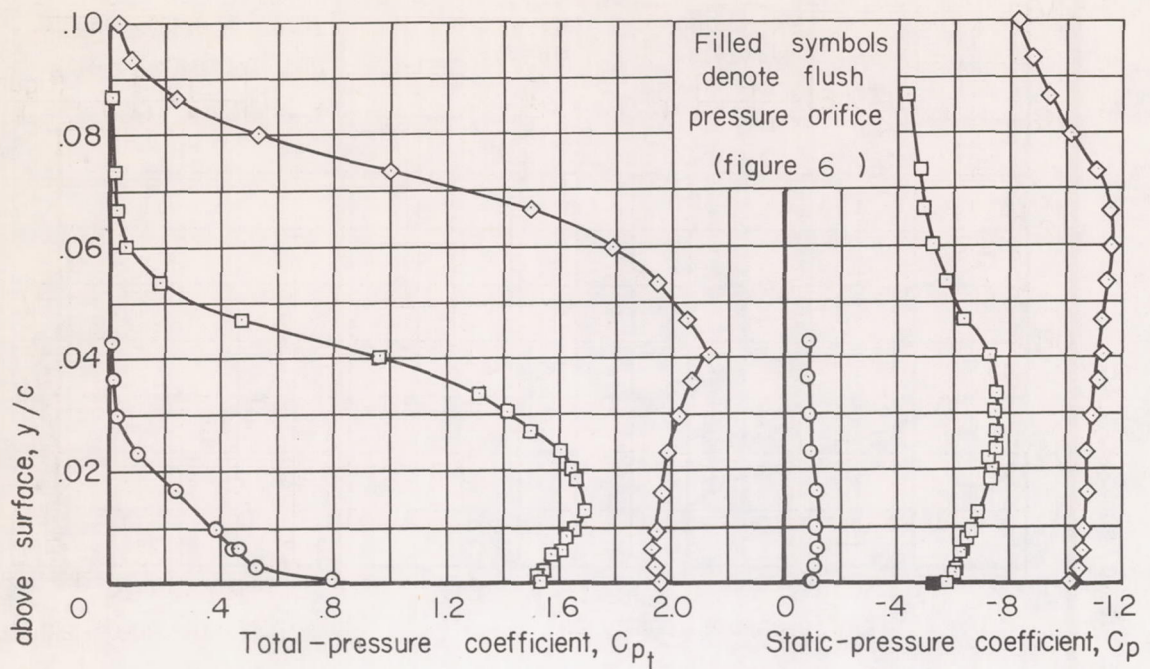
(e) x/c = 0.20

Figure 7.- Continued.
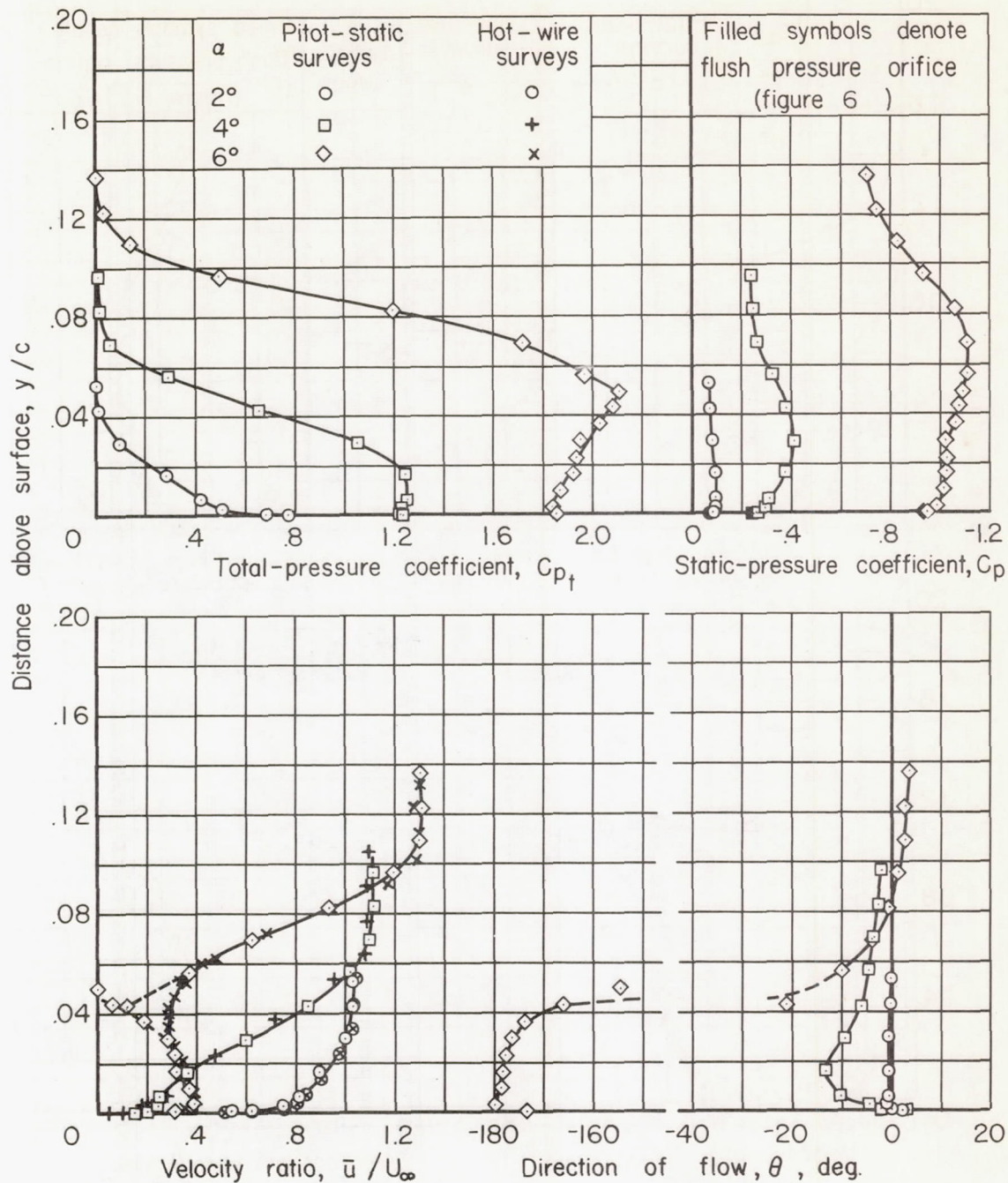
(f) x/c = 0.30

Figure 7.- Continued.

(g) x/c = 0.45

Figure 7.- Continued.

.20

.16

.12

y/c

.08

above surface,

.04

0

Distance

$\alpha$ | Pitot-static surveys | Hot-wire surveys

2° | ○ | ⊗

4° | □ | +

6° | ◇ | ×

Filled symbols denote flush pressure orifice (figure 6 )

.4  .8  1.2  1.6  2.0

Total-pressure coefficient, $C_{p_t}$

0  -.4  -.8  -1.2

Static-pressure coefficient, $C_p$

.20

.16

.12

.08

.04

0

.4  .8  1.2  1.6

Velocity ratio, $\bar{u}/U_\infty$

-20  0  20  160  180

Direction of flow, $\theta$, deg
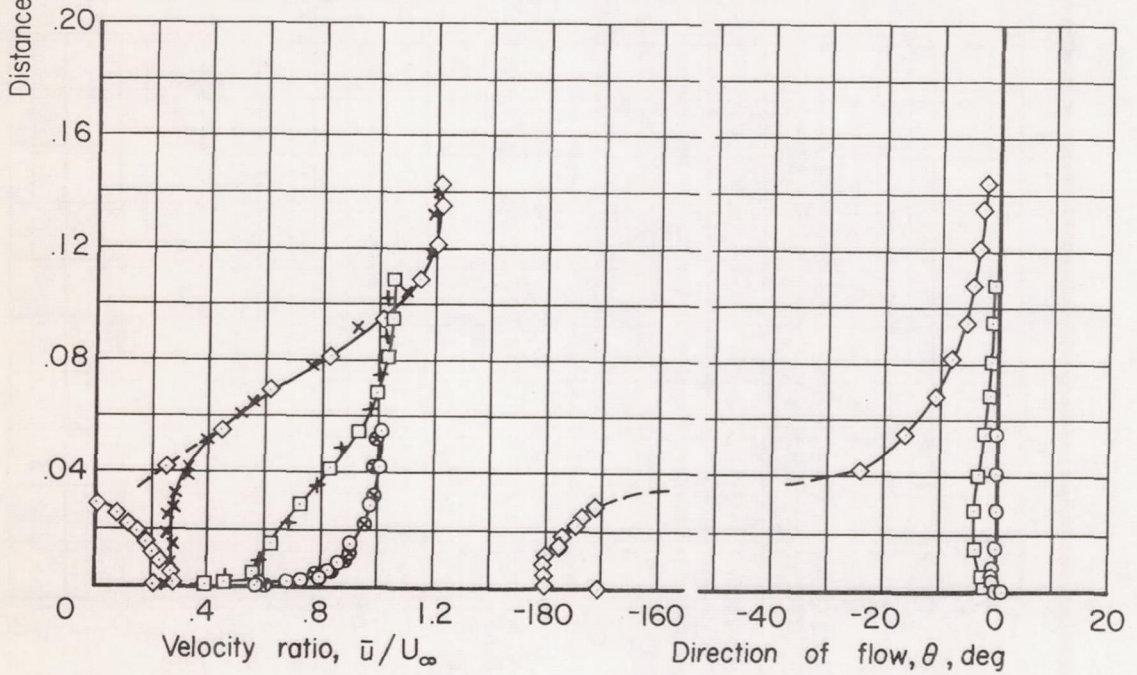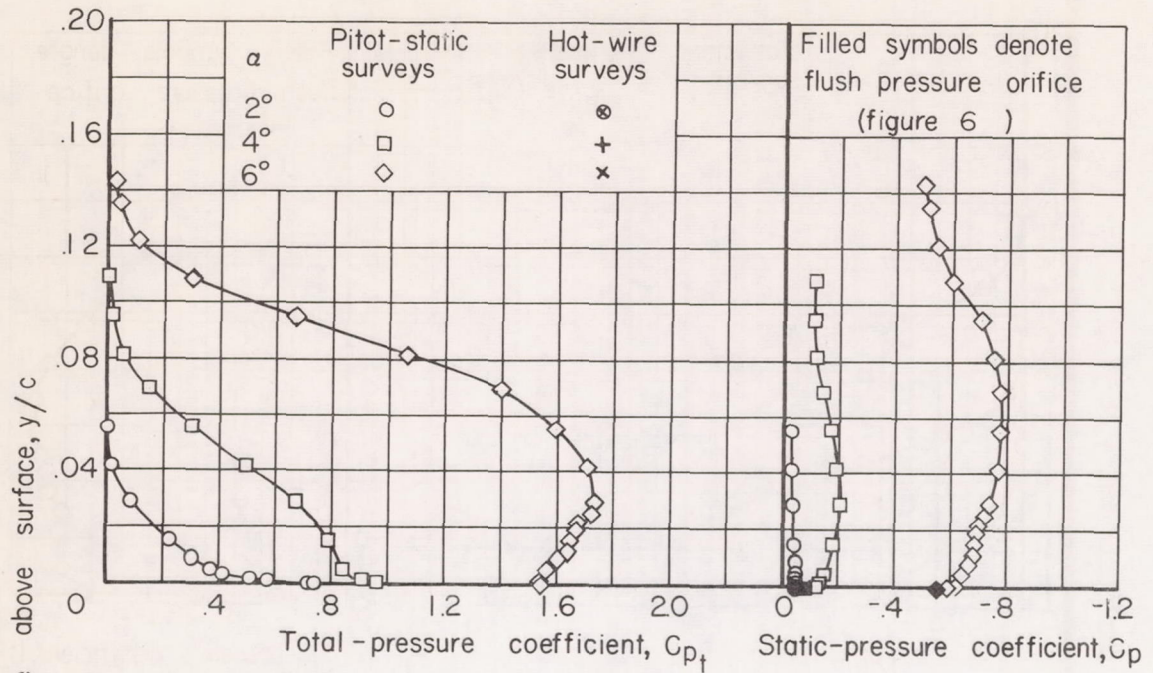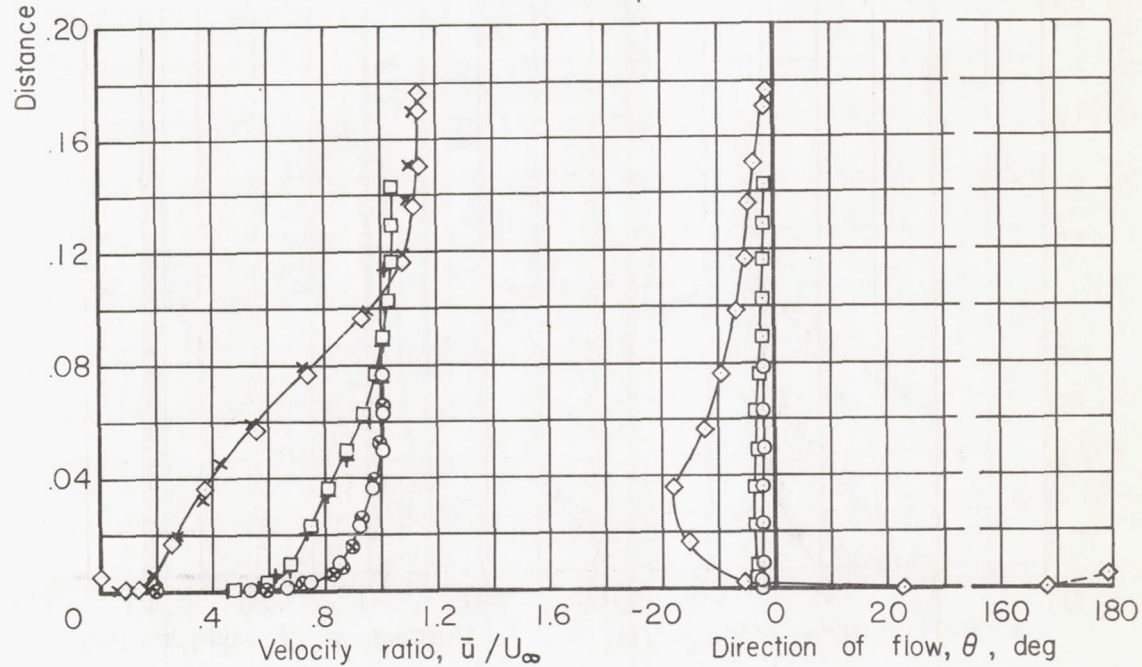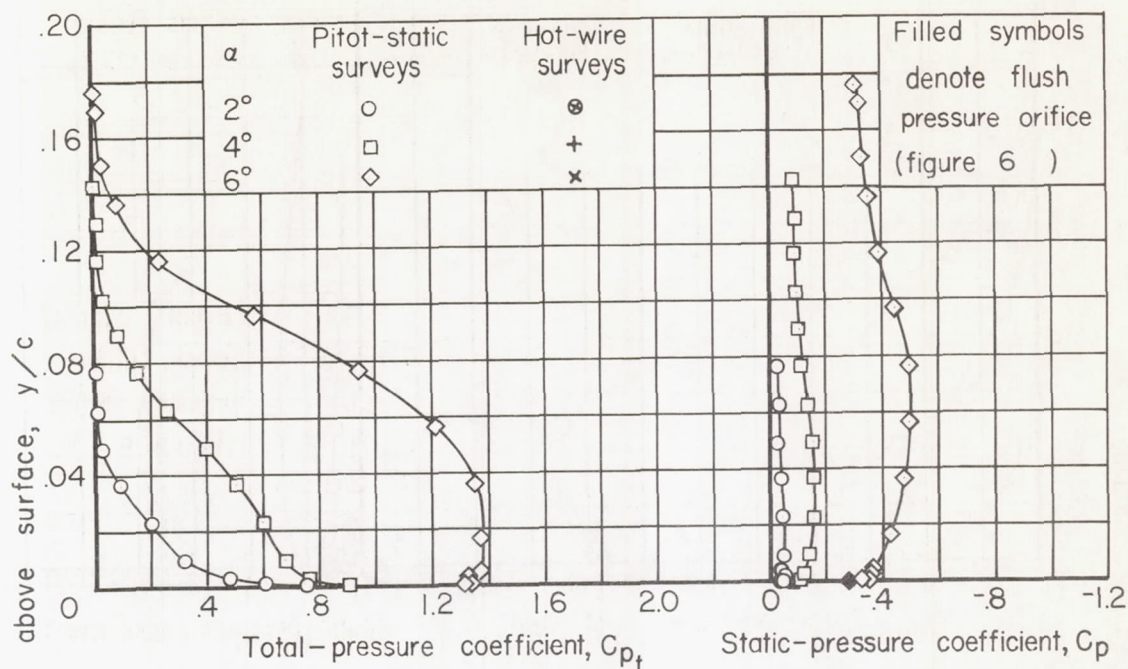
(h) x/c = 0.60
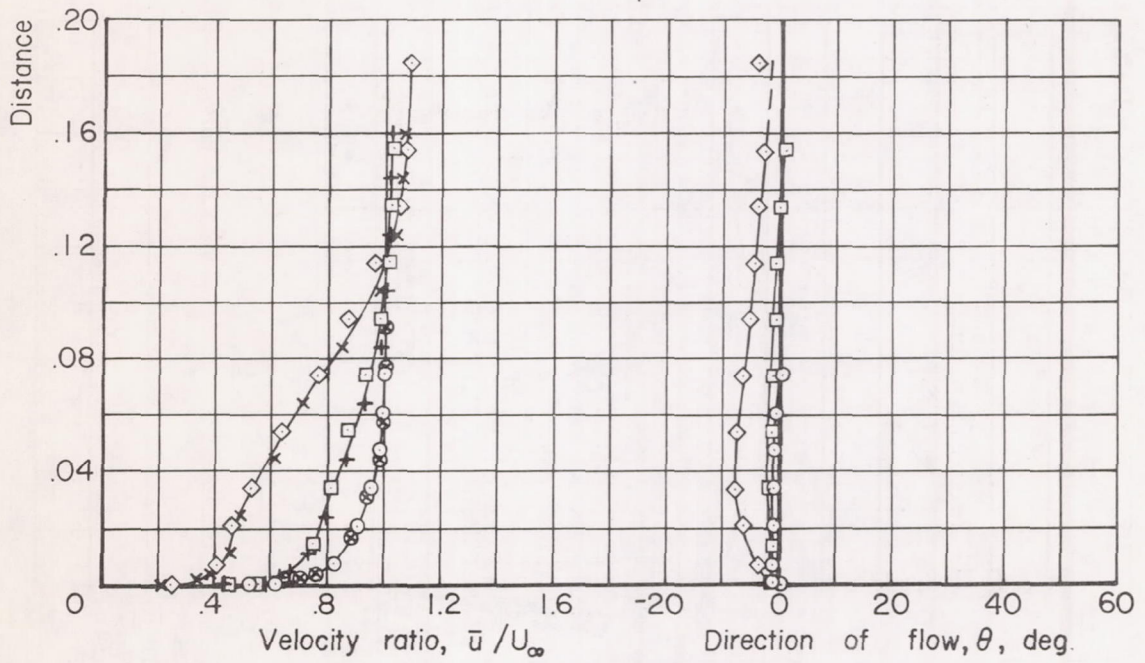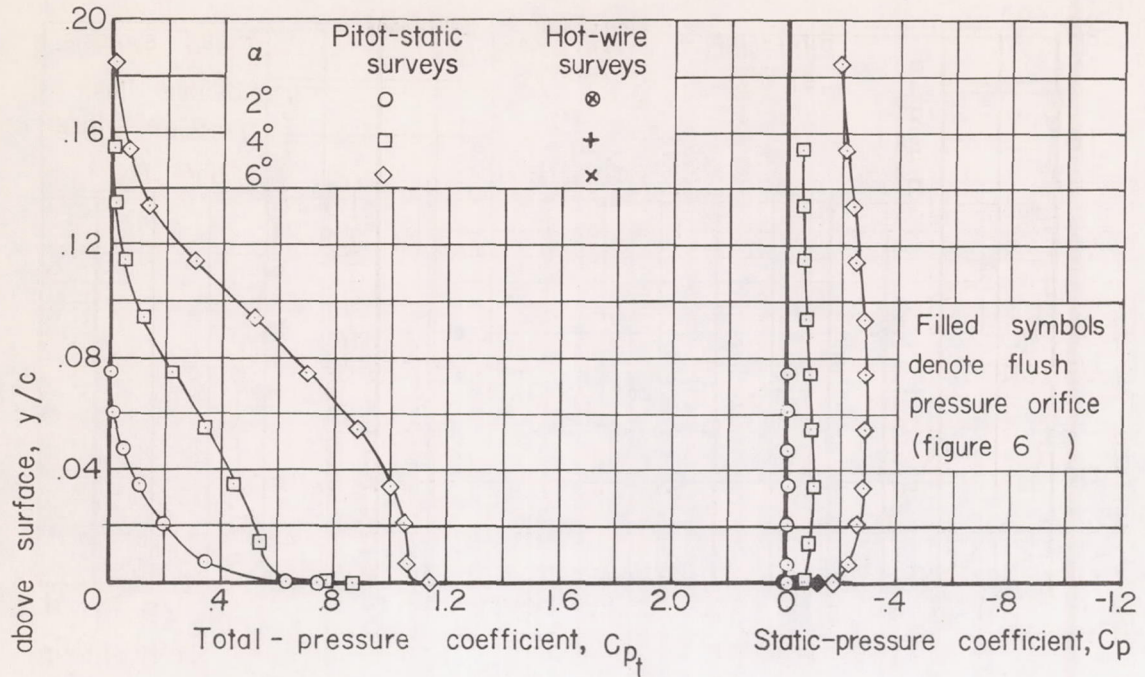
Figure 7.- Continued.

(i) x/c = 0.80

Figure 7.- Concluded.
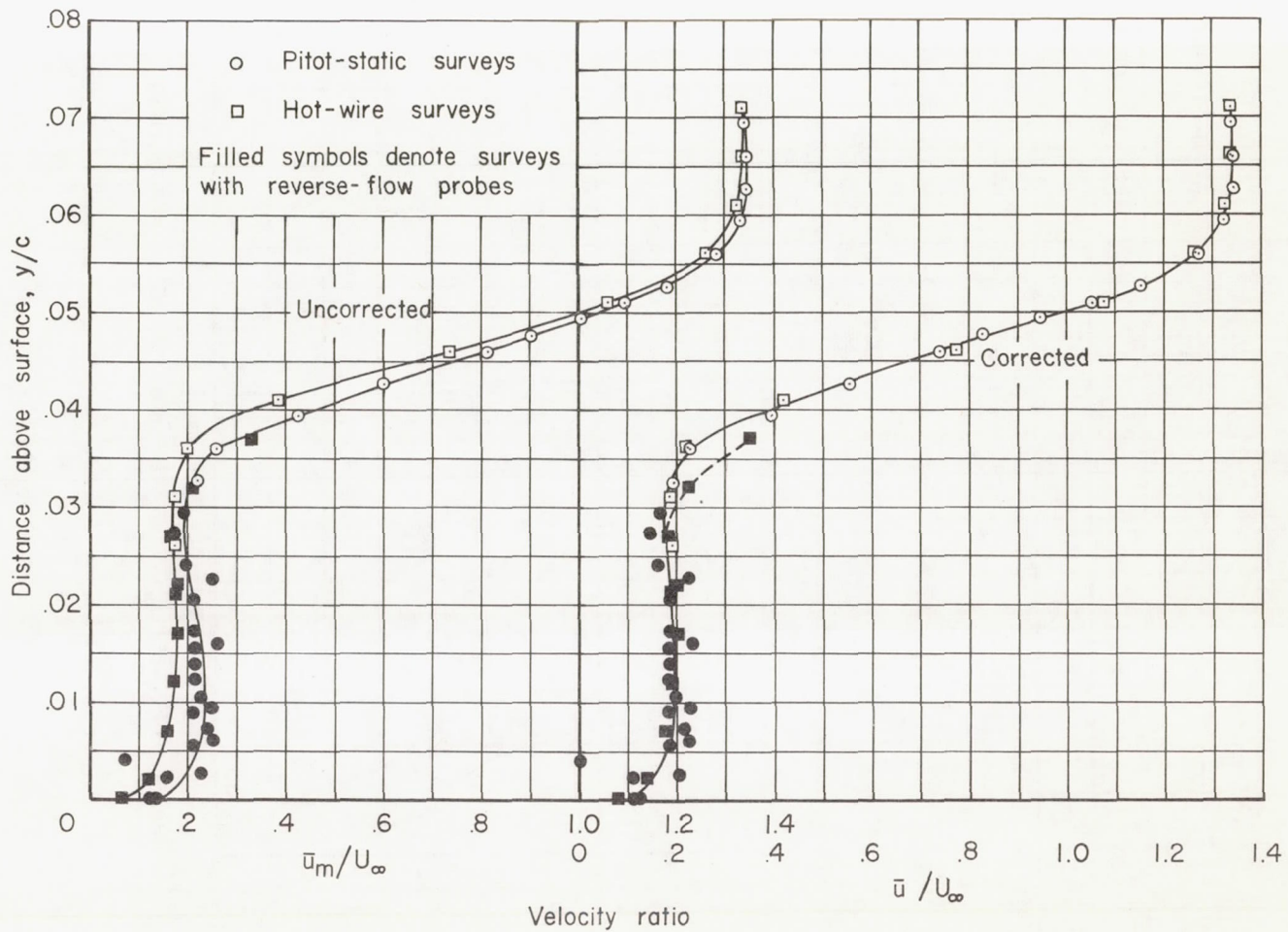
(a) x/c = 0.10

Figure 8.- Typical comparison between pitot-static and hot-wire determinations of the mean velocity; α = 6°.
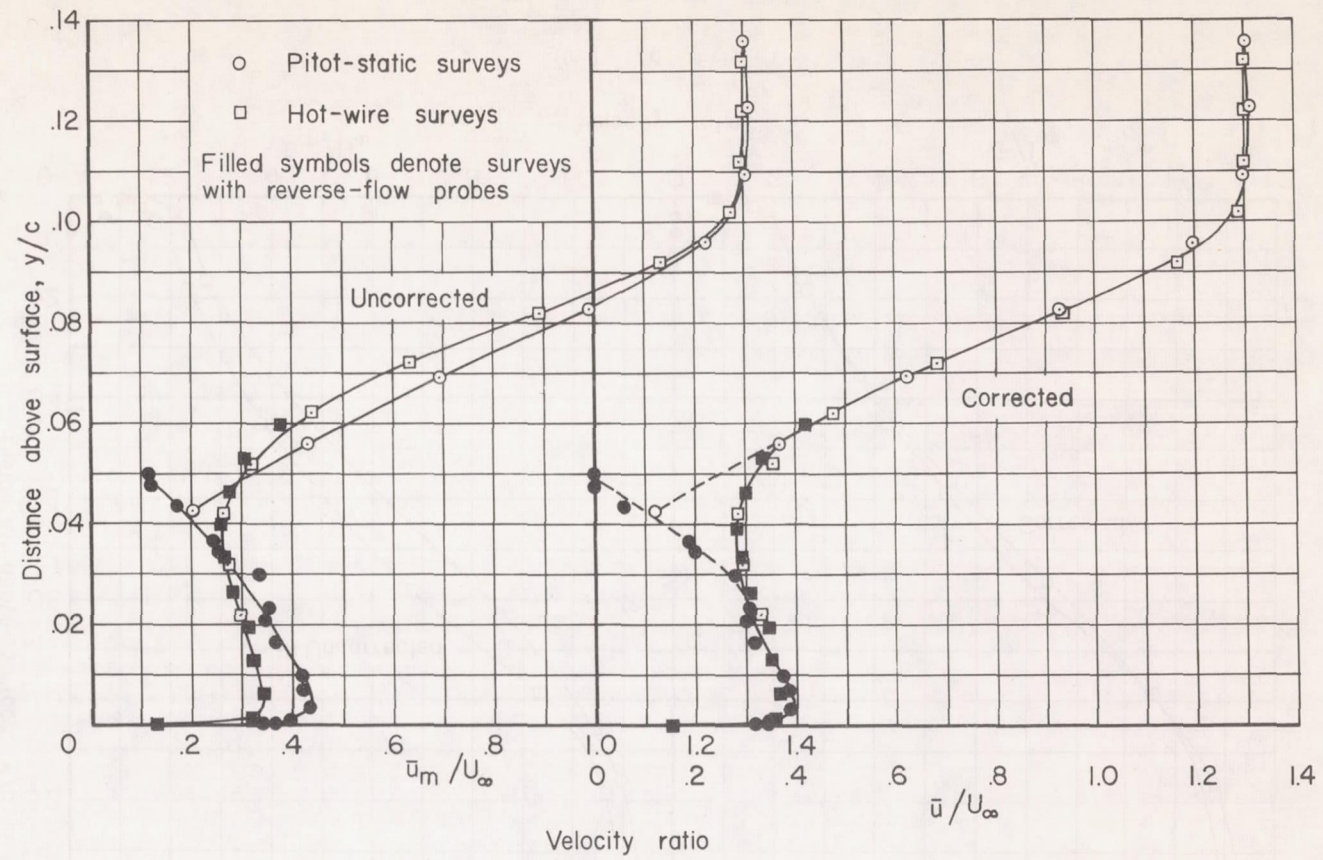
(b) x/c = 0.30

Figure 8.- Continued.
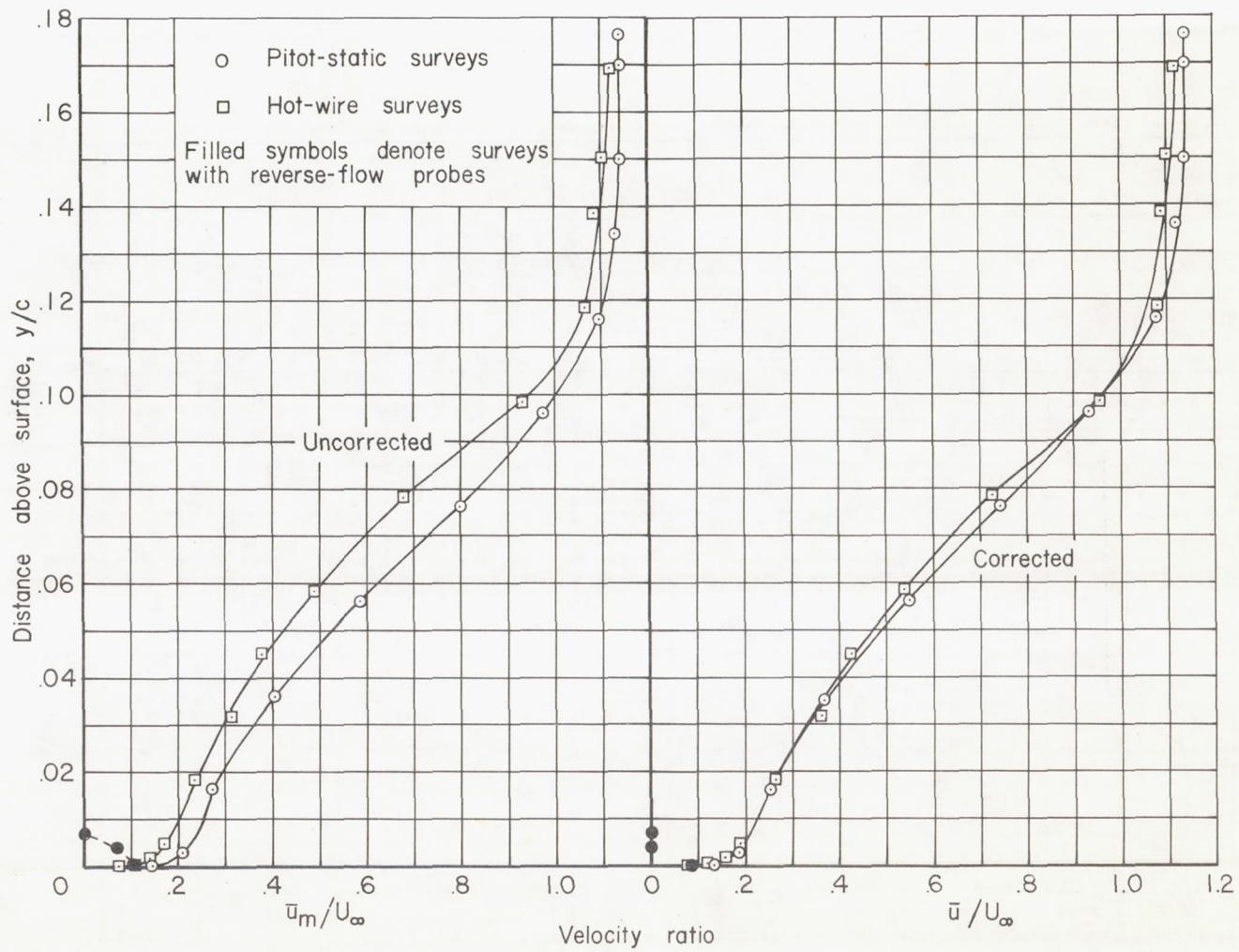
(c) x/c = 0.60

Figure 8.- Concluded.
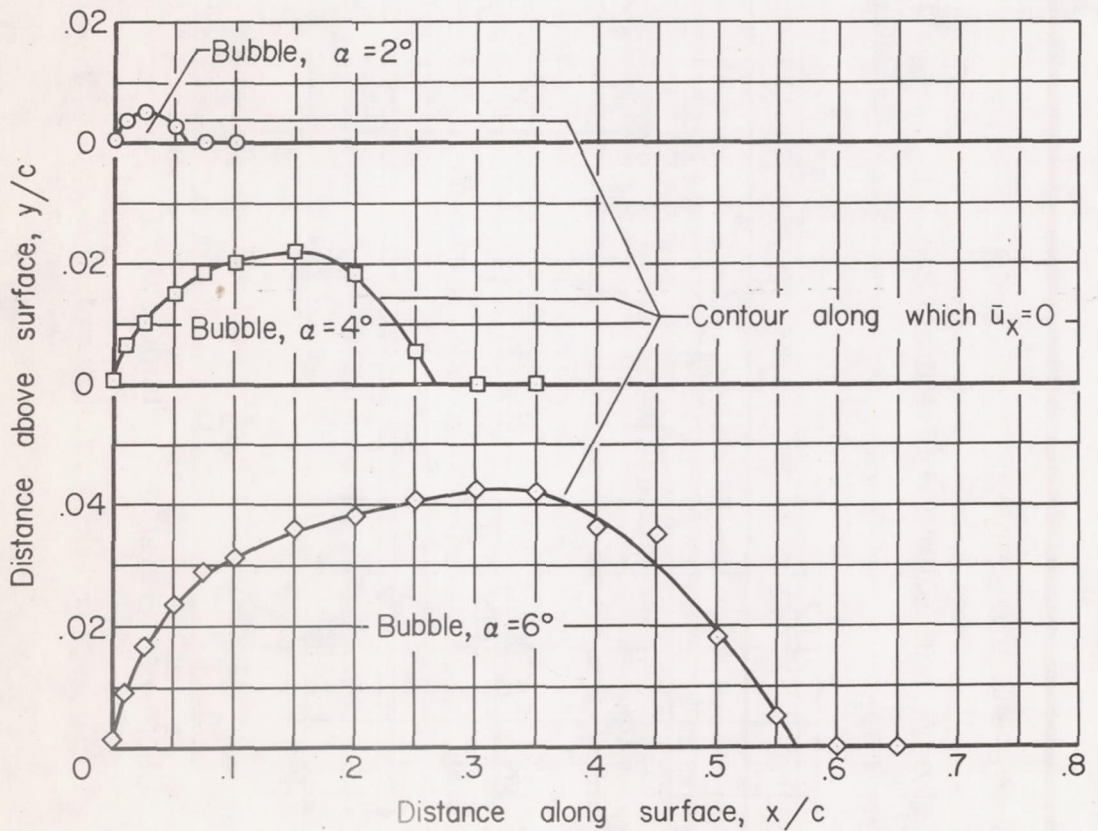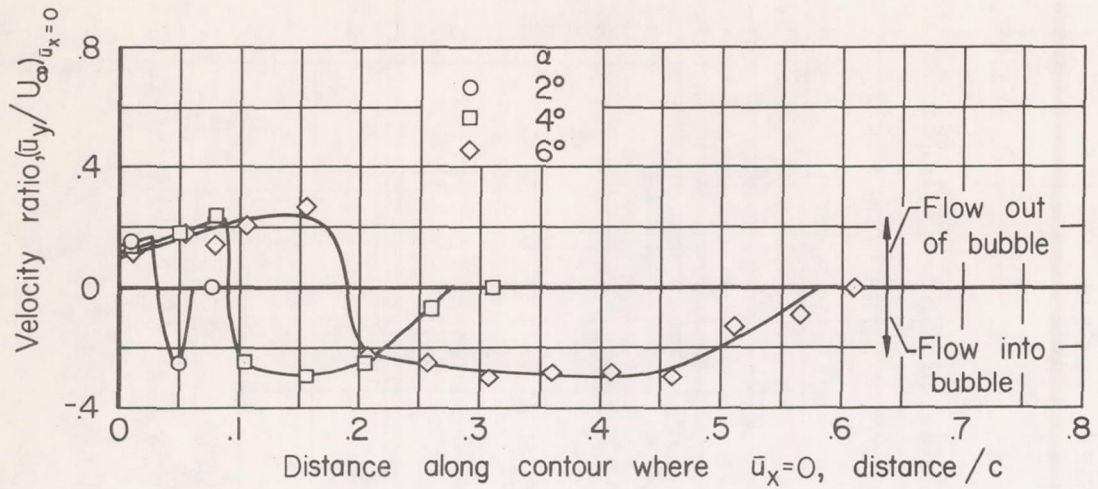
Figure 9.- Bubble shapes derived from the mean-flow surveys and estimated inflow and outflow velocities across the upper contour of the bubbles.
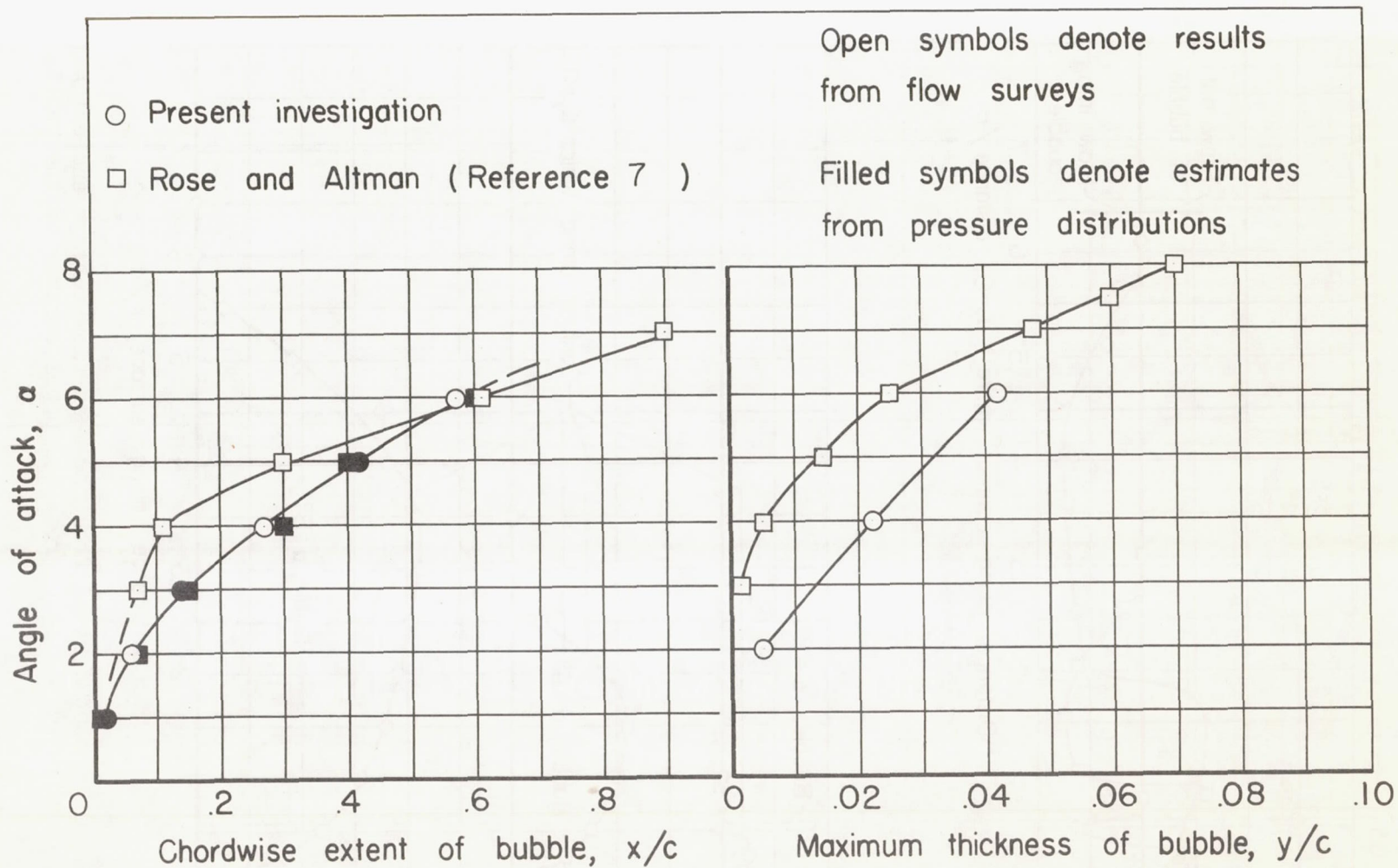
Figure 10.- A comparison of the chordwise extent and maximum thickness of the bubbles with those reported in reference 7.
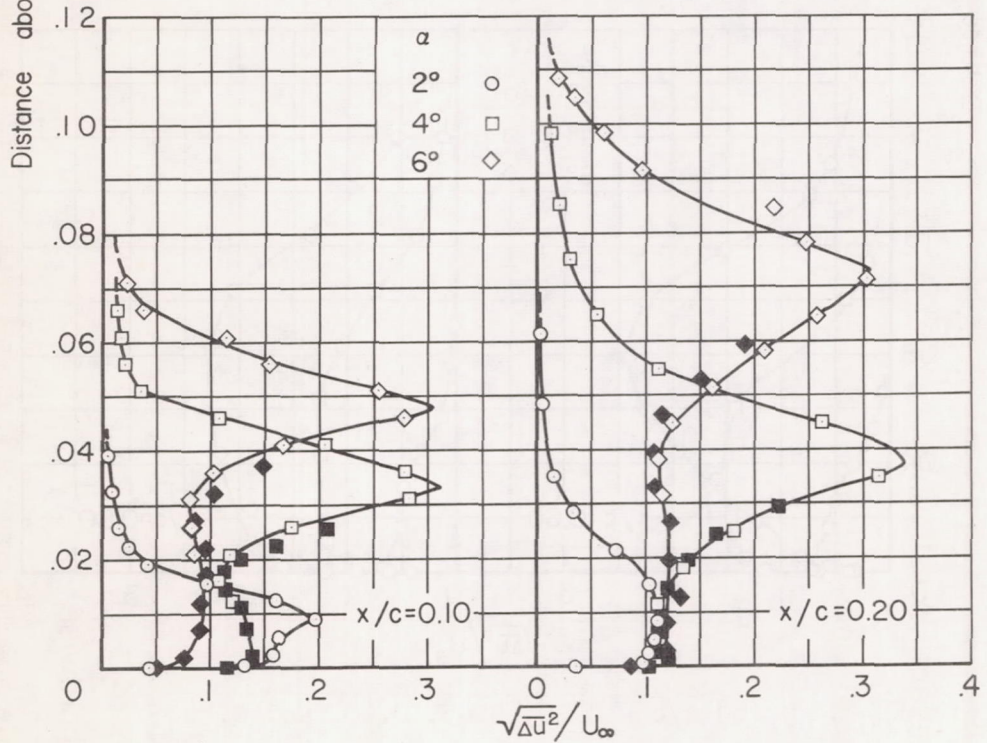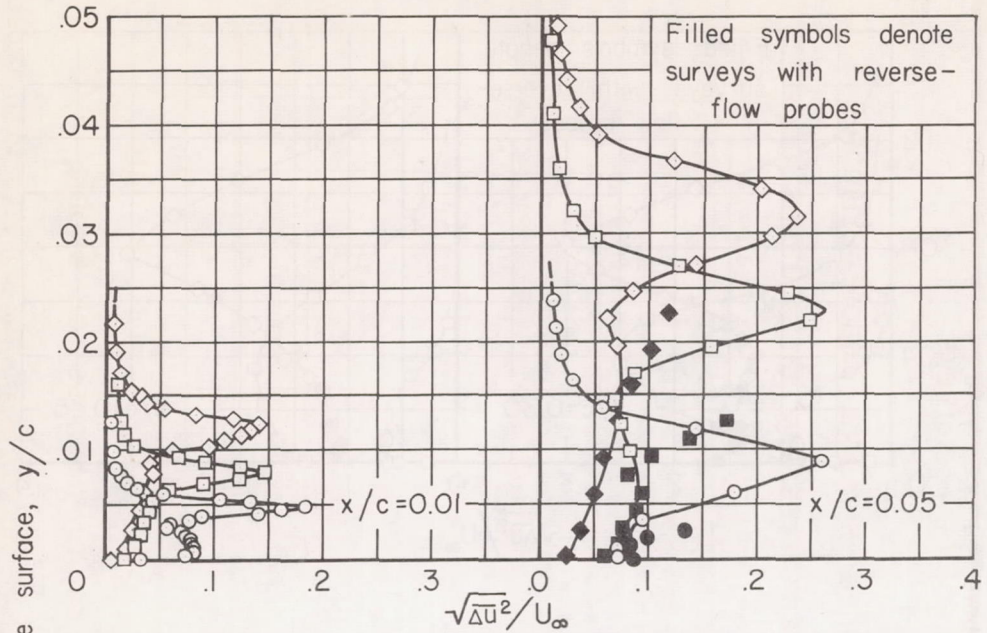
(a) x/c = 0.01, 0.05, 0.10, and 0.20

Figure 11.- Results from the hot-wire anemometer measurements of the velocity fluctuations.
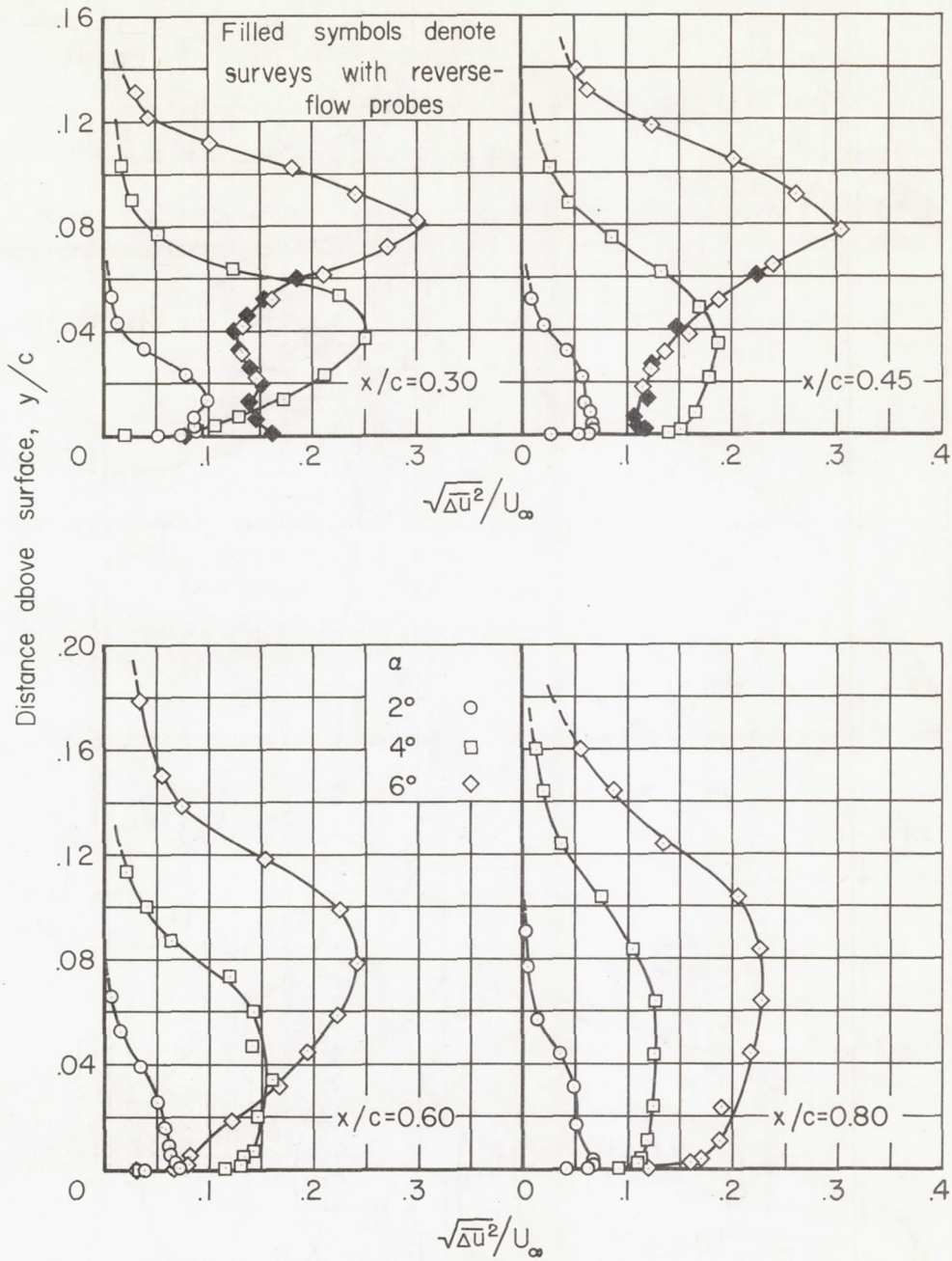
(b) x/c = 0.30, 0.45, 0.60, and 0.80

Figure 11.- Concluded.
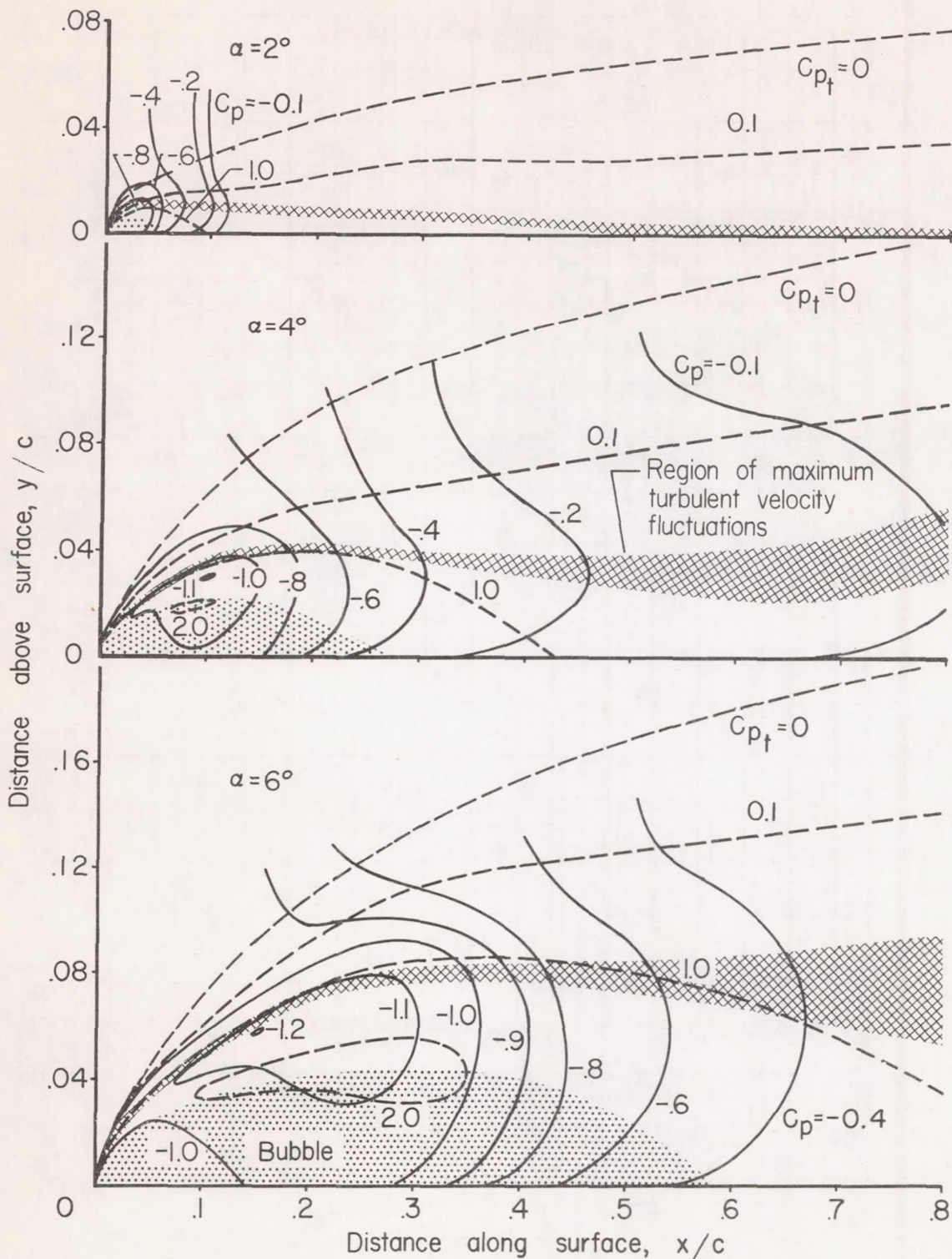
Figure 12.- Graphical summary of the flow surveys.
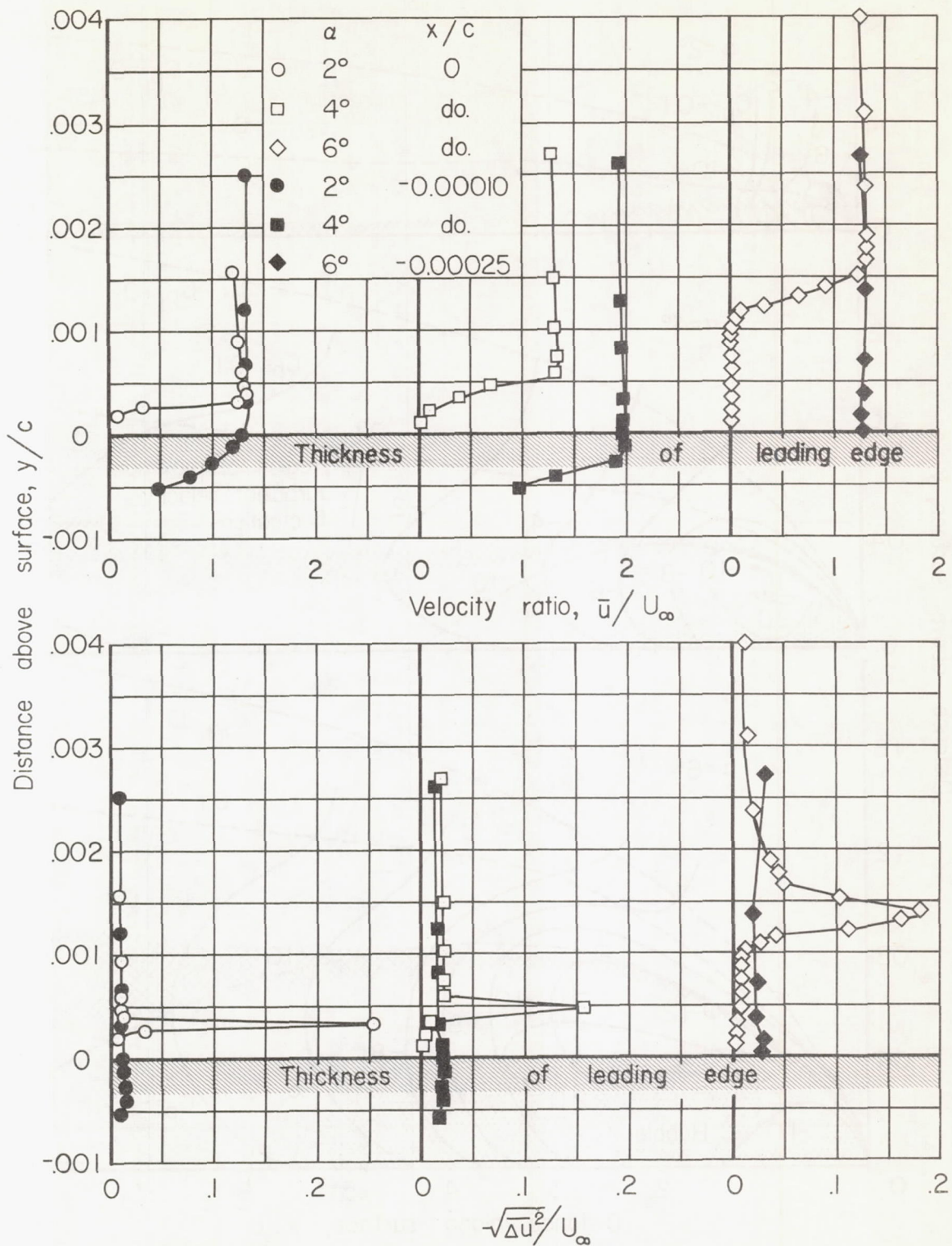
Figure 13.- Results from the hot-wire anemometer measurements in the
immediate vicinity of the leading edge of the plate.
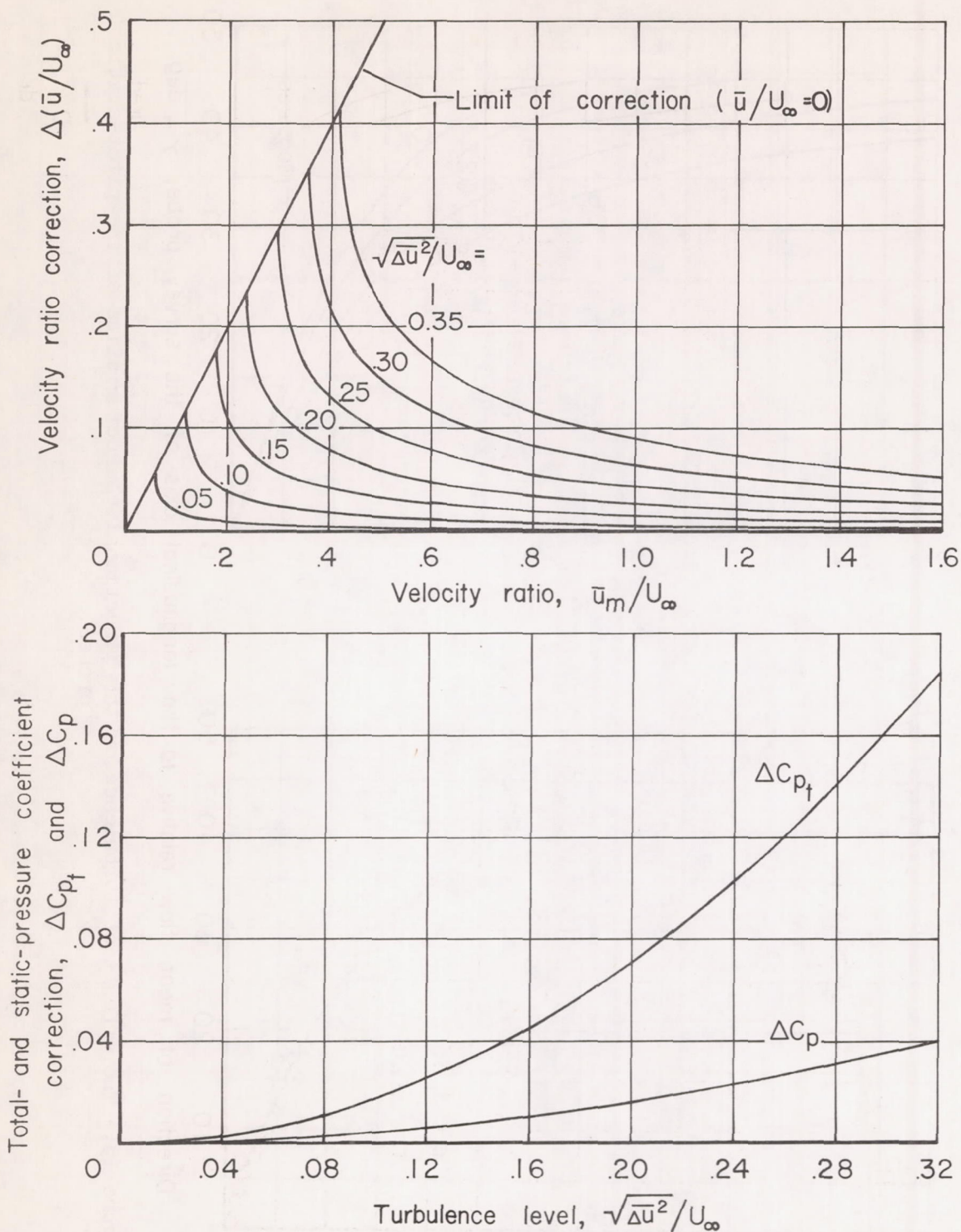
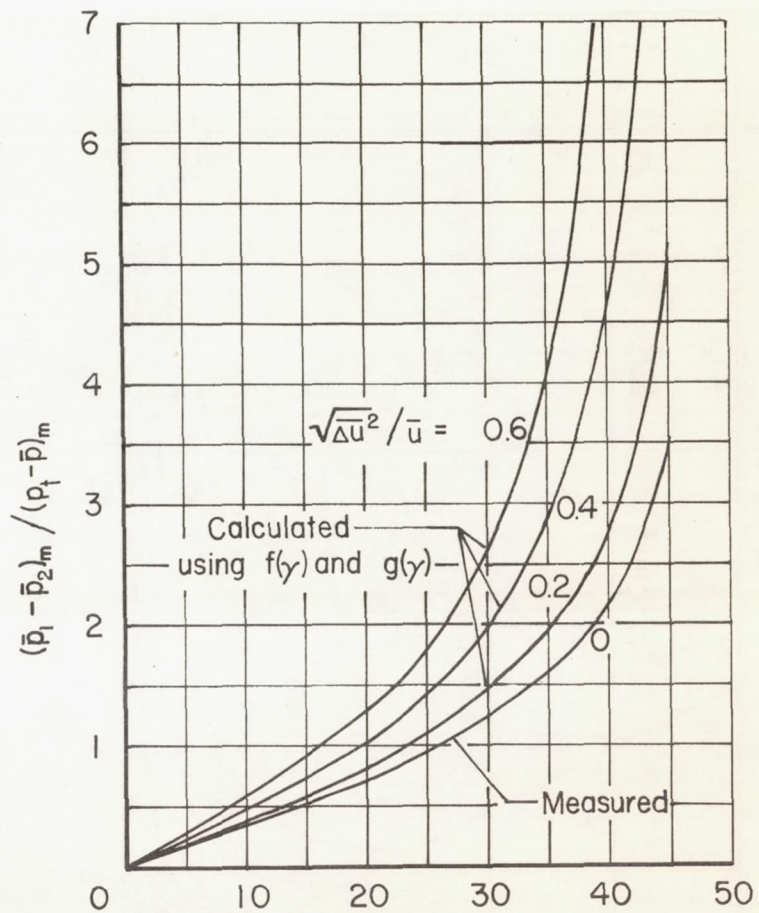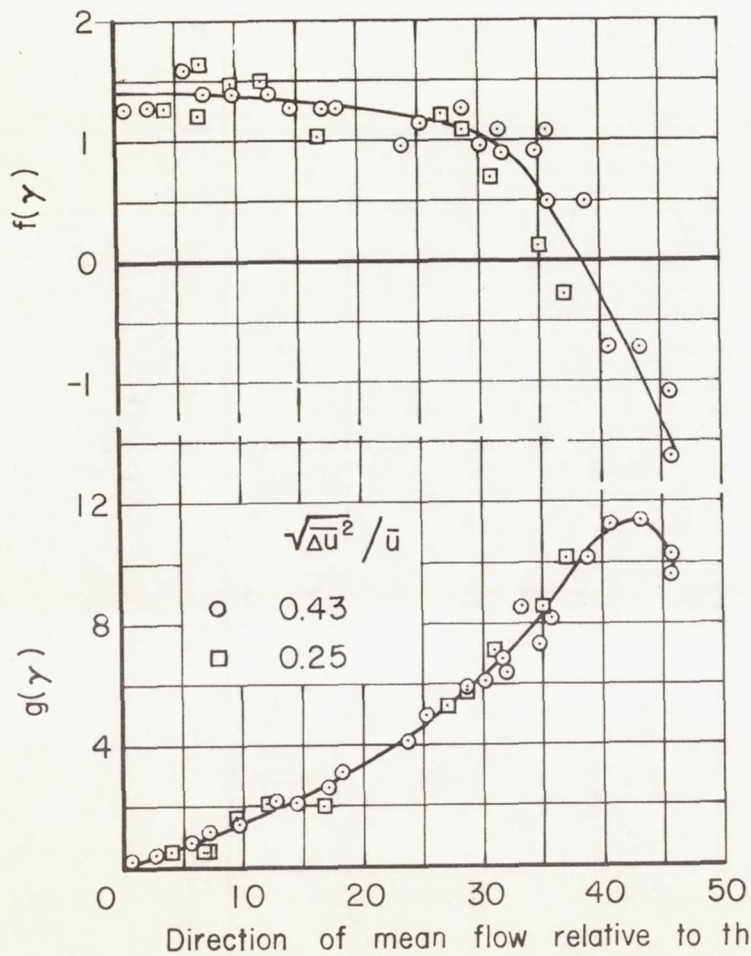Figure 14.- Corrections applied to the pitot-static measurements for the effects of turbulent flow.

Figure 15.- The effects of turbulence on the directional characteristics of the pitot-static probes.